Diss. ETH No 14595

Measures to enhance the NO$_x$ conversion in urea-SCR systems for automotive applications

A dissertation submitted to the

SWISS FEDERAL INSTITUTE OF TECHNOLOGY ZURICH

for the degree of

DOCTOR OF TECHNICAL SCIENCES

presented by

GIUSEPPE SALVATORE MADIA

Dipl. Chem. Eng., University of Calabria (Italy)

born December 1, 1973

from Italy

accepted on the recommendation of

Prof. Dr. A. Wokaun, examiner

Prof. Dr. A. Baiker, co-examiner

Dr. M. Koebel, co-examiner

2002

alla mia famiglia, al mio paese

Acknowledgments

I would like to thank Prof. Dr. A. Wokaun for the supervision of this work. I appreciated his interest in my work and his encouragement to fruitful collaborations between different research groups within the Department of General Energy at PSI. I'm grateful to Prof. Dr. A. Baiker, co-examiner of this work, for devoting his attention in refereeing this thesis.

My special thanks are due to Dr. M. Koebel for the precious support during the last three years. Manfred was an untiring teacher and spent a lot of time in proof-reading our publications and this thesis.

I'm very grateful to Mr. M. Elsener for the help, the precious advises and the efficient contribution to this work. Martin was a partner of fruitful discussions as well as many jogging hours and mushroom excursions in Rotberg and PSI surroundings.

Many thanks are due to my "compare" F. Raimondi whose co-operation was very helpful to my research. Fabio carried out the XPS and Raman experiments and provided also ideas which are involved in this work. I'm sorry to leave him with the big regret of not winning even a single kicker match against me!

I would like to express my thanks for their contribution to: Mrs. Friederike Geiger (BET measurements), Mr. Alwin Frei (XRD analysis) and Mr. Rolf Keil (ICP-AES). I wish to thank also all left unnamed who contributed in several ways to this thesis.

Thanks are also due to all colleagues who have contributed to make enjoyable the last three years at PSI. Their presence, their humor and their comradeship created a nice working atmosphere. I'm happy for the hours we spent together inside and outside PSI. I will always remember the several exciting trips, the amusing evenings, the heated discussions, the funny adventures, the social cases, the good and bad times...and the not-ending soccer matches with "papa Jorn" shouting "zurück!".

In the past few years I won new friends: They represent the best reward of my staying in Switzerland and I'm sure "che non ci perderemo mai!"

Table of Contents

Table of Contents

Table of Contents

Summary

The Selective Catalytic Reduction (SCR) of nitrogen oxides (NO_x) by ammonia is currently considered the most effective technology for high NO_x removal from lean exhaust of stationary plants. The most qualified SCR catalysts are based on TiO_2-WO_3-V_2O_5 and show their optimum performance in the temperature range 300-400°C. On the other hand, the automotive application of the process calls for a high NO_x removal over a much wider temperature range (150-550°C). The aim of the present work was to investigate the possibilities of widening the temperature window of the SCR reaction in order to adapt the process to the applications with mobile diesel engines.

The work can be subdivided in the following main topics:

- Preparation of TiO_2-WO_3-V_2O_5 catalysts with enhanced activity, selectivity and thermal stability;

- Investigations of the effects of NO_2 on the activity and selectivity of the SCR process.

In order to boost the intrinsic activity of the TiO_2-WO_3-V_2O_5 catalysts, the concentration of vanadia was increased up to ≈2.5 wt-%. Higher vanadium contents have negative effects on the thermal stability of the catalyst and on the SCR selectivity. In the automotive application of the SCR process, coated catalysts should have definite advantages compared to the classical extruded catalysts. This is due to their lower amount of active mass per volume of catalyst resulting in a lower amount of adsorbed ammonia. This will cause a considerable reduction of the ammonia peaks desorbed at sudden load/temperature increases. A second advantage of using coated catalysts is that they allow for higher cell densities, resulting in a higher ratio of geometric area/volume.

This will lower the mass transfer resistance, resulting in a higher volumetric activity of the catalyst.

The steady state performances of the catalysts were measured both in laboratory tests with synthetic gas mixtures and in diesel test stand experiments with real exhaust gas. Gaseous ammonia was used as reducing agent in the laboratory tests, whereas an aqueous solution of urea (32.5 wt-% urea) was used in the investigations at the diesel test stand.

The thermal behavior of TiO_2-WO_3-V_2O_5 catalysts with various vanadia contents (1, 2 and 3 wt-% V_2O_5) was investigated using X-ray diffraction (XRD), X-ray photoelectron spectroscopy (XPS), Raman spectroscopy and BET surface area determination. The activity and selectivity of the fresh and thermally aged catalysts (up to 650°C) were tested in the SCR reaction. Both structural and catalytic investigations have shown that the vanadia content has a strong effect on the thermal stability of the SCR catalysts. The structural investigations evidenced anatase sintering, increase of polymeric vanadyl surface species and three dimensional growth of supported vanadia upon ageing. The catalytic tests have shown that the SCR activity of catalysts containing 1 - 2 wt-% V_2O_5 increased upon ageing, whereas the SCR performance of the catalyst with 3 wt-% V_2O_5 decreased. The observed improvement of the SCR performance is attributed to an increase of the amount of polymeric vanadyl surface species upon ageing. The decrease of the SCR performance of the catalyst with 3 wt-% V_2O_5 is due to the extensive loss of surface area and to the three dimensional growth of supported vanadia upon ageing. The catalyst containing 2 wt-% V_2O_5 represents the best compromise between high SCR activity and good thermal stability.

Another topic of the work pertained the use of NO_2 to enhance the NO_x conversion at temperatures below 300°C. The higher rates of the fast SCR reaction requiring ammonia and the equimolar mixture of NO + NO_2 allow for higher NO_x conversions, and this effect is most pronounced at low temperatures. The nitrogen oxides of a diesel exhaust gas are mainly composed of NO (>90%), therefore the main reaction occurring on the SCR catalyst is the standard SCR reaction involving NO and ammonia. In order to make

Summary

use of the fast SCR reaction, the NO_2 content can easily be increased by oxidizing part of the NO on a Pt-based oxidation catalyst.

The influence of NO_2 on the NO_x conversion (DeNOx) on an SCR catalyst was investigated using feeds with various NO_2 contents. The NO_x conversion increases with increasing NO_2 fraction from 0% to 50% of total NO_x, as an increasing amount of NO_x reacts with ammonia in the fast SCR reaction. On the other hand, the removal of NO_x decreases with increasing NO_2 fraction from 50% to 100% of total NO_x, as an increasing amount of NO_2 reacts slowly with ammonia in the NO_2-SCR reaction. The highest NO_x conversion is obtained for NO_x composed of an equimolar mixture of NO + NO_2. The above considerations call for a proper design of the oxidation catalyst in order to possibly avoid conversions of NO to NO_2 higher than 50%.

The reactions of NO and NO_2 with ammonia in the temperature range 150-450°C were investigated in laboratory tests. At temperatures below 200°C the simultaneous presence of NO_2 and ammonia may lead to the formation of ammonium nitrate which may deposit as a solid on the catalyst causing its deactivation due to pore clogging. Ammonium nitrate decomposes into nitric acid and ammonia upon heating the reactor and the catalyst recovers its original activity. The formation of ammonium nitrate imposes a lower possible operating temperature for the SCR process.

The role of NO_2 in the mechanism of the fast SCR reaction was investigated with in-situ Raman experiments and transient catalytic tests. NO_2 was found to be involved in the reoxidation of the vanadium sites, which seems to be the rate limiting step in the standard SCR reaction at temperatures below 300°C. NO_2 is very effective in speeding up this critical step, thus enhancing the reaction rate of the SCR process at low temperatures.

Further experiments were made in order to investigate the side reactions of the SCR process with various NO_2 fractions. It was found that the selective catalytic oxidation of ammonia (SCO) and the formation of undesired nitrous oxide compete with the SCR reactions at high temperatures. Water strongly inhibits the SCO of ammonia and the formation of nitrous oxide, thus increasing the selectivity for the SCR reactions. However, water also inhibits the SCR reaction, most pronounced at low temperatures. NO_2

fractions exceeding 50% enhance the formation of nitrous oxide at low temperatures. Ammonium nitrate probably plays the role of an intermediate in the N_2O formation under these conditions.

The SCR-performances of both a simple SCR catalyst and a combined system with an upstream oxidation catalyst were investigated in laboratory tests. The addition of an oxidation catalyst was found to enhance the removal of NO_x at temperatures below 350°C. The beneficial effects of the added oxidation catalyst are due both to the oxidation of unburned hydrocarbons and to the NO_2 enhancement of the oxidation catalyst.

The effects of the oxidation catalyst on the NO_x conversion were also investigated in experiments at the diesel test stand. At temperatures below 300°C, the combined system including the oxidation catalyst showed a higher NO_x conversion than the SCR catalyst alone. Transient tests simulating typical automotive operations have shown that an aftertreatment system based on the SCR process can reduce the NO_x emissions of heavy-duty diesel engines to values below the forthcoming EURO IV emission standards.

Summary

Sommario

La riduzione catalitica selettiva (SCR) degli ossidi di azoto (NO_x) con ammoniaca e' considerata attualmente la piu' efficiente tecnologia per un'elevata rimozione degli NO_x dai gas di scarico magri di impianti stazionari. I piu' qualificati catalizzatori per la SCR sono a base di TiO_2-WO_3-V_2O_5 ed hanno prestazioni ottimali nell'intervallo di temperature tra 300°C e 400°C. La tecnologia di SCR non puo' essere direttamente impiegata su autoveicoli poiche', in questo ultimo caso, e' richiesta un'elevata rimozione degli NO_x in un intervallo di temperature molto piu' ampio (150-550°C). Per l'impiego della SCR su autoveicoli sono, dunque, necessari catalizzatori con maggiore attivita' intrinseca e migliore stabilita' termica di quelli attualmente impiegati negli impianti stazionari.

Nel presente lavoro di tesi e' stata indagata la possibilita' di ampliare l'intervallo di temperature operative del processo di SCR al fine di consentirne l'impiego su autoveicoli a motore diesel. A tal scopo

- sono stati preparati diversi catalizzatori a base di TiO_2-WO_3-V_2O_5 e le loro caratteristiche di attivita', selettivita' e stabilita' termica sono state studiate in diverse condizioni operative;

- e' stata analizzata l'influenza dell'NO_2 sull'attivita' e selettivita' del processo di SCR.

Nell'impiego della SCR su autoveicoli i catalizzatori supportati presentano alcuni vantaggi rispetto a quelli estrusi. La minore massa attiva per volume di catalizzatore, infatti, comporta un minore quantitativo di ammoniaca adsorbita e, di conseguenza, il quantitativo di ammoniaca desorbita in seguito a repentini aumenti della temperatura dei gas di scarico diminuisce notevolmente. Un ulteriore vantaggio dei catalizzatori

supportati consiste nella maggiore densita' di canali. Questo risulta in un piu' alto rapporto tra superficie geometrica e volume e, pertanto, comporta un aumento dell'attivita' volumetrica del catalizzatore (minori resistenze al trasporto di materia).

Le prestazioni dei catalizzatori di SCR in condizioni stazionarie sono state studiate in laboratorio con miscele gassose sintetiche e su un impianto pilota in condizioni reali. Negli esperimenti in laboratorio, come agente riducente e' stata impiegata ammoniaca gassosa, mentre una soluzione acquosa di urea (32.5% in peso di urea) e' stata impiegata negli esperimenti sull'impianto pilota.

La stabilita' termica dei catalizzatori a base di TiO_2-WO_3-V_2O_5 con diversi contenuti di vanadio (1, 2 e 3% in peso di V_2O_5) e' stata studiata mediante diffrazione ai raggi X (XRD), spettroscopia fotoelettrica ai raggi X (XPS), spettroscopia Raman ed analisi BET della superficie specifica. L'attivita' e la selettivita' per la SCR sono state indagate con catalizzatori freschi e dopo vari trattamenti termici (fino a 650°C). I risultati delle indagini strutturali e catalitiche hanno mostrato che il contenuto di vanadio ha una notevole influenza sull'attivita' e sulla stabilita' termica dei catalizzatori di SCR. In seguito ai trattamenti termici si evidenzia la sinterizzazione dell'anatase, l'aumento delle specie polimeriche superficiali di vanadio e la crescita tridimensionale degli ossidi di vanadio supportati. L'attivita' dei catalizzatori con 1 ed 2% V_2O_5 cresce in seguito ai trattamenti termici, mentre quella del catalizzatore con 3% V_2O_5 diminuisce. Il miglioramento dell'attivita' di SCR e' dovuto ad un aumento delle specie polimeriche superficiali di vanadio. Viceversa, la diminuzione dell'attivita' di SCR del catalizzatore con 3% V_2O_5 e' dovuta ad una notevole diminuzione della superficie specifica ed alla crescita tridimensionale degli ossidi di vanadio supportati. Il catalizzatore con 2% V_2O_5 rappresenta il miglior compromesso tra un'elevata attivita' di SCR ed una buona stabilita' termica.

L'analisi dell'influenza dell'NO_2 sulla rimozione degli NO_x ha evidenziato che le piu' alte velocita' di reazione della "fast SCR" tra ammoniaca e la miscela equimolare di NO ed NO_2 permettono una maggiore rimozione degli NO_x a temperature inferiori a 300°C. Gli ossidi di azoto nei gas di scarico dei motori diesel sono composti principalmente da NO (> 90%); pertanto, la tipica reazione di SCR coinvolge NO ed ammoniaca

Sommario

("standard SCR"). Per poter sfruttare i vantaggi della reazione di "fast SCR", il quantitativo di NO_2 nei gas di scarico puo' essere aumentato ossidando parte dell'NO su di un catalizzatore a base di platino.

L'influenza dell'NO_2 sulla conversione degli NO_x ad azoto (DeNOx) e' stata indagata in laboratorio usando miscele gassose con vari contenuti di NO_2. La DeNOx cresce all'aumentare della percentuale di NO_2 negli NO_x dallo 0% al 50%, poiche' un crescente quantitativo di NO_x reagisce con ammoniaca nella reazione di "fast SCR". D'altro lato, la DeNOx diminuisce all'aumentare della percentuale di NO_2 negli NO_x dal 50% al 100%, poiche' un crescente quantitativo di NO_2 reagisce con ammoniaca nella "NO_2 SCR", che ha una bassa velocita' di reazione. La piu' alta conversione degli NO_x e' stata osservata in corrispondenza di NO_x costituiti da una miscela equimolare di $NO + NO_2$ (reazione di "fast SCR"). Da quanto detto, risulta che e' necessario un corretto dimensionamento del catalizzatore di ossidazione al fine di evitare conversioni di NO ad NO_2 maggiori del 50%.

Le reazioni di NO ed NO_2 con ammoniaca nell'intervallo di temperatura tra 150°C e 450°C sono state studiate in laboratorio. A temperature inferiori a 200°C la simultanea presenza di NO_2 ed ammoniaca puo' portare alla formazione di nitrato d'ammonio. Quest'ultimo puo' depositarsi sul catalizzatore bloccandone i pori e causandone la disattivazione. Aumentando la temperatura, il nitrato d'ammonio si decompone in acido nitrico ed ammoniaca ed il catalizzatore recupera la sua attivita' originaria. La formazione di nitrato d'ammonio impone, dunque, un limite inferiore alla temperatura operativa del processo di SCR.

Il ruolo dell'NO_2 nel meccanismo della reazione di "fast SCR" e' stato indagato tramite esperimenti Raman in-situ e test catalitici in transitorio. Questi esperimenti hanno evidenziato che NO_2 partecipa alla riossidazione dei siti di vanadio, che rappresenta lo stadio limitante della reazione di "standard SCR" a temperature inferiori a 300°C. NO_2 e' molto efficiente nell'accelerare questo stadio e conseguentemente aumenta la velocita' di reazione della SCR a basse temperature.

Ulteriori esperimenti sono stati condotti per indagare le reazioni parallele alla SCR in caso di miscele gassose con varie concentrazioni di NO_2. Gli esperimenti hanno

dimostrato che a temperature inferiori a 400°C il sistema presenta un'elevata selettivita' per il processo di SCR. L'ossidazione selettiva catalitica (SCO) dell'ammoniaca ad azoto e la formazione di ossido nitroso (N_2O) competono, invece, con la SCR a temperature superiori a 400°C. La presenza di acqua inibisce fortemente la SCO dell'ammoniaca e la formazione di ossido nitroso, aumentando di conseguenza la selettivita' per la SCR. La presenza di acqua, pero', inibisce anche la SCR. Percentuali di NO_2 negli NO_x al di sopra del 50% aumentano la formazione di ossido nitroso a basse temperature. In questo caso, il meccanismo che porta alla formazione di ossido nitroso passa, presumibilmente, attraverso uno stadio intermedio rappresentato dal nitrato d'ammonio.

Nelle ricerche condotte in laboratorio sono state studiate anche le prestazioni nel processo di SCR di un sistema contenente il solo catalizzatore di SCR e di un sistema combinato contenente il catalizzatore di SCR ed un pre-catalizzatore di ossidazione. L'aggiunta del catalizzatore di ossidazione aumenta la rimozione degli NO_x a temperature inferiori a 350°C. Gli effetti benefici del catalizzatore di ossidazione derivano dall'ossidazione degli idrocarburi incombusti presenti nei gas di scarico e dalla conversione di parte di NO ad NO_2.

Gli effetti del catalizzatore di ossidazione sulla conversione degli NO_x sono stati indagati anche sull'impianto pilota. Il sistema combinato contenente il catalizzatore di ossidazione ha portato ad una maggiore rimozione degli NO_x in confronto al sistema costituito dal solo catalizzatore di SCR. Gli esperimenti sull'impianto pilota hanno dimostrato che un sistema di trattamento dei gas di scarico basato sul processo di SCR puo' ridurre le emissioni degli NO_x dai veicoli diesel pesanti a valori inferiori a quelli imposti dalla futura legislazione EURO IV.

Sommario

1

Introduction

1.1   Nitrogen oxide emissions

Almost 90% of the current energy production is based on the combustion of fossil fuels and biomass [1]. Energy scenarios predict that the combustion of fossil fuels and biomass will still allow for 50% of the world energy consumption in 2100 [2]. In the last few decades, the environmental effects of pollutant emissions from combustion sources (nitrogen oxides, sulfur oxides, soot particles, CO, volatile organic compounds) have become increasingly serious. Accordingly, the use of catalytic systems for pollution abatement has grown in the last decades from a virtually non-existing to a multi-billion-dollar worldwide business due to the increasingly severe emission legislation.

Nitrogen oxides (NO_x) were found to be responsible for photochemical smog, acid rains, tropospheric ozone formation and stratospheric ozone depletion [3,4]. The major amount (66%) of total NO_x emissions is caused by human activities involving combustion processes. The remaining NO_x emissions derive from natural sources such as lightning (16%) and microbiological activities (16%) or as input from the stratosphere [5].

Different sources of anthropogenic NO_x emissions are known. The transport sector is responsible for 50% of global man-made NO_x emissions [6]. The remainder originates from stationary sources, like power plants, internal combustion engines, industrial

boilers, waste and sludge incinerators, process heaters and gas turbines. Figure 1.1 reports the contributions of several human activities to the nitrogen oxide emissions in Switzerland [7]. The lion share of the NO_x emissions is produced by traffic. Since 1985 the emissions by traffic dropped due to the introduction of the catalyst technology for cars. However, an efficient technology for the removal of NO_x from automotive lean burn engines does currently not exist, therefore the contribution of diesel powered vehicles to the NO_x emissions will increase in the future. The development of a DeNOx technology for vehicles equipped with lean-burn gasoline or diesel engines represents the main challenge of automotive emission control in the forthcoming years.
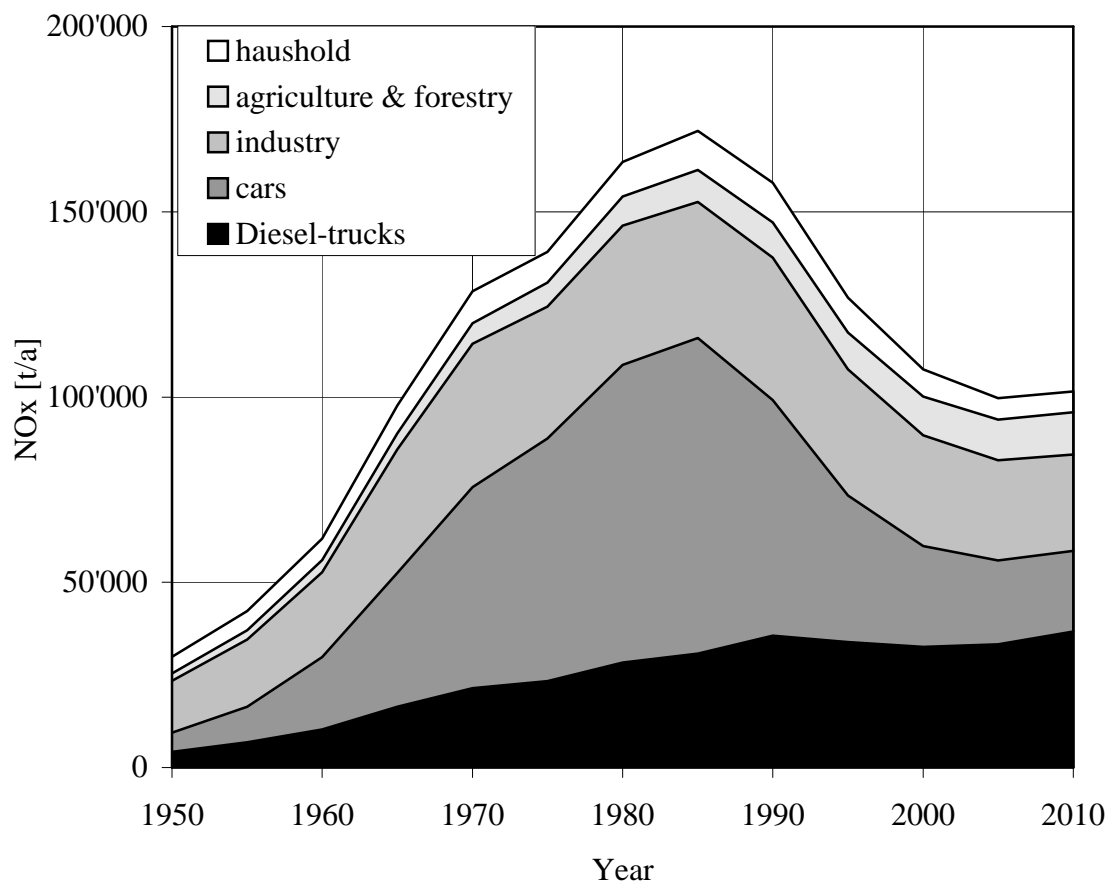
Figure 1.1   Evolution of the nitrogen oxide emissions in Switzerland from 1950 to 2010 [7]

1.2   Nitrogen oxide removal from automotive exhaust

The Three Way Catalyst (TWC) technology allows for a deep removal of NO_x from the exhaust of vehicles equipped with a gasoline engine [8]. This technology is possible due to the absence of oxygen in the exhaust resulting from a stoichiometric combustion in the cylinder. On the three-way catalyst, the nitrogen oxides react with the unburned hydrocarbons or CO in such a way that the oxygen of NO_x is consumed for the oxidation of the unburned hydrocarbons or CO yielding carbon dioxide and water; accordingly, NO_x are reduced to N_2. A minor drawback of the TWC technology is the partial reduction of NO_x to undesired nitrous oxide or ammonia under certain operating conditions of the engine.

The practical application of diesel and lean-burn spark ignition gasoline engines has become increasingly important in recent years. These engines operate with a high air-fuel ratio, thus allowing fuel-economy improvements [9]. The TWC technology can not be applied for the aftertreatment of exhaust from lean burn engines due to the low NO_x conversion in the presence of oxygen.

In many instances it was possible to reduce the NO_x emissions from automotive diesel engines using primary measures [10-12]. The primary measures aim at preventing the NO_x formation during the combustion process by lowering flame temperatures, avoiding local oxygen deficit, favoring a slower combustion (see Table 1.1). Conversely, the primary measures lead to higher emissions of unburned products, especially soot, CO and hydrocarbons, thus resulting in a trade-off between the emissions of NO_x and unburned products. However, whilst being relatively inexpensive, primary measures are usually insufficient to meet the increasingly strict emission standards set by the legislation. It is now generally assumed that the EURO IV emission standards for heavy-duty diesel engines (i.e. trucks and buses) proposed for the year 2005 will no longer be feasible by primary measures alone but will require additional aftertreatment techniques.

Table 1.1 Primary measures for the reduction of NO_x emissions. Reprint from [12].

Reduction of the flame temperature	Avoidance of local oxygen deficit	Slow combustion
■ delayed injection timing ■ exhaust gas recirculation (EGR) ■ water-fuel mixture injection ■ combustion air cooling	■ central trough-shaped combustion zone ■ central injection ■ reduction of the ignition delay ■ increase of cetane number ■ control of the combustion air temperature	■ prolonged injection ■ control of the injected fuel ■ smaller dose diameter ■ use of common rail system ■ increase of cetane number

Figure 1.2 shows the large gap between feasible raw emissions of heavy-duty diesel engines and forthcoming emission standards [13]. The emissions from diesel engines show a trade-off between particulate matter and NO_x. Two basic strategies exist to attain the new standards:

(a) optimize the combustion with respect to a low emission of NO_x, leading to a high emission of unburned material (soot, CO and hydrocarbons); use a particulate filter in the aftertreatment;

(b) optimize the combustion with respect to a low emission of unburned material, leading to a high emission of NO_x; use a DeNOx process in the aftertreatment.
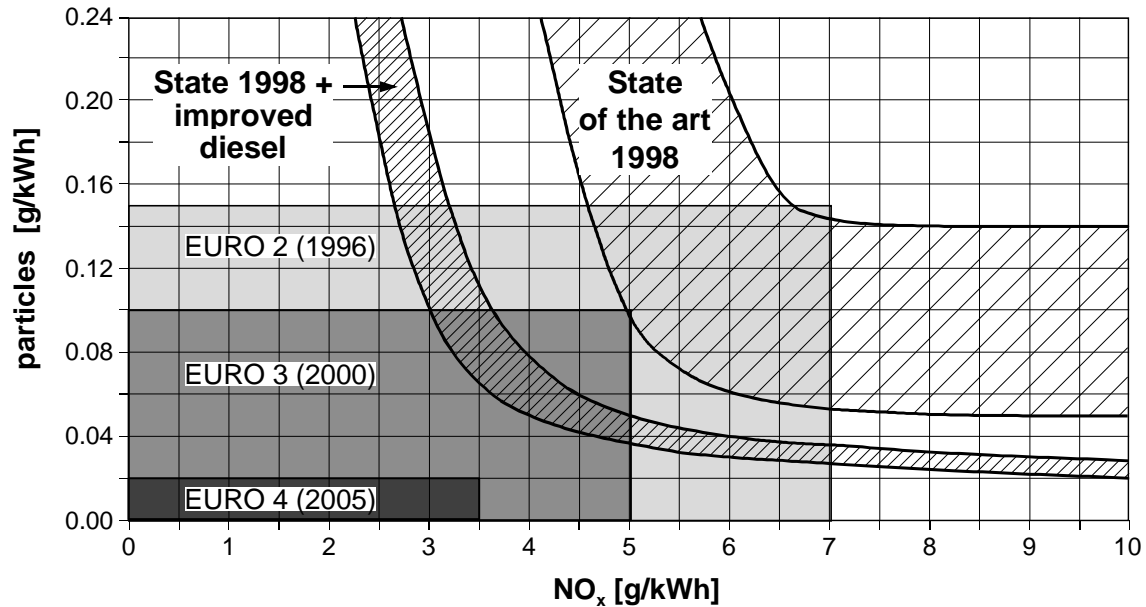
Figure 1.2 Trade-off between particulate matter and NO_x for heavy-duty truck engines and prospected EURO emission standards [13].

Because a better fuel economy is attained with route (b), various processes have been studied in recent years for selectively reducing NO_x in competition to O_2 in lean exhaust gases. The reduction of NO_x in lean exhaust requires a reducing agent which reacts selectively with NO_x in the presence of oxygen.

1.3 Technologies for the removal of NO_x from lean exhaust

1.3.1 HC-SCR (Hydrocarbon Selective Catalytic Reduction)

This process uses hydrocarbons as the reducing agent in combination with a suitable catalyst. It has been shown that even diesel fuel can be used as reducing agent and, therefore, no special chemical must be carried on board of the vehicle. The first catalyst reported to possess activity for HC-SCR under strongly oxidizing conditions was Cu-ZSM-5 (highly copper exchanged ZSM-5) [14]. Later also Pt-based catalysts have been found to be active for this reaction [15].

Many fundamental and more applied works have been devoted to understand the basic mechanism of HC-SCR [16] and to develop better catalysts. However, despite all these efforts, HC-SCR does not yet fulfill the basic requirements for its practical applicability in automotive DeNOx.

In fact, most of catalysts suitable for HC-SCR show a very narrow temperature window where a useful NO_x reduction can be obtained [17]. Generally, the HC-SCR process shows a maximum in DeNOx. On Pt-based catalyst, the maximum in DeNOx is reached at $\approx 230°C$, whereas with Cu-ZMS-5 this maximum is less pronounced and is situated at $\approx 350°C$. The low selectivity of the catalyst requires a high excess of reducing agent, thus resulting in a considerable fuel penalty. Only a small fraction (typically 1/25) of the reducing agent is used for the reduction of NO_x, whereas the main fraction is burnt with oxygen forming CO, CO_2 and water. Moreover, it has been observed that on Pt-based catalysts the major fraction of NO is reduced only to undesired N_2O. Due to the facts reported above, only a moderate removal of NO_x may be obtained in a typical test cycle, typically 20% to 40%.

Summing up all these disadvantages, the HC-SCR process is not suitable for the NO_x abatement in vehicles equipped with diesel engines. Only if much more selective and stable catalysts become available, this process should be considered again for an automotive application.

1.3.2   NSR (NO_x Storage and Reduction)

This process is based on Pt- or Ir-based catalysts on γ-Al_2O_3 as support [18-21]. Moreover, metal oxides with basic properties are added to the support (e.g. barium oxide, lanthanum oxide) as adsorbing sites for NO_x. The process requires alternating lean and rich operating periods of the engine. During the lean period, the nitrogen oxides will be adsorbed in the form of barium or lanthanum nitrates. In typical diesel exhaust, the nitrogen oxides are mainly composed of NO. The adsorption of NO includes the following two steps:

$$2 \, NO \, + \, O_2 \, \rightarrow \, 2 \, NO_2 \qquad\qquad \text{(on the Pt sites)}$$

$$BaO \, + \, 3 \, NO_2 \, \rightarrow \, Ba(NO_3)_2 \, + \, NO \qquad\qquad \text{(on the BaO sites)}$$

The adsorption of NO_x will gradually consume the basic storage sites of the NSR catalyst. The equilibrium adsorption/desorption will be reached and the NO_x abatement is no longer feasible without regenerating the adsorbing material. This is accomplished by switching to rich operation of the engine for a short period. During the regeneration, the nitrates are reduced to nitrogen by reaction with the hydrocarbons contained in the exhaust. The ratio of lean to rich operating periods is typically of the order of 10 to 100, the duration of one cycle being typically one minute. The realization of the rich operating period can be achieved with both in-cylinder and after-combustion measures [19].

The NSR process is interesting because normal fuel may be used as the reducing agent for the nitrates. Alternating lean and rich periods implies fuel savings in comparison to the HC-SCR process. However, the main problem of the NSR process is the poisoning of the catalyst due to the formation of stable sulfates on the adsorbing sites. The decomposition of these sulfates requires temperatures as high as 600-650°C [21] and reducing (rich) conditions. Such a reducing period will considerably increase the average fuel consumption and can also lead to thermal degradation of the adsorption properties of the catalyst (i.e. formation of barium or lanthanum aluminate species).

The NSR catalyst is presently considered in Europe to be the favorite candidate for passenger cars driven by lean gasoline or diesel engines. The application of the NSR technology calls for a very low sulfur fuel (< 5 ppm S).

1.3.3   Plasma techniques

Plasma techniques for pollution control have been intensively investigated using dielectric barrier discharge reactors [22-25] and corona discharge reactors [26]. Using discharge reactors, the main reaction is the dissociation of oxygen leading to oxidizing radicals. This is due to the formation of electric field strengths which are optimal for the dissociation of oxygen [23] but insufficient for breaking up the triple bond of N_2. The

O-radicals formed will therefore oxidize NO and not reduce it. The main products of such reactions are NO_2 and nitric acid (HNO_3).

High NO_x removals can be obtained combining plasma techniques with other DeNOx technologies, i.e. SCR [27,28]. The advantage of using plasma techniques relies in the formation of NO_2 - a useful intermediate to accelerate other important reactions used in aftertreatment, especially Selective Catalytic Reduction (SCR) [29] and direct soot oxidation [30].

The main disadvantage of the plasma techniques is the high electric power requirement. Hammer et al. [23] have reported specific energy consumption of the order of 5-20 kWh/Kg NO_x (as NO_2). However, NO_2 is presently produced more easily and without additional energy input by strong oxidizing catalysts based on Pt-metals. Only if the energy efficiency of non-thermal plasma reactors could be significantly enhanced, they might have a chance to replace the simpler oxidation catalysts.

1.3.4 SCR (Selective Catalytic Reduction)

The Selective Catalytic Reduction (SCR) process was introduced in the seventies in Japan for reducing the NO_x emissions from the lean exhaust of stationary plants. Since then, SCR has gained wide acceptance as being the most effective technology for deep NO_x removal from lean exhaust of stationary plants (power plants, industrial boilers, process heaters, gas turbines, incinerators) [31-33].

The Selective Catalytic Reduction, using urea as reducing agent, is presently considered the most promising technique for the removal of nitrogen oxides from the exhaust of heavy-duty diesel vehicles, e.g. trucks [34]. Very high conversions of NO_x may be obtained and the reducing agent is consumed very selectively for the reduction of NO_x. In automotive applications, urea is preferred to ammonia as reducing agent for toxicological and safety reasons [35]. Urea is a solid storage compound of ammonia which is actually involved in the reduction of NO_x. In typical exhaust, the nitrogen oxides are

mainly composed of NO (> 90%), so the SCR catalyst favors the conversion of NO and NH_3 into nitrogen and water.

The SCR catalysts exhibit optimum activity and selectivity for SCR in the temperature range 300-400°C. The classical commercial SCR catalysts for stationary applications are extruded catalysts of TiO_2-WO_3-V_2O_5 in monolithic configuration. The major challenges in developing catalysts for the automotive application of the urea-SCR process are the increase of the SCR activity at low temperatures and the improvement of the thermal stability for temperatures above 500°C.

Moreover, an optimized dosage strategy is required in order to avoid undesired slip of ammonia and iso-cyanic acid. A serious problem is the sensitivity of the SCR catalysts to basic compounds and to phosphorus deriving from the combustion of motor oil. However, the main disadvantage of the urea-SCR process is the need for a special reducing agent which must be carried on board of the vehicle.

1.3.5 Summary

Table 1.2 summarizes the advantages and disadvantages of the different technologies for the removal of NO_x from automotive lean exhausts. Urea SCR is considered the most promising technology for reducing NO_x from heavy duty vehicles, especially trucks. In the case of lean-burn gasoline or diesel passenger cars the requirement of an additional reducing agent (urea) is unlikely to be accepted by the consumers; moreover, the exhaust temperatures in a typical test cycle are so low that the SCR process may lead only to a modest removal of NO_x. Therefore, for passenger cars the NSR technology is probably the best choice.

Table 1.2   Comparison of the technologies for the removal of NO_x from automotive lean exhaust.

Aftertreatment technique	Advantages	Disadvantages
HC-SCR	• no additional reducing agent	• low selectivity (formation of N_2O) • low DeNOx (20-40%) • higher fuel consumption
NSR	• no additional reducing agent • high DeNOx at low temperatures	• realization of fuel-to-rich operating periods • catalyst poisoning by sulfur • higher fuel consumption
Plasma + SCR	• high DeNOx at low temperatures	• high energy requirements (i.e. higher fuel consumption) • additional tank for the reducing agent
SCR	• high selectivity • high DeNOx at high temperatures (>300°C)	• additional tank for the reducing agent • low DeNOx at low temperatures (<300°C)

Chapter 1

1.4   SCR process

1.4.1   Chemistry

In the automotive application of the SCR process, the preferred reducing agent is urea due to toxicological and safety reasons [35]. An aqueous solution of urea (32.5 wt-% urea) is usually atomized into the hot exhaust upstream of the SCR catalyst. The thermohydrolysis of urea into ammonia and carbon dioxide precedes the SCR reaction [35].

The first step is the evaporation of water from the droplets, thus leading to solid or molten urea:

$$NH_2\text{-}CO\text{-}NH_2(aqueous) \; \rightarrow \; NH_2\text{-}CO\text{-}NH_2(molten) \; + \; x\,H_2O(gas) \tag{1.1}$$
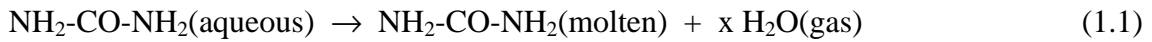
Molten urea will then heat up and decompose thermally according to:

$$NH_2\text{-}CO\text{-}NH_2(molten) \; \rightarrow \; NH_3(gas) \; + \; HNCO(gas) \qquad \Delta H^{298} = +186\,kJ \tag{1.2}$$

Equimolar amounts of ammonia and isocyanic acid are thus formed. Isocyanic acid is very stable in the gas phase, but hydrolyzes easily on many solid oxides reacting with water vapor originating from the combustion process:

$$HNCO(gas) \; + \; H_2O(gas) \; \rightarrow \; NH_3(gas) \; + \; CO_2(gas) \qquad \Delta H^{298} = -96\,kJ \tag{1.3}$$

The thermohydrolysis of urea is globally an endothermic process - the heat being provided by the hot exhaust. Kleemann et al. [36] have found that SCR catalysts are also effective in the hydrolysis of isocyanic acid (reaction 1.3). Reactions (1.1) and (1.2) may also occur in the gas phase upstream of the catalyst, whereas the hydrolysis of the isocyanic acid (reaction 1.3) proceeds mainly on the SCR catalyst itself. Catalytic tests have shown that the reaction rates of HNCO hydrolysis are much higher than the rates of the standard SCR reaction at low to medium temperatures on usual SCR catalysts. Therefore, Kleemann et al. [36] suggested that ammonia is the effective reducing agent also when urea is used.

Due to the fact that the nitrogen oxides of a diesel exhaust gas are primarily composed of NO, the main reaction occurring on the SCR catalyst is:

$$4\,NH_3 \ + \ 4\,NO \ + \ O_2 \ \rightarrow \ 4\,N_2 \ + \ 6\,H_2O \qquad\qquad \text{(standard SCR reaction)} \qquad (1.4)$$

This reaction implies a 1:1 stoichiometry for ammonia and NO and the consumption of some oxygen. The reaction of ammonia and NO in the absence of oxygen is very slow and is definitely not relevant in lean conditions:

$$4\,NH_3 \ + \ 6\,NO \ \rightarrow \ 5\,N_2 \ + \ 6\,H_2O \qquad\qquad\qquad\qquad\qquad\qquad\qquad (1.5)$$

At high temperatures N_2O can be formed in the incomplete reduction of NO with ammonia:

$$4\,NH_3 \ + \ 4\,NO \ + \ 3\,O_2 \ \rightarrow \ 4\,N_2O \ + \ 6\,H_2O \qquad\qquad\qquad\qquad\qquad (1.6)$$
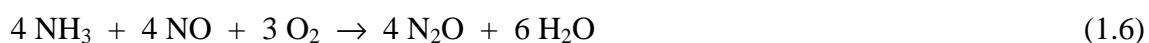
The Selective Catalytic Oxidation of ammonia (SCO) to N_2 becomes increasingly important at high temperatures:

$$4\,NH_3 \ + \ 3\,O_2 \ \rightarrow \ 2\,N_2 \ + \ 6\,H_2O \qquad\qquad\qquad\qquad\qquad\qquad\qquad (1.7)$$

Although this reaction does not lead to the formation of undesired products, it is highly undesirable due to an increase in the consumption of reducing agent.

1.4.2 Kinetics and mechanism

Many mechanistic studies of the Selective Catalytic Reduction of NO by NH_3 were carried out on vanadia based catalysts. All proposed mechanisms converge on the suggestion that the DeNOx reaction involves a strongly adsorbed NH_3 species and a gaseous or weakly adsorbed NO species, but the various proposals differ in the nature of the adsorbed reactive ammonia species and the associated reaction intermediates. Moreover, all proposed mechanisms agree on the fact that the SCR reaction takes place on the vanadia sites of the catalyst.

For the case of a complete coverage of the catalyst surface with ammonia, the reaction order has been found to be 1 for NO and 0 for NH_3 [37-43]. Recent works [44-48] report the possibility of NO reacting from a weakly adsorbed state, thus resulting in a

reaction order for NO lower than 1. Accordingly, Tufano and Turco [49] found that the reaction order for NO decreases from 1 to 0.85 when the temperature is decreased from 300 to 200°C.

Ramis et al. [50] proposed a nitrosamidic intermediate species which is formed from gaseous NO and ammonia adsorbed dissociatively on Lewis acid centers:

$$V^{+5}=O \ + \ NH_3 \ \rightarrow \ HO\text{-}V^{+4}\text{-}N^{\bullet}H_2 \tag{1.8}$$

$$HO\text{-}V^{+4}\text{-}N^{\bullet}H_2 \ + \ ^{\bullet}NO \ \rightarrow HO\text{-}V^{+4}\text{-}(NH_2)\text{-}NO \tag{1.9}$$

$$HO\text{-}V^{+4}\text{-}(NH_2)\text{-}NO \ \rightarrow \ HO\text{-}V^{+4} \ + \ N_2 \ + \ H_2O \tag{1.10}$$

$$HO\text{-}V^{+4} \ + \ 1/4 \, O_2 \ \rightarrow \ V^{+5}=O \ + \ 1/2 \, H_2O \tag{1.11}$$
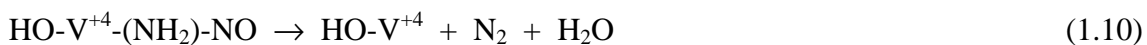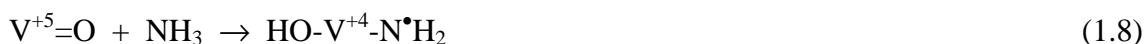
On the basis of adsorption and co-adsorption experiments of NO, NO_2 and NH_3 on TiO_2 and V_2O_5/TiO_2, Ramis et al. [50] suggest that the Lewis acid centers are essential for SCR activity, whereas ammonium ions bonded to Bronsted acid centers are not involved in the SCR reaction.

On the basis of temperature programmed in-situ FTIR and online mass spectroscopy studies, Topsoe et al. [51] proposed a mechanism which combines two cycles, involving the acid-base and the redox functions of the catalyst (Figure 1.3). The acid-base cycle involves V^{+5}-OH species, whereas the redox cycle is associated with V^{+5}=O species. In contradiction to the proposal of Ramis et al. [50], Topsoe et al. [51] suggest that ammonia involved in the SCR reaction is ammonia adsorbed on Bronsted acid centers, which are therefore essential in the SCR process.

In both mechanisms, ammonia is first oxidatively activated to a N^{-2} species by V^{+5}, which is simultaneously reduced to V^{+4}. In the mechanism proposed by Ramis et al. [50] this species is ($-N^{\bullet}H_2$), whereas according to Topsoe et al. [51] it is $(N^{\bullet}H_3)^{+}$. Traces of amide species ($-N^{\bullet}H_2$) have been actually found both in the IR spectra of adsorbed

Introduction

ammonia on several SCR catalysts and in the gas-phase during the so-called SNCR (selective non-catalytic reduction) process. Nitrosamide NH_2NO was detected by mass spectrometry among the reaction products of SCR on vanadia based catalysts [52] and traces of it were also found by IR spectroscopy at the catalyst surface [50]. Moreover, a nitrosamide species was suggested as intermediate in the mechanism of the SNCR process [53]. On the other hand, $(N^{\bullet}H_3)^+$ species seem to be less likely. Therefore, the so-called "amide-nitrosamide" mechanism proposed by Ramis et al. [50] is actually considered the most likely [44].

Acid - Base Cycle   Redox - Cycle
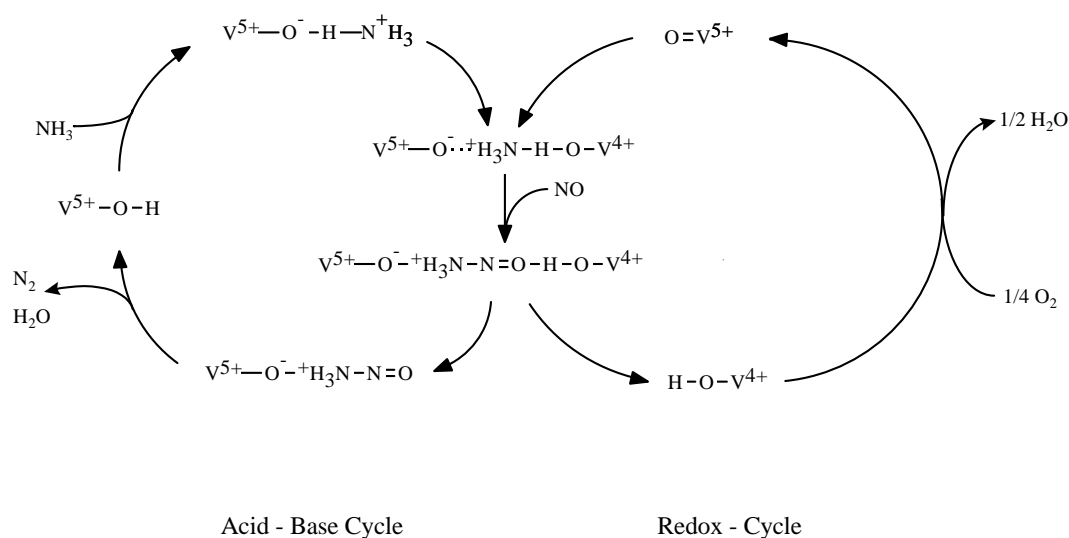
Figure 1.3   Reaction scheme proposed by Topsoe. Reprint from [51].

Summarizing, both mechanisms assume the following steps:

1. activating adsorption of ammonia on V^{+5} sites, which are simultaneously reduced to V^{+4};

2. reaction of gaseous or weakly adsorbed NO with adsorbed ammonia forming an intermediate species;

3. decomposition of the intermediate species to N_2 and H_2O;

4. re-oxidation of V^{+4} to V^{+5} by oxygen.

Chapter 1

1.5   Scope of the thesis

Typical vanadia-tungsta-titania catalysts show their optimum SCR performance at temperatures of 300-400°C. On the other hand, the automotive application of the SCR process calls for a high NO_x removal in a much wider temperature range (150-550°C). The scope of this thesis was to investigate the possibilities of widening the temperature window of the SCR reaction in order to adapt the process to the applications with mobile diesel engines.

In order to boost the intrinsic activity of the catalyst, the concentration of vanadia was increased up to 2.5 wt-%. Higher vanadium contents may be detrimental to the thermal stability of the catalyst and to the selectivity for SCR. Coated catalysts were preferred to the classical extruded catalysts in order to minimize the slip of ammonia in unsteady-state applications. The steady-state performance of the SCR catalysts were investigated both in laboratory with synthetic exhaust and at a test stand under real exhaust gas conditions. Gaseous ammonia was used as reducing agent in the laboratory tests, whereas an aqueous solution of urea (32.5 wt-% urea) was used in the investigations at the test stand.

The thermal behavior of SCR catalysts with several vanadium contents (1, 2 and 3 wt-% V_2O_5) was investigated by X-ray diffraction (XRD), X-ray photoelectron spectroscopy (XPS), Raman spectroscopy and BET surface area determination.

NO_2 was used as a key molecule for enhancing the removal of NO_x at temperatures below 300°C. The higher rates of the fast SCR reaction between the equimolar mixture of NO-NO_2 and NH_3 may enhance the NO_x removal at low temperatures. The reactions of NO, NO_2 and NH_3 in the temperature range 150-450°C were investigated in laboratory tests.

NO_2 can be produced by oxidizing part of the exhaust NO either on a Pt-based catalyst or by using plasma techniques. The effects of a pre-oxidation catalyst on the removal of NO_x were investigated both in laboratory and test stand experiments.

The potentiality of urea-SCR for reducing the NO_x emissions below the limits set by the EURO IV legislation was investigated at the diesel test stand in unsteady-state experiments simulating actual automotive operations.

1.6   References

[1]   World Energy Council and International Institute for Applied System Analysis, *Global energy perspectives and beyond*, World Energy Council, London (1995)

[2]   N. Nakicenovic and A. Grübler, *General energy perspectives*, Cambridge University Press, Cambridge (1998)

[3]   J. Hoigné, *Umweltchemie I*, ETH Zurich, Switzerland (1993)

[4]   R.A. Cox and S.A. Penkett, *Acid Deposition*, *D. Reidel Publishing Co.*, Dordrecht (1983)

[5]   H.B. Singh, *Environ. Sci. Technol.* **21** (1987), 320

[6]   CONCAWE 1989 *Trends in Motor Vehicle Emissions and Fuel Consumption Regulation*, p. 86, CONCAWE, The Hague, Netherlands, 1989

[7]   Bundesamt für Umwelt, Wald und Landschaft (BUWAL), *Schriftenreihe Umwelt: Von Menschen verursachte Luftschadstoffemissionen in der Schweiz von 1900 bis 2010*, N. 255, BUWAL, Bern, Schweiz, (1995)

[8]   P. Eastwood, *Critical Topics in Exhaust Gas Aftertreatment*, Research Studies Press, Baldock (2000)

[9]   Engineering Clean Air, *The Continuous Improvement of Diesel Engine Emission Performance*, Diesel Technology Forum, March 2001

[10]   J. Makansi, *Power* **11** (1993), 11

[11]   S.C. Wood, *Chem. Eng. Prog.* **90** (1994) I, 33

[12]   W. Kind, *Beitrag zur NO$_x$-Verminderung im Abgas von Dieselmotoren durch se-lektive katalytische Reduktion mit Harnstoff*, Fortschritts-Berichte VDI, Reihe 12, Nr. 355, VDI-Verlag, Düsseldorf (1998)

[13]   G. Emmerling and F.I. Zuther, *Motorische Verbrennung - aktuelle Probleme und moderne Lösungsansätze*, A. Leipertz (Editor), Berichte zur Energie- und Ver-fahrenstechnik, Schriftenreihe Heft 99.1, Erlangen (1999), 581

[14]   M. Iwamoto and H. Hamada, *Catal. Today* **10** (1991), 57

[15]   M. Shelef, *Chem. Rev.* **95** (1995), 209

[16]   D.K. Captain and M.D. Amiridis, *J. Catal.* **184** (1999), 377

[17]   T. Wahl, E. Jacob and W. Weisweiler, *MTZ* **57** (1996), 505

[18]   W. Weisweiler, *Möglichkeiten der NO$_x$-Entfernung aus Abgasen von Diesel- und Magermotoren*, 3. Dresdener Motorenkolloquium, Mai 20-21, 1999, p. 60

[19]   T. Cartus, G. Holy et al., *Integration of the NO$_x$-adsorber technology in future gasoline and diesel engine concepts*, 19th International Vienna Motor Symposium, May 7-8, 1998, p. 343

[20]   M. Krämer, J. Abthoff et al., *Chancen von Abgasreinigunskonzepten für den PKW-Dieselmotor mit schwefelfreiem Kraftstoff*, 19th International Vienna Motor Symposium, May 7-8, 1988, p. 247

[21]   S. Brandt, U. Dahle et al., *Entwicklungsforschritte bei NO$_x$-Adsorber-katalysatoren für magerbetriebene Ottomotoren*, 3. Stuttgarter Symposium, 23-25 Februar 1999, p. 82

[22]   S. Bröer, *Plasmainduzierte Entstickung dieselmotorischer Abgase - Der Einfluss gasförmiger Additive sowie die Kombination mit katalytischen und reaktiven Ma-terialen*, Thesis TU Munich (1998)

[23] T. Hammer and T. Zens, *Reinigung von Pkw-Dieselabgasen durch plasma-gestützte selektive katalytische Reduktion*, Berichte zur Energie- und Ver-fahrenstechnik, Heft 99.1 (1999), p. 599

[24] T. Hammer and S. Bröer, *SAE Paper* No. 982428 (1998)

[25] S. Müller, J. Conrads and W. Best, *Dieselabgasreinigung mit einem Plasmaver-fahren*, 3. Dresdener Motorenkolloquium, Mai 20-21, 1999, p. 124

[26] B.M. Penetrante and S.E. Chultheis, *Non-thermal Plasma Techniques for Pollu-tion Control*, NATO Advanced Research Workshop at Cambridge University, September 21-25, 1992, NATO ASI Series G, Vol. 34

[27] S. Bröer and T. Hammer, *Appl. Catal. B* **28** (2001), 101

[28] M. Kim, K. Takashima, S. Katasura and A. Mizuno, *J. Phys. D. Appl. Phys.* **34** (2001), 604

[29] G. Tuenter, W. Leeuwen and L. Snepvangers, *Ind. Eng. Chem. Prod. Res. Dev.* **25** (1986), 633

[30] S.J. Jelles, R.R. Krul, M. Makkee and J.A. Moulijn, *Catal. Today* **53** (1999), 623

[31] P. Forzatti and L. Lietti, *Heter. Chem. Rev.* **3** (1996), 33

[32] H. Bosch and F. Janssen, *Catal. Today* **2** (1998), 369

[33] R.M. Heck and R.J. Farrauto*, Catalytic Air Pollution Control: Commercial Tech-nology*, Engelhard Corporation Research and Development, New York, USA (1995)

[34] M. Koebel, M. Elsener and M. Kleemann, *Catal. Today* **59** (2000), 335

[35] B. Maurer, E. Jacob and W. Weisweiler, *MTZ* **60** (1999), 308

[36] M. Kleemann, M. Elsener, M. Koebel and A. Wokaun, *Ind. Eng. Chem. Res.* **39** (2000), 4120

Chapter 1

[37] J. Svachula, L.J. Alemany, N. Ferlazzo, P. Forzatti, E. Tronconi and F. Bregani, *Ind. Eng. Chem. Res.* **32** (1993), 826

[38] S.N. Orlik, V.A. Ostapyuk and M.G. Martsenyuk-Kukharuk, *Kinet. Katal.* **36** (1995), 284

[39] M. Inomata, A. Miyamoto and Y. Murakomi, *J. Catal.* **62** (1980), 140

[40] W.C. Wong and K. Nobe, *Ind. Eng. Chem. Prod. Res. Dev.* **23** (1984), 564

[41] I. Nam, J.W. Eldridge and I.R. Kittrell, *Ind. Eng. Chem. Prod. Res. Dev.* **25** (1986), 1186

[42] L.J. Pinoy and L.H. Hosten, *Catal. Today* **17** (1993), 151

[43] J. Marangozis, *Ind. Eng. Chem. Res.* **31** (1992), 387

[44] G. Busca, L. Lietti, G. Ramis and F. Berti, *Appl. Catal. B* **18** (1998), 1

[45] M. Koebel and M. Elsener, *Chem. Eng. Sci.* **53** (1998), 657

[46] J.A. Odriozola, H. Heinemann, G.A. Somorjai, J.F. Garcia de la Banda and P. Pereira, *J. Catal.* **119** (1989), 71

[47] R.J. Willey, H. Lai and J.B. Peri, *J. Catal.* **130** (1991), 319

[48] R. Willi, B. Roduit, R.A. Köppel, A. Wokaun and A. Baiker, *Chem. Eng. Sci* **51** (1996), 2897

[49] V. Tufano and M. Turco, *Appl. Catal. B* **2** (1993), 9

[50] G. Ramis, G. Busca, F. Bregani and P. Forzatti, *Appl. Catal.* **64** (1990), 259

[51] N.Y Topsoe, J.A. Dumesic and H. Topsoe, *J. Catal.* **151** (1995), 241

[52] M. Farber and S.P. Harris, *J. Phys. Chem.* **88** (1994), 680

[53] M.N. Hughes, T.D.B. Morgan and G. Stedman, *J. Chem. Soc. B* (1968), 344

<div align="right">

2

</div>

<div align="right">

Experimental

</div>

2.1   Experimental setup

2.1.1   Description of the apparatus for the laboratory tests

The experimental setup for the laboratory tests is shown in Figure 2.1. The composition of the base feed gas was adapted to a typical diesel exhaust gas, containing 10% O_2 and 5% H_2O with balance N_2. CO_2 was found to have no influence on the SCR process. Consequently, it was omitted in the test gas mixture, as it might disturb the measurements. NH_3 was used as reducing agent. The feed gas was obtained by diluting gas mixtures of higher concentrations (Carbagas). The composition and purity of the gas mixtures are reported in Table 2.1. The flow rates were controlled by mass flow controllers (Brooks 5850S). Liquid water was dosed by means of a liquid mass flow controller (Brooks 5881) through a capillary tube into an electrically heated evaporator. The mass flow controllers were regulated from a computer using a self implemented program (Microsoft QBasic) with access to AD cards. All lines of the experimental apparatus were heated to 150°C by heating tapes.

A partial stream of about 250 l_N/h of the gas leaving the reactor was extracted by a heated membrane-pump, filtered by a heated PTFE-membrane-filter and delivered to

the gas-cell of the FTIR spectrometer. The gas cell (for details see paragraph 2.2) was thermostated at 175°C.
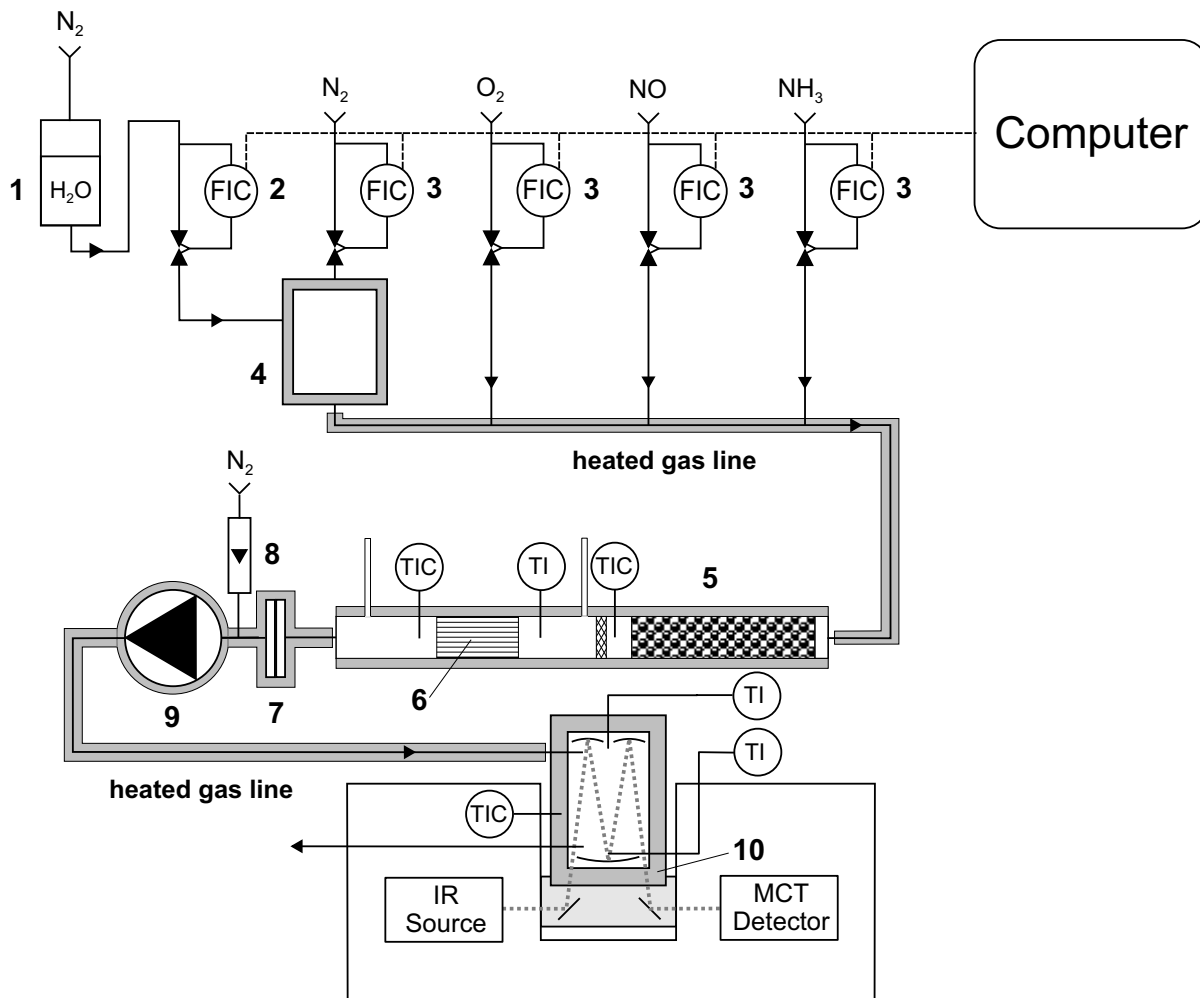
Figure 2.1   Experimental setup: 1, water reservoir; 2, liquid mass flow controller; 3, mass flow controller; 4, water evaporator; 5, reactor; 6, catalyst sample; 7, filter; 8, flow meter; 9, diaphragm pump; 10, gas cell

2.1.2   Reactor for testing monolithic catalysts

A glass reactor was used to test the monolithic catalysts (Figure 2.1). It was composed of a glass tube with an inner diameter of 28 mm. The reactor consisted of a pre-heating zone filled with steatite pearls and of a second zone for the monolithic catalyst. These

zones were heated independently by two separate heating tapes connected to individual temperature controllers. The temperature control was based on two thermocouples placed in front of the pre-heating zone and after the catalyst, respectively. A third thermocouple was placed just in front of the catalyst entrance in order to measure the temperature of the gas feed.

Table 2.1   Gas mixtures used in the preparation of the model gas for the laboratory tests.

Species	Concentration	Purity	Concentration in the test gas mixture
N_2	100%	99.999%	carrier gas
O_2	100%	99.5%	0-10%
NO	5% in N_2	99.9%	0-1500 ppm
NO_2	1% in synthetic air	99%	0-1000 ppm
NH_3	5% in N_2	99.999%	0-1500 ppm
N_2O	200 ppm in N_2	99.999%	0-200 ppm

2.1.3   Micro-reactor for testing powdered catalysts

Figure 2.2 depicts the micro-reactor used for determining the intrinsic kinetics of powdered catalyst samples. The reactor consisted of a stainless steel tube with an inner diameter of 6.5 mm. The reactor was placed in the experimental apparatus reported in Figure 2.1. In the micro-reactor, the catalyst was placed between two layers (3-4 mm) of quartz wool. A thermocouple was inserted into the quartz wool for measuring the temperature at the catalyst outlet. The preheating zone consisted of a stainless steel tube in spiral configuration and with a length of ≈70 cm. The micro-reactor was placed into a stainless steel cylinder heated by a heating tape. A valve system allowed the gas to by-

Experimental

pass the reactor for measuring the composition of the gas feed. A blank experiment confirmed that no reaction between NO and NH_3 occurs in the void space of the reactor.
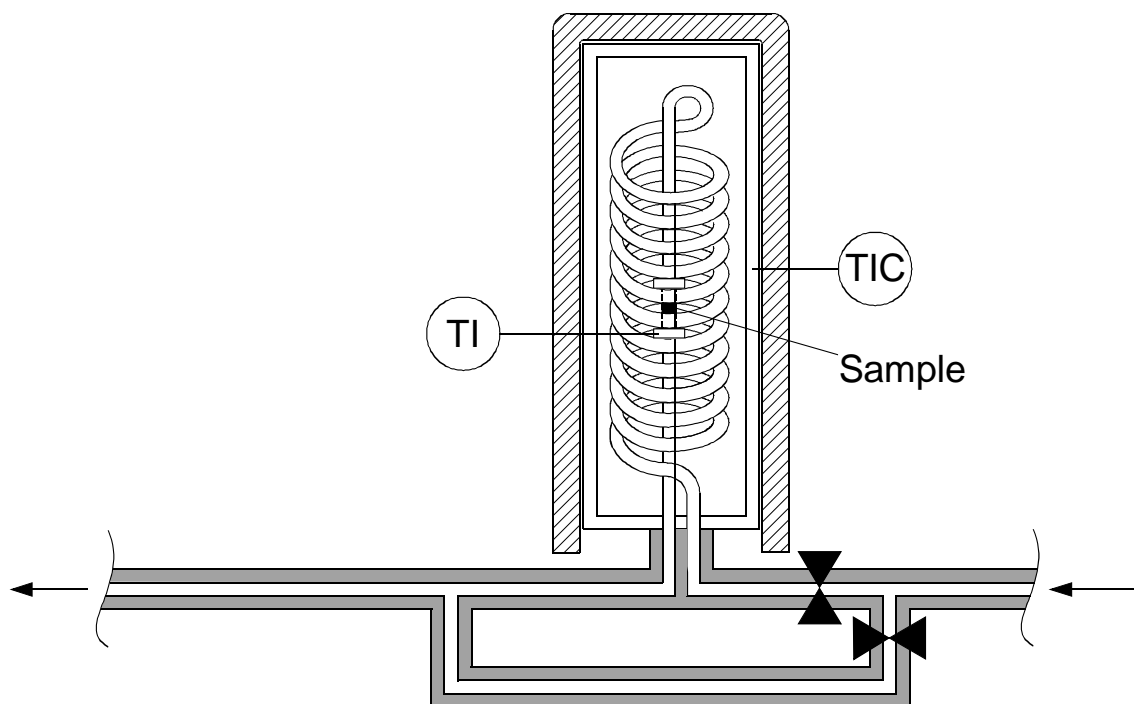
Figure 2.2   Scheme of the micro-reactor used for testing the powdered catalyst samples.

2.2   FTIR gas analysis

An FTIR spectrometer (Nicolet Magna 560 with MTC detector) was used to quantify the concentrations of the gas species. The FTIR spectrometer allows the fast and simultaneous measurement of the concentrations of several species. A minor drawback of the FTIR analysis is the interference of the adsorbance bands of NO and NO_2 with the ones of water, thus limiting the lower limit of detection in the measurements of NO_x.

A multi-path White cell was used for the FTIR analysis. The cell could be heated up to 200°C. The path length could be varied in the range 0.4-2.8 m (cell length = 10 cm) according to the number of reflections. A fixed path length of 2 m was used in the experi-

ments. The volume of the gas cell was 275 cm^3. Considering a typical flow of 350 l$_N$/h the residence time of the gas in the cell was about 2-4 seconds. The sequence of the measurements was limited by the scanning rate of the FTIR spectrometer and was between 5 and 10 seconds for the data processing (8 scans per spectrum at a resolution of 0.5 cm^{-1}).

The quantification of the various gaseous species was carried out with the software QuantPad Version 2.1. This software is based on the CLS process (classic least square fit) and allows to correct the spectral adsorbance in the region of non linearity. Table 2.2 reports the ranges and the limits of detection of the various species. CO_2 was omitted from the test gas mixture as it interferes with N_2O, thus disturbing the measurement of this gas.

Table 2.2 Detection limits of various components in dry and wet model gas.

Species	Detection Range [cm^{-1}]	Detection Limits without water	Detection Limits with 5% vol. water
NO	1850-1940	3 ppm	5 ppm
NO_2	1634-1678	1 ppm	3 ppm
N_2O	2134-2266	0.5 ppm	0.5 ppm
NH_3	831-1147	1 ppm	1 ppm
HNO_3	836-917	10 ppm	10 ppm
H_2O	2953-3017	300 ppm	---

2.3 Data evaluation

2.3.1 Space velocity

The space velocity is an important design parameter for chemical reactors and represents the number of reactor volumes of feed, measured at normal conditions, processed per unit of time [1]. Usually, the gas hourly space velocity (GHSV) is used and it is defined as:

$$\text{GHSV} = \frac{V_N^*}{V_C} \qquad (2.1)$$

V_N^* = volumetric gas flow in normal conditions [cm_N^3/h]

V_C = catalyst volume [cm^3]

The volumetric activities of two catalysts can be compared considering the conversions obtained at the same value of GHSV. A GHSV representative of typical operative conditions with automotive diesel exhaust is 40000-60000 h^{-1}. Accordingly, in the laboratory tests the performance of the SCR catalysts were investigated at GHSV=52000 h^{-1}.

2.3.2 NO$_x$ conversion

The NO$_x$ conversion (DeNOx) is defined as follows:

$$\text{DeNOx} = \frac{NO_{x,IN} - NO_{x,OUT}}{NO_{x,IN}} \cdot 100 \qquad (2.2)$$

The definition of DeNOx is based on the conversion of $NO_x = NO + NO_2$. The main product of the NO$_x$ reduction is generally N_2, a high DeNOx indicating a high SCR activity of the catalyst. If the selectivity for SCR is low, the reduction of NO$_x$ is not complete and nitrous oxide may be formed (e.g. reaction 1.6). However, the formation

of nitrous oxide consumes NO, thus enhancing the DeNOx according to equation 2.2. Therefore, in the case of low SCR selectivity, a high DeNOx does not correspond to a high SCR activity of the catalyst (see chapter 7).

2.3.3 Stoichiometric ratio α

The stoichiometric ratio α represents the ratio between the moles of nitrogen added as reducing agent and the moles of NO_x contained in the feed. A value of α =1 means that, in case of a high selectivity for SCR, the amount of reducing agent added to the feed allows the total removal of NO_x. If ammonia is used as reducing agent, then α is evaluated as follows:

$$\alpha = \frac{NH_{3,IN}}{NO_{x,IN}}$$
(2.3)

For automotive applications, urea is used as the reducing agent. In this case α is evaluated as follows:

$$\alpha = \frac{2 \cdot urea_{IN}}{NO_{x,IN}}$$
(2.4)

2.3.4 Curves of DeNOx vs. NH₃-slip

The practical application of the SCR process calls for a high NO_x removal and simultaneously a low slip of ammonia (i.e. 10 ppm). The practically interesting values of DeNOx at 10 ppm NH₃-slip can be read from the curves of DeNOx vs. NH₃-slip. These curves are obtained by increasing stepwise the ammonia concentration at a constant flow of 1000 ppm NO and at a fixed operative temperature.

Figure 2.3 reports the curves of DeNOx vs. NH₃-slip for the PSI catalyst K51 in the temperature range 200-450°C and at GHSV=52000 h^{-1}, typical for automotive applications. It can be seen that the SCR process has a high DeNOx potential at temperatures above 300°C.
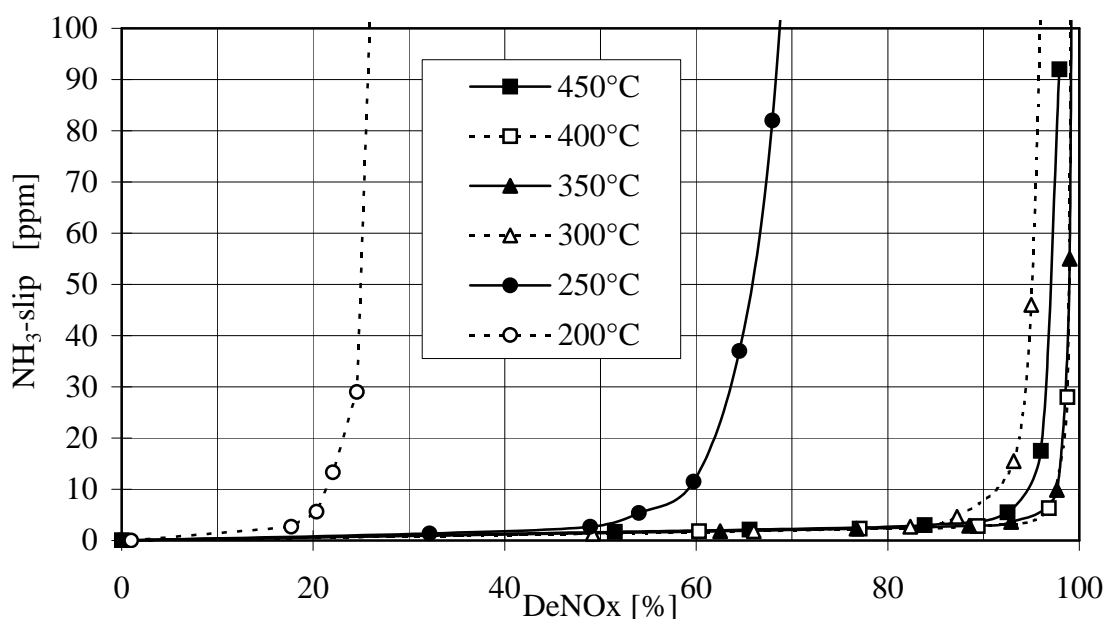
Figure 2.3   Curves of DeNOx vs. NH$_3$-slip for the reference PSI catalyst K51. GHSV=52000 h^{-1}.

The NO$_x$ conversion at 100 ppm of NH$_3$-slip is the "maximum DeNOx" and mainly depends on the intrinsic activity of the catalyst. Depending on the slope of the curves of DeNOx vs. NH$_3$-slip, different values of DeNOx at 10 ppm NH$_3$-slip may correspond to the same value of maximum DeNOx at a fixed operative temperature: the steeper the curve, the higher the value of DeNOx at 10 ppm NH$_3$-slip. Kleemann et al. [2,3] have found that the surface acidity of the catalyst influences the slope of the curves of DeNOx vs. NH$_3$-slip: the higher the surface acidity, the steeper the curve.

2.3.5   Investigations with the micro-reactor

The investigations with the micro-reactor were carried out with powdered catalyst samples showing particle diameters of 160-200 µm. The amount of catalyst used in these experiments was 150-200 mg. The total gas flow rate was 150 l$_N$/h, thus resulting in gas hourly space velocities of about 500000 h^{-1}. At these conditions the temperature increase measured over the catalyst bed was 2 K. The pressure drops on the catalyst bed

(Δp_{bed}), depending on the temperature and the flow of the exhaust, were always below 0.3 bar.

In the evaluation of the results, the average pressure in the catalyst bed was assumed to be:

$$p_{av} = p_{atm} + \Delta p_{bed} / 2 \tag{2.5}$$

Kinetic parameters (k_m) were evaluated assuming a first order law with respect to the concentration of NO_x:

$$k_m = -\frac{V^*}{W} \cdot \ln\left(1 - \frac{DeNOx}{100}\right) \tag{2.6}$$

k_m = kinetic parameter/constant (referred to the catalyst mass) [cm^3/g·s]

V* = volumetric gas flow at the actual T and p [cm^3/s]

W = catalyst mass [g]

DeNOx = NO_x conversion [%]

The values of k_m were found to be useful parameters for comparing the rates of the various reactions between NO, NO_2 and NH_3 occurring on the SCR catalyst. In the case of the standard SCR reaction (1.4), the values of k_m correspond to the kinetic constants, as the kinetic law of this reaction was found to be first order with respect to the concentration of NO [4].

2.4   References

[1]   O. Levenspiel, *Chemical Reaction Engineering*, John Wiley & Sons Inc. (1972)

[2]   M. Kleemann, *Beschichtung von Cordierit-Wabenkörpern für die selektive Katalytische Reduktion von Stickodiden*, Thesis ETH N. 14301, Zurich (1999)

Experimental

[3]   M. Kleemann, M. Elsener, M. Koebel and A. Wokaun, *Appl. Catal. B* **27** (2000), 231

[4]   M. Koebel and M. Elsener, *Chem. Eng. Sci.* **53** (1998) 4, 657

3

Catalyst preparation

3.1   Introduction

Many supported metal oxides are reported to be active for the SCR reaction. In these investigations, TiO_2 anatase is usually used as catalyst support. V_2O_5, WO_3, MoO_3, Cr_2O_3, Fe_2O_3, Mn_2O_3, Pt were investigated individually or in combination [1]. The metal oxide showing the highest activity and selectivity for SCR was V_2O_5. The drawback of Fe_2O_3, WO_3, MoO_3 and Mn_2O_3 is the low activity and selectivity for the SCR reaction. Recently, Willi et al. [2] reported on Cr_2O_3/TiO_2 catalysts with higher SCR activity than V_2O_5/TiO_2 catalysts at low temperatures. However, the low resistance to sulfur poisoning is a major drawback of the Cr_2O_3/TiO_2 catalysts.

At low temperatures, the Pt-based catalysts show the highest activity. However, the selectivity of these catalysts begins to decrease above 250°C, leading to the reduction of NO_x to highly undesirable N_2O. Moreover, above 350°C a relevant amount of the reducing agent is oxidized to NO.

The commercial SCR catalysts are made from homogeneous mixtures of titanium dioxide, tungsten trioxide (or molybdenum trioxide) and vanadium pentoxide [3-6]. TiO_2 in the anatase form is used as a support of high surface area for the active components. Vanadia is responsible for the SCR activity but may also cause the (undesired) oxidation of SO_2 to SO_3 (SO_2 derives from the combustion of the sulfur impurities of the fuel).

Therefore, the vanadia content should be kept as low as possible. Its concentration is typically below 1 wt-% in high sulfur applications. WO_3 or MoO_3 are added in larger amounts (10 and 6 wt-% for WO_3 and MoO_3, respectively). They act as "chemical" and "structural" promoters by widening the temperature window of the SCR reaction, limiting the oxidation of SO_2 and improving the mechanical, structural and morphological properties of the catalysts. Moreover, WO_3 and MoO_3 increase the thermal stability of the SCR catalyst. Silico-aluminates and glass fibers are added to improve the mechanical strength in the case of extruded catalysts. The commercial SCR catalysts are employed in the form of honeycomb monoliths or plates because of the following main advantages over the packed bed arrangement:

1. lower pressure drops by two or three orders of magnitude;

2. superior attrition resistance and lower tendency to plugging by fly ash;

3. comparable geometric surface area per unit volume of catalytic reactor.

The surface structure of V_2O_5/TiO_2 catalysts has a pronounced effect on the catalytic activity and selectivity for the SCR reaction. Raman investigations [7] have shown that, at vanadia loadings below the monolayer, the vanadia is present on the surface of the support as monomeric vanadyl and polymeric vanadate species. As the loading of vanadia is increased above the dispersive capacity of the support, crystallites of V_2O_5 form at the expense of the polymeric species. Analysis of the turnover frequency for NO conversion in the SCR reaction indicated that the polymeric species are approximately ten times more active than the monomeric species. Cristalline vanadia was found to have a low selectivity for the SCR reaction, leading to more direct oxidation of ammonia to nitrogen and to the formation of nitrous oxide [8-10].

3.2   Preparation of monolithic and powdered SCR catalysts

The inert of monoliths were coated with active mass consisting of TiO_2-WO_3-V_2O_5. Both ceramic (cordierite) and metal monolithic carriers were used for the preparation of the catalysts (Table 3.1).

The coating implies dipping of the monolith into a suspension of the active mass. A binder was used in order to increase the mechanical stability of the coating mass and its adherence to the support. In order to coat the desired amount of active mass, the dipping step had to be repeated several times. After each dipping step the catalyst was dried in hot air (80°C). Finally, the catalyst was calcined at 550°C for 50 hours in air.

For the preparation of the powdered samples, the suspension was poured on a watch glass and the resulting film was successively dried. The dried layer was then scraped off the watch glass and calcined at 550°C as reported above. The powder was crushed in a mortar and sieved in order to get particles in the 160-200 μm range.

The composition of the active mass was determined by ICP (inductively coupled plasma) analysis after decomposing the catalyst in a $KHSO_4$ melt. The active mass coated on catalysts K51 and M11 contained 3.1 wt-% V_2O_5, 8 wt-% WO_3 and TiO_2.

3.3   Impregnation technique

The impregnation technique is decisive for the type of anchorage of the vanadia on the support surface, influencing the dispersion of the V_2O_5 on the support and the formation of polyvanadate surface species. The formation of three-dimensional vanadia species on the support surface should be avoided [8-10]. The duration of the impregnation procedure should guarantee an even distribution of V_2O_5 over the whole layer. This is especially important for the catalyst activity at low temperatures where the whole layer thickness is used for the SCR reaction.

Table 3.1   Specifications of the monolithic SCR catalysts used in the laboratory experiments.

Reference catalysts	K51	M11
support material	cordierite (2 MgO· 2 Al$_2$O$_3$·5 SiO$_2$)	heat resistant steel
cell density	400 cpsi	600 cpsi
cell geometry	square	approximately triangular
pitch* *without coating	1.32 mm	1.05 mm
wall thickness* *without coating	180 μm	30 μm
specific surface* *without coating	2400 m^2/m^3	3400 m^2/m^3
catalyst geometry	parallelepiped	cylinder
catalyst length	30 mm	21 mm
catalyst volume	6.8 cm^3	7.3 cm^3
frontal dimensions	17.2 × 13.2 mm	diameter = 21 mm
coating thickness	≈50 μm	≈50 μm
active mass (coated)	1.4 g (200 g/l)	1.4 g (200 g/l)

Chapter 3

A high dispersion of V_2O_5 on the support surface can be realized by equilibrium impregnation. The principle of this impregnation technique is based on ion exchange between support oxide and precursor ions. In an aqueous solution containing the precursor ions, the surface of the support oxide is positively or negatively charged depending on the pH value. Consequently, the precursor ions can interact electrically with the charged support surface. Important parameters are the iso-electric point of the support oxide, the pH value of the solution and the nature of the precursor ions. If the pH of the solution is lower than the iso-electric point of the support oxide, the surface of the support oxide has a positive charge. If the precursor ions present in the solution are negatively charged, a strong interaction will occur between support oxide and precursor ions. On the other hand, no interaction will occur if the precursor ions present in the solution are also positively charged.

Vice versa, if the pH of the solution is higher than the iso-electric point of the support oxide, then the surface of the support oxide is negatively charged and can interact with a positively charged precursor ion.

TiO_2 anatase and WO_3 have iso-electric points of ≈ 6 and < 0.5, respectively. At pH values of 0.5-6 TiO_2 is positively charged, whereas WO_3 is negatively charged. At pH values above 6 both TiO_2 and WO_3 are negatively charged.

Ammonium vanadate (NH_4VO_3) is a very common V_2O_5 precursor. The dissolution of ammonium vanadate in an aqueous solution leads to the formation of several vanadate and polyvanadate species depending on the pH value and on the total concentration of vanadium (Figure 3.1).

At pH values below 5.5 and vanadium concentrations above 10^{-3} mol·l^{-1}, decavanadate ions $HV_{10}O_{28}^{5-}$ are formed in the aqueous solution. At these pH values the support oxide TiO_2 is positively charged and interacts with the decavanadate ions. Consequently, polyvanadate species are formed on the surface of the TiO_2 anatase. On the other hand, no interaction occurs between the decavanadate ions and the WO_3 of the support as they are both negatively charged.
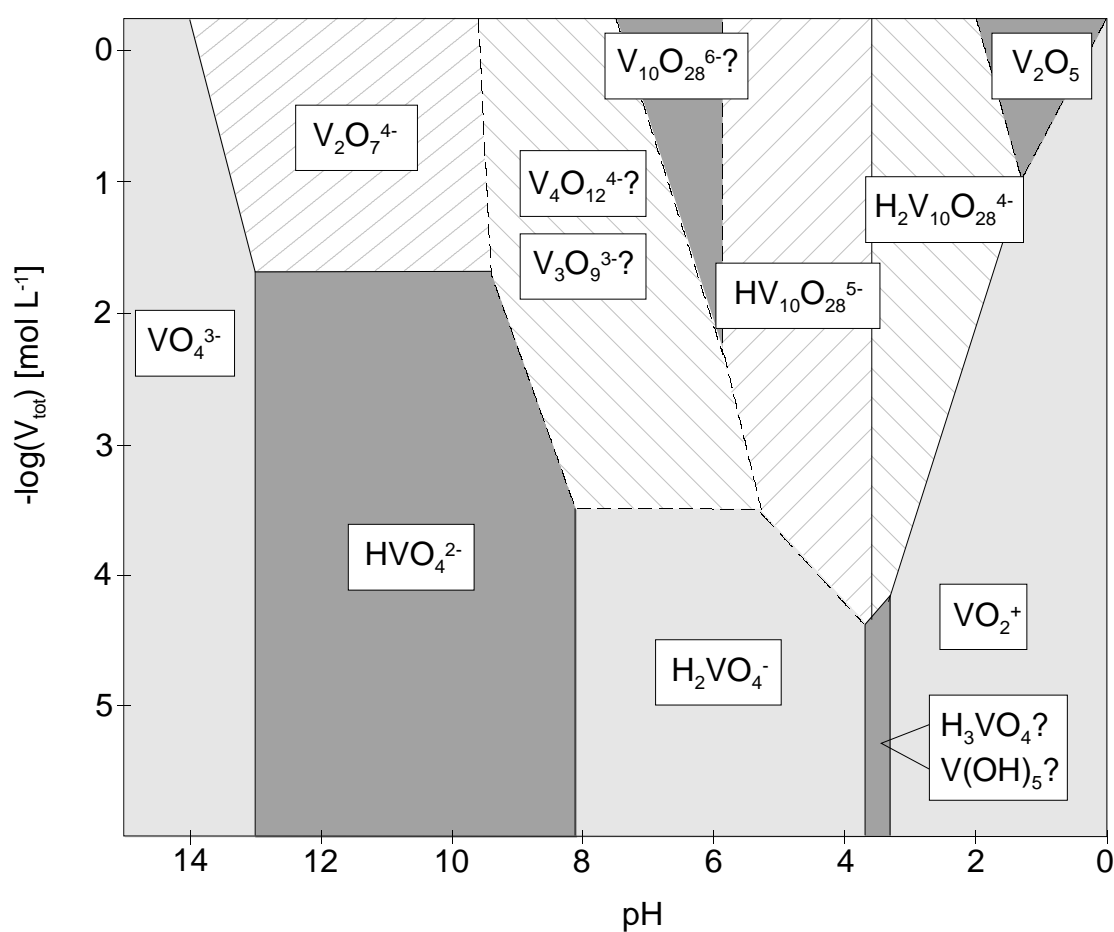
Figure 3.1   Formation of the several vanadate and polyvanadate species as a function of the pH value and of the total vanadium concentration. Reprinted from [11].

3.4   Comparison of coated and extruded catalysts

The classical commercial SCR catalysts were mainly extruded monolithic catalysts. In this case the entire wall consists of TiO_2-WO_3-V_2O_5 with admixtures of binders and glass fibers to increase the mechanical properties. On the other hand, coated catalysts have only a layer of active mass coated on the carrier, thus containing less active mass per volume of the monolith.

Koebel et al. [12] have modeled the performance of SCR catalysts for various operative conditions. Fig. 3.2 shows the relative concentration profiles of NO or NH_3 (α=1) in the wall of a 200 cpsi extruded catalyst at 250 and 450°C.
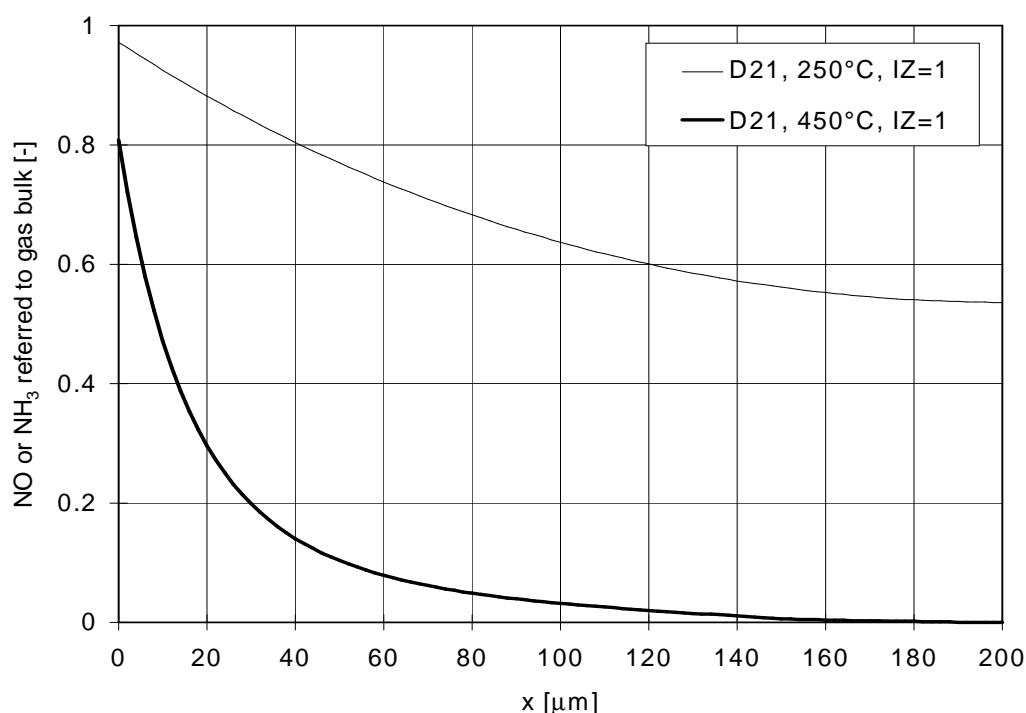
Figure 3.2   Calculated concentration profiles at 250 and 450°C in the catalyst wall of a 200 cpsi extruded catalyst at GHSV = 25000 h^{-1} and 1000 ppm each of NO and NH_3. The abscissa x indicates the depth in the monolith wall. Reprint from [13].

It is evident that the reaction takes place mainly in the top layer of the catalyst at 450°C. This is no longer true at 250°C: at this temperature even in the center of the wall, the relative concentration of NO or NH_3 still amounts to $\approx$ 0.5. At high temperatures, the deeper layers of the catalyst have almost no contribution to the SCR reaction; consequently, extruded and thinly coated catalysts will be practically equally effective. This is no longer true at low temperatures, where the deeper layers of the catalyst contribute

Catalyst preparation

to the SCR reaction. Therefore extruded catalysts will outperform coated catalysts at low temperatures [12].

Figure 3.2 shows that, due to the high reaction rates, the mass transfer resistance in the gas laminar layer at the channel wall is important at 450°C but negligible at 250°C (relative concentrations at x = 0 are ≈ 0.8 and ≈ 0.97, respectively). Therefore, an increased cell density will be effective at the higher temperatures. Moreover, high cell densities allow for lower coating thickness, thus reducing the internal mass transfer resistance. In short, increasing the cell density enhances the volumetric activity of the catalyst.

Although the coated catalysts show a lower SCR performance at low temperatures, they are probably more suitable for automotive applications due to the reduced ratio of active mass/volume, resulting in less ammonia stored [13]. Ammonia stored in the active mass is responsible for ammonia peak emissions caused by sudden increases of the engine load: the exhaust temperature will rise and this will cause the desorption of some ammonia adsorbed on the catalyst.

3.5   References

[1]   H. Bosch and F. Janssen, *Catal. Today* **2** (1988), 53

[2]   R. Willi, M. Maciejewski, U. Göbel, R.A. Koppel and A. Baiker, *J. Catal.* **166** (1997), 356

[3]   S.C. Wood, *Chem. Eng. Prog.* **90** (1994) I, 47

[4]   P. Forzatti and L. Lietti, *Heterogeneous Chem. Rev.* **3** (1996), 33

[5]   K. Kartte and H. Nonnenmaker, US Patent No. 3 279 884 (1966)

[6]   F. Nakajima, M. Tacheuci, S. Matsuda, S. Umo, T. Mari, Y. Matanche and M. Inamuri, US Patent No. 4 085 193 (1976)

[7] G.T. Went, L.J. Leu, R.R. Rosin and A.T. Bell, *J. Catal.* **134** (1992), 492

[8] U.S. Ozkan, Y. Cai and M.W. Kumthekar, *J. Catal.* **149** (1994), 390

[9] C.U.I. Odenbrand, P.L.T. Gabrielsson, J.G.M. Brandin and L.A.H. Andersson, *Appl. Catal.* **78** (1991), 109

[10] M. Kotter, H.G. Lintz, T. Turek and D.L. Trimm, *Appl. Catal.* **52** (1989), 225

[11] N.N. Greenwood and A. Earnshaw, *Chemie der Elemente*, VCH Verlag Gesellschaft, Weinheim (1990), p. 1267

[12] M. Koebel and M. Elsener, *Ind. Eng. Chem. Res.* **37** (1998), 327

[13] M. Koebel, M. Elsener and M. Kleemann, *Catal. Today* **59** (2000), 335

4

SCR with NO and NO$_2$

4.1 Introduction

Typical SCR catalysts based on TiO$_2$-WO$_3$-V$_2$O$_5$ show their optimum performance at temperatures of 300-400°C. On the other hand, the automotive application of the SCR process calls for a high NO$_x$ conversion in a much wider temperature range (150-550°C). Therefore, a new process has recently been proposed in order to increase the rate of the SCR reaction [1]. It relies on the fact that the SCR reaction will be much faster with a mixture of NO-NO$_2$ than with pure NO [2,3].

NO$_2$ is a more reactive molecule than NO. It is already known from the process of nitric acid production that NO$_2$ easily dimerizes to N$_2$O$_4$, which, in the presence of water, disproportionates into NO and HNO$_3$:

$$3 \, N_2O_4 \; + \; 2 \, H_2O \; \rightarrow \; 2NO \; + \; 4 \, HNO_3 \hspace{3cm} (4.1.a)$$

$$6 \, N^{+4} \hspace{2cm} \rightarrow \; 2 \, N^{+2} \; + \; 4 \, N^{+5} \hspace{3cm} (4.1.b)$$

Moreover, NO$_2$ is a stronger oxidizing agent than oxygen [4], dissociating easily into an O-atom and NO. The simultaneous presence of NO, NO$_2$ and NH$_3$ gives rise to an highly interesting chemistry.

This chapter reports the experiments carried out in a micro-reactor using feeds with various NO_x compositions: pure NO, an equimolar mixture of $NO + NO_2$, pure NO_2. The SCR catalyst was a powder of TiO_2-WO_3-V_2O_5 with particle size in the range 160-200 μm. It was prepared according to the recipe reported in chapter 3. The intraparticle mass transfer resistance could be neglected at temperatures below 350°C [5,6]. The feed was adapted to a typical diesel exhaust and consisted of 1000 ppm NO_x, 1000 ppm NH_3, 5% H_2O, 10% O_2, balance N_2.

The measured values of NO_x conversion were converted into kinetic parameters k_m assuming a first order rate law and applying the well known equation for a plug flow reactor:

$$k_m = -\frac{V^*}{W} \cdot \ln\left(1 - \frac{DeNOx}{100}\right) \qquad (4.2)$$

with k_m = kinetic parameter/constant (referred to the catalyst mass) [cm^3/g·s]

   V^* = gas flow at actual conditions [cm^3/s]

   W = catalyst weight [g]

   DeNOx = NO_x conversion [%]

The values of k_m have been plotted in Arrhenius plots. These values of k_m do not represent the proper kinetic constants of the considered reactions but are practically useful for a rough comparison of different reaction rates. In the following, the comparison of the different reaction rates was based on the values of k_m, because the kinetics of the various reactions between NO, NO_2 and NH_3 are not known.

4.2 Results and Discussion

4.2.1 Experiments with NH_3 and NO

Figure 4.1 reports the values of k_m resulting from experiments carried out with a feed containing NO only. At temperatures below 350°C, NO and NH_3 react in a 1:1 stoichiometry according to the standard SCR reaction:

Chapter 4

$$4\,NH_3 \;+\; 4\,NO \;+\; O_2 \;\rightarrow\; N_2 \;+\; 6\,H_2O \tag{4.3}$$

Above 350°C, traces of N_2O were detected at the catalyst outlet indicating a certain loss of selectivity for SCR. At temperatures above 350°C, the change of slope in the Arrhenius plot must be attributed to intraparticle mass transfer resistance [5,6].

Many authors [5,7-9] have found a reaction order for NO of $\approx$ 1 for the standard SCR reaction (4.3). Therefore, the values of k_m calculated using equation (4.2) represent the kinetic constants for this reaction. The values of activation energy and pre-exponential factor resulting from the regression analysis below 350°C are 85 kJ/mol and $8.35 \cdot 10^{10}$ $cm^3/(g \cdot s)$. These values are close to the ones reported in literature.
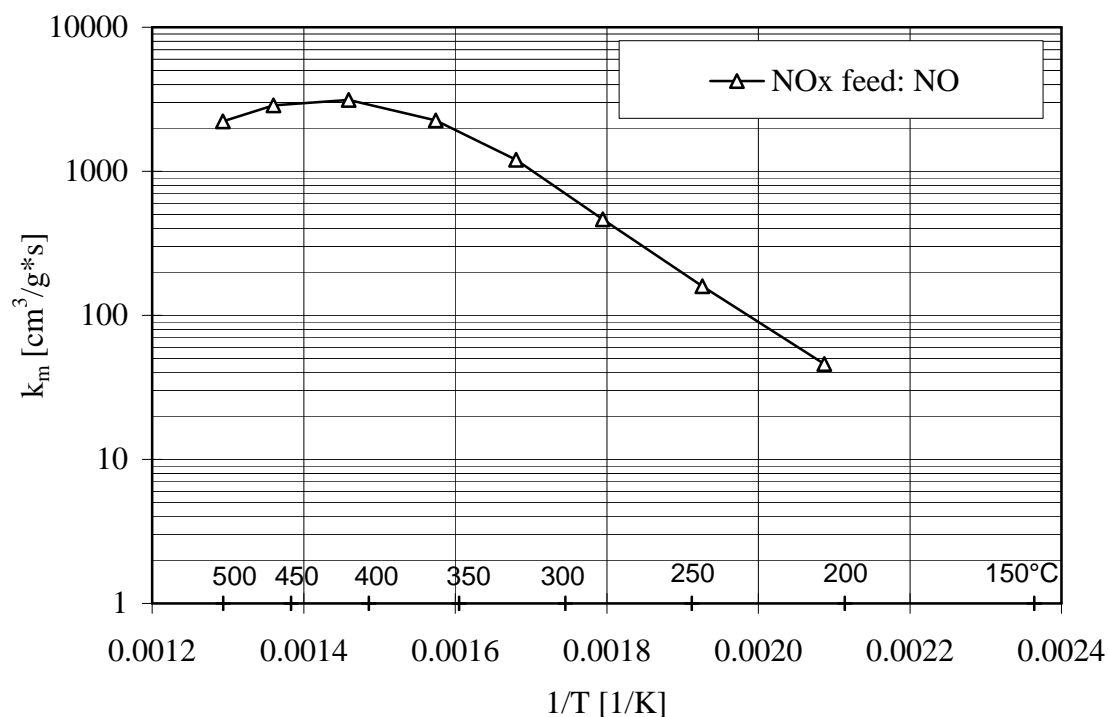
Figure 4.1 Temperature dependence of k_m. Feed: 1000 ppm NO, 1000 ppm NH_3, 5% H_2O, 10% O_2, balance N_2. GHSV=$5.0 \cdot 10^5$ h^{-1}.

4.2.2 Experiments with NH$_3$ and NO-NO$_2$

Figure 4.2 reports the values of k$_m$ resulting from experiments carried out with a feed containing an equimolar mixture of NO + NO$_2$. At temperatures below 350°C, NO and NO$_2$ were consumed in equimolar amounts. Accordingly, the amount of reacted NH$_3$ was equal to the sum of NO and NO$_2$ consumed in the process. This is in agreement with the stoichiometry of the fast SCR reaction:

$$4\,NH_3 + 2\,NO + 2\,NO_2 \rightarrow 4\,N_2 + 6\,H_2O \tag{4.4}$$

At temperatures above 350°C, the amount of NO detected at the catalyst outlet was higher than NO$_2$. This is due to the thermodynamic equilibrium NO$_2 \Leftrightarrow$ NO + 0.5 O$_2$ which shifts to the right side with increasing temperature (see paragraph 8.3.1). In analogy to the standard SCR reaction, at temperatures above 350°C the rates of the fast SCR reaction were limited by intraparticle mass transfer resistance.
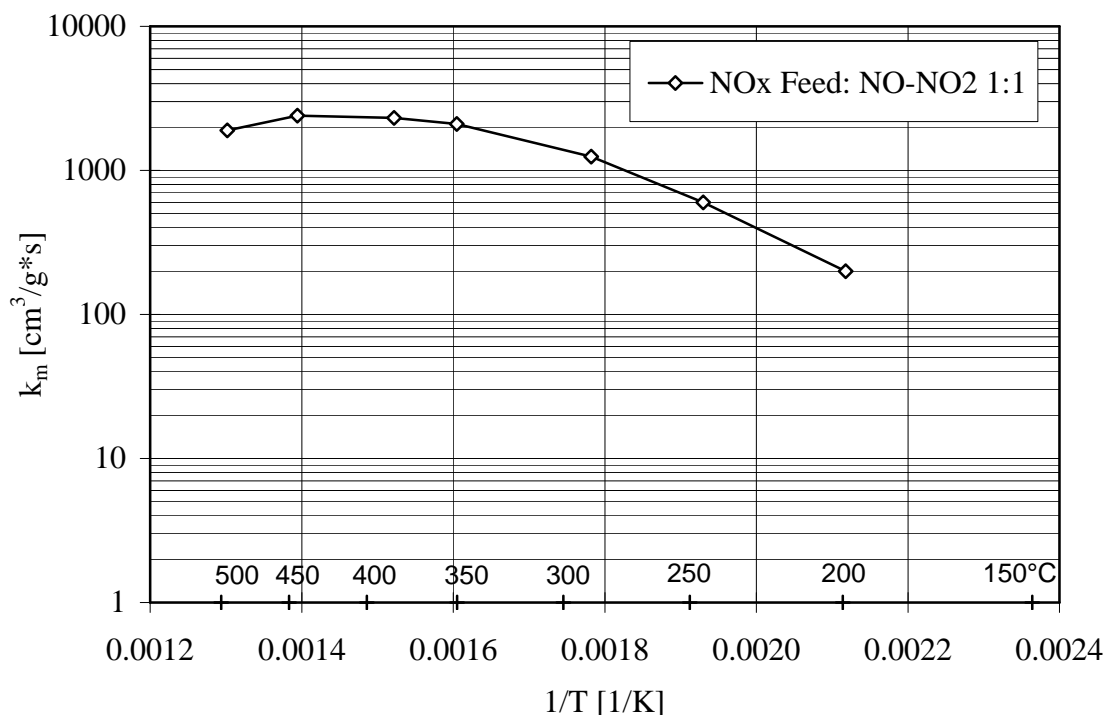
Figure 4.2 Temperature dependence of k$_m$. Feed: 500 ppm NO, 500 ppm NO$_2$, 1000 ppm NH$_3$, 5% H$_2$O, 10% O$_2$, balance N$_2$. GHSV=5.0·10^5 h^{-1}.

Chapter 4

4.2.3 Experiments with NH_3 and NO_2

Figure 4.3 reports the results of experiments carried out with a feed containing NO_2 only. The values of k_m exhibit a minimum at $\approx 275°C$ suggesting that NO_2 and NH_3 react according to two different mechanisms depending on the operative temperature. At temperatures below 275°C, NO_2 and NH_3 were found to react with a 1:1 stoichiometry under the formation of ammonium nitrate:

$$2\,NH_3 + 2\,NO_2 \rightarrow NH_4NO_3 + N_2 + H_2O \tag{4.5}$$
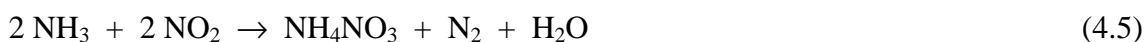
The rate constants of reaction (4.5) increase with decreasing temperature. A detailed discussion of reaction (4.5) will be reported in Chapter 5.
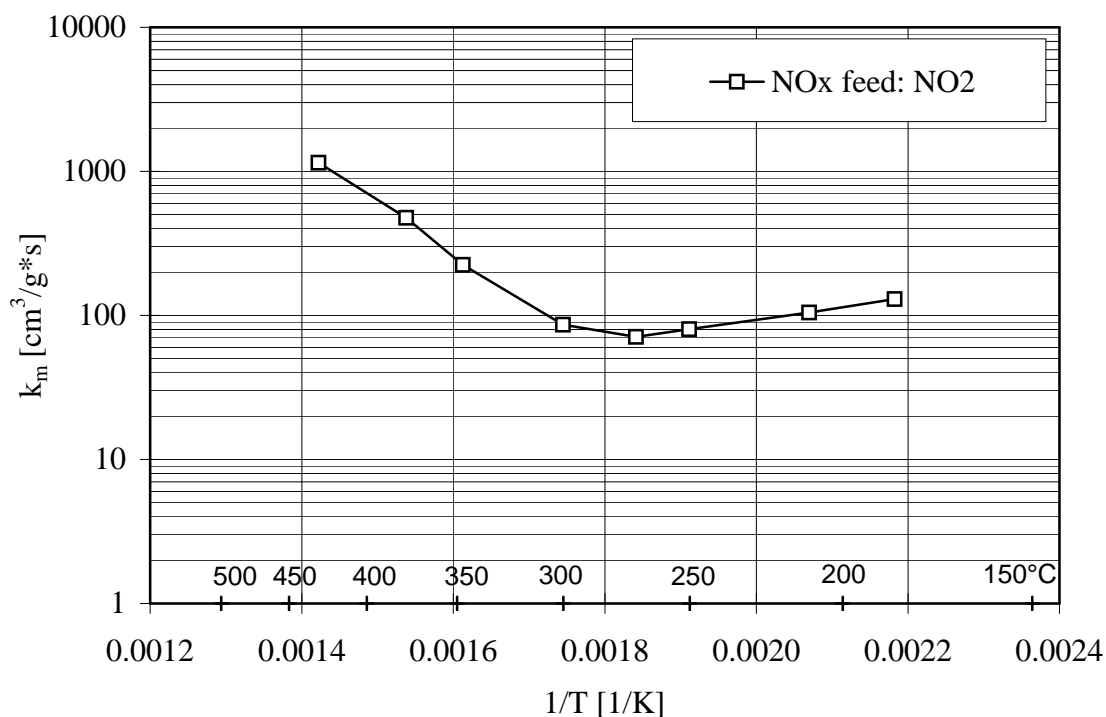
Figure 4.3 Temperature dependence of k_m. Feed: 1000 ppm NO_2, 1000 ppm NH_3, 5% H_2O, 10% O_2, balance N_2. GHSV=$5.0\cdot10^5$ h^{-1}.

SCR with NO and NO$_2$

At temperatures above 300°C, ammonia and NO_2 were found to react with a 4:3 stoichiometry according to the NO_2-SCR reaction:

$$4\,NH_3 \;+\; 3\,NO_2 \;\rightarrow\; 3.5\,N_2 \;+\; 6\,H_2O \tag{4.6}$$

The rates of the NO_2-SCR reaction (4.6) show the usual positive temperature dependence.

4.2.4 Reactions between NO, NO_2 and NH_3

Figure 4.4 summarizes the results obtained in the experiments reported above.
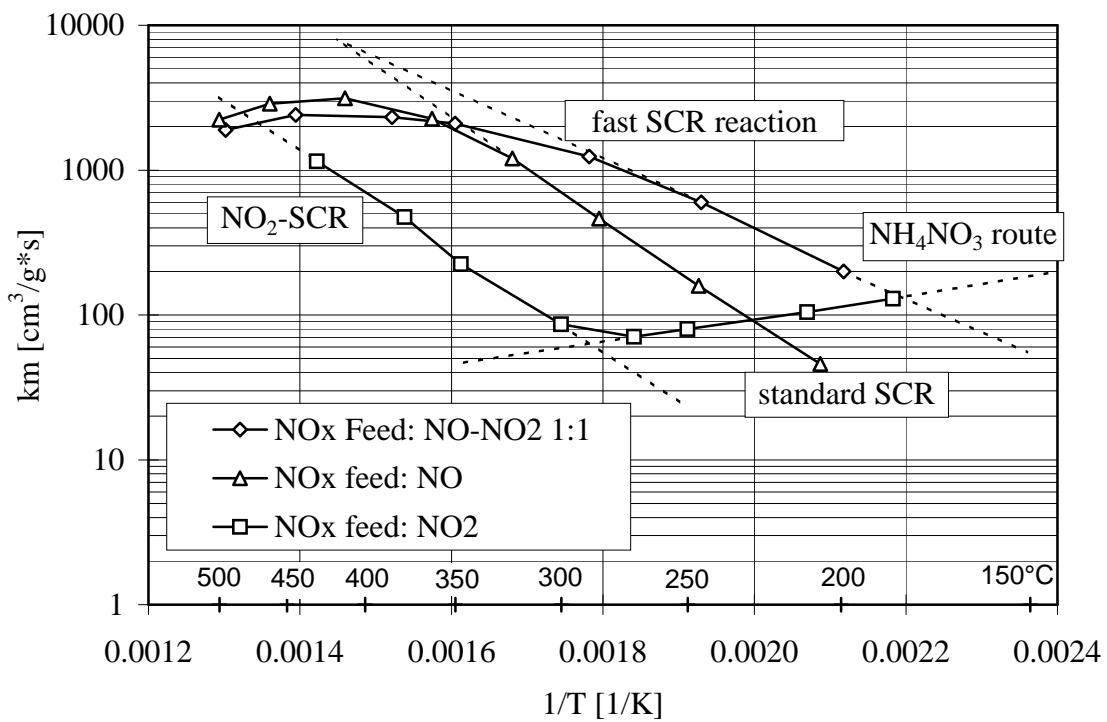
Figure 4.4   Comparison of the values of k_m determined in the experiments reported in Figure 4.1, 4.2 and 4.3.

Three zones can be distinguished in Figure 4.4:

1. at temperatures below $\approx 170°C$ the ammonium nitrate route (4.5) has the highest reaction rates;

2. in the temperature range $170 < T < 350°C$, the fast SCR reaction has the highest reaction rates; the difference in the rates of the fast and the standard SCR reaction decreases with increasing temperature: at $200°C$ this difference amounts to a factor of ≈ 10, whereas the values of k_m of the fast and standard SCR reactions converge at $T \approx 350°C$;

3. at temperatures above $350°C$, the fast and standard SCR reactions show similar values of k_m, as both reactions are mass transfer limited at these operative conditions.

The NO_2-SCR reaction (4.6) is the slowest reaction at temperatures above $275°C$.

The different reaction rates determine which reactions occur on the catalyst: the higher the reaction rate, the higher the catalyst selectivity for that reaction. However, the ratio NO_2/NO_x of the feed plays also an important role.

The above considerations were also confirmed by experiments carried out with monolithic SCR catalysts under typical exhaust gas conditions (for more details, see paragraphs 5.3.1, 7.5.2 and 8.3.2). Investigations with an equimolar mixture $NO + NO_2$ showed that:

- $T = 140\text{-}170°C$: a higher amount of NO_2 than NO reacted on the catalyst. Accordingly, the amount of NH_3 reacted was equal to the sum of NO and NO_2 consumed. This suggested that the ammonium nitrate route (4.5) and the fast SCR reaction (4.4) both occurred on the SCR catalyst.

- $T = 170\text{-}350°C$: NO, NO_2 and NH_3 reacted on the SCR catalyst according to the stoichiometry of the fast SCR reaction (4.4).

- $T = 350\text{-}450°C$: at temperature above $350°C$ part of NO_2 was converted to NO because of the thermodynamic equilibrium $NO_2 \Leftrightarrow NO + 0.5\ O_2$ (see paragraph 8.3.1),

SCR with NO and NO$_2$

556

so the fast SCR (4.4) and the standard SCR (4.3) reaction both contributed to the removal of NO_x.

In the case of NO_x with $NO_2/NO_x < 50\%$, the contribution of the standard SCR reaction was found to increase when the NO_2 content decreased. On the other hand, in the case of NO_x with $NO_2/NO_x > 50\%$, the contribution of the NO_2-SCR reaction increased with increasing NO_2 content. These results can be exhaustively explained considering the kinetic parameters reported in Figure 4.4.

4.3   Conclusions

Under typical exhaust gas conditions, the main reactions between NO, NO_2 and NH_3 on the SCR catalyst are the ammonium nitrate route, the standard SCR reaction, the fast SCR reaction and the NO_2 SCR reaction. The operating temperature and the ratio NO_2/NO_x of the feed are the main parameters determining which reactions occur on the catalyst. The fast SCR reaction has higher rate constants than the standard SCR reaction at temperatures below 350°C. At 200°C the fast SCR reaction is about ten times faster than the standard SCR reaction, thus providing a much higher DeNOx potential. The NO_2-SCR is even slower than the standard SCR reaction. The ammonium nitrate route becomes important at temperatures below 200°C.

4.4   References

[1]   E. Jacob, G. Emmerling et al., *NO_x-Verminderung für Nutzfahrzeugmotoren mit Harnstoff-SCR-Kompaktsystemen*, 19th International Vienna Motor Symposium, May 7-8, 1998

[2]   A. Kato, S. Matsuda, F. Nakajima, H. Kuroda and T. Narita, *J. Phys. Chem.* **85** (1981), 4099

[3]   G. Tuenter, W. Leeuwen and L. Snepvangers, *Ind. Eng. Chem. Prod. Res. Dev.* **25** (1986), 633

[4]   S.J. Jelles, M. Makkee, J. A. Moulijn, G.J.K. Acres and J.D. Peter-Hoblyn, *SAE Paper* N. 990113 (1989).

[5]   M. Koebel and M. Elsener, *Chem. Eng. Sci.* **53** (1998) 4, 657

[6]   M. Kleemann, *Beschichtung von Cordierit-Wabenköorpern für die selektive katalytische Reduktion von Stickoxiden*, Thesis ETH Zurich N. 13401 (1999)

[7]   M. A. Buzanowski and R.T. Yang, *Ind. Chem. Eng. Res.* **29** (1990), 2074

[8]   J.W. Beeckman and L.L. Hegedus, *Ind. Chem. Eng. Res.* **30** (1991), 969

[9]   E. Tronconi, P. Forzatti, J.P. Gomez Martin and S. Malloggi, *Chem. Eng. Sci.* **47** (1992), 2401

5

Formation of ammonium nitrate

5.1   Introduction

The automotive application of the urea-SCR process calls for an enhanced SCR activity at low temperatures [1]. As shown in the previous chapter, in the case of NO_x composed of a mixture of NO and NO_2, the operative window of the SCR process can be widened to temperatures below 300°C [1-4]. However, it is well known from the manufacturing process of nitric acid that the simultaneous presence of NO_2 and NH_3 may lead to the formation of solid ammonium nitrate at low temperatures [5,6]:

$$2\,NH_3 \;+\; 2\,NO_2 \;\rightarrow\; NH_4NO_3 \;+\; N_2 \;+\; H_2O \tag{5.1}$$

This reaction may also be considered as a selective DeNOx reaction; the maximal NO_x reduction could be 50% because half the NO_2 reacted in (5.1) is reduced to N_2. The ammonium nitrate condenses at 170°C at atmospheric pressure and may thus lead to solid deposits on SCR catalysts [5-7]. The formation of solid deposits of ammonium nitrate imposes a lowest possible operative temperature for the SCR process.

Reaction (5.1) is composed of several individual steps:

$$2\,NO_2 \;\Leftrightarrow\; N_2O_4 \tag{5.2}$$

$$N_2O_4 \;+\; H_2O \;\rightarrow\; HNO_3 \;+\; HNO_2 \tag{5.3}$$

$$HNO_3 + NH_3 \rightarrow NH_4NO_3 \tag{5.4}$$

$$HNO_2 + NH_3 \rightarrow NH_4NO_2 \tag{5.5}$$
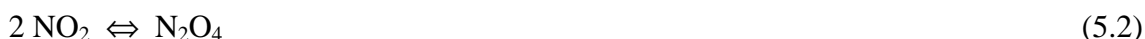
Ammonium nitrite is known to be a very unstable compound, decomposing explosively at temperatures above 60°C [8]. It may also be considered as the hydrate of nitrosoamine (NH_2–NO), which is known to be unstable with respect to nitrogen and water:

$$NH_4NO_2 \rightarrow NH_2\text{–NO} + H_2O \tag{5.6}$$

$$NH_2\text{–NO} \rightarrow N_2 + H_2O \tag{5.7}$$

The sum of reactions (5.2) to (5.7) yields reaction (5.1). The ammonium nitrate formed in reaction (5.1) will deposit as solid or liquid (melting point = 170°C) if the product of the partial pressures of NH_3 and HNO_3 exceeds the equilibrium constant K_P of the decomposition reaction:

$$NH_4NO_3 \Leftrightarrow NH_3 + HNO_3 \tag{5.8}$$

$$K_p = p_{NH_3} \cdot p_{HNO_3} \tag{5.9}$$

Conversely, ammonium nitrate can decompose with increasing temperature into NH_3 and HNO_3. The decomposition of ammonium nitrate can also yield nitrous oxide and water [9]:

$$NH_4NO_3 \rightarrow N_2O + 2\,H_2O \tag{5.10}$$

The explosive decomposition under initial ignition is also possible and yields nitrogen, oxygen and water [9]:

$$2\,NH_4NO_3 \rightarrow 2\,N_2 + O_2 + 4\,H_2O \tag{5.11}$$

Chapter 5

In the following, we will determine experimentally which of the previous decomposition pathways contributes most to the decomposition of ammonium nitrate in typical exhaust gas conditions. Other main goals are to determine the threshold temperature for ammonium nitrate deposition, the nature of the catalyst poisoning by ammonium nitrate, and the parameters influencing the formation and decomposition of ammonium nitrate on SCR catalysts.

5.2   Experimental

The description of the experimental apparatus has been reported in chapter 2. A method was implemented for the on-line measurement of nitric acid by Fourier Transform Infra-Red (FTIR) spectroscopy. The main difficulty in developing such a method is the instability of nitric acid, thus preventing the preparation of a stable calibration gas. Therefore, the calibration gas was prepared by bubbling a stream of pure nitrogen through a wash bottle containing an aqueous solution of nitric acid (45 wt-% HNO_3). The equilibrium partial pressures of HNO_3 and H_2O over a solution of this concentration at 25°C and atmospheric pressure are 0.23 and 12.7 mmHg [10]. The resulting gaseous mixture contains the equilibrium concentration of nitric acid:

$$HNO_3 = \frac{0.23}{760} \times 10^6 = 303 \, ppm$$

This value was further confirmed by titration and HPLC analysis. The FTIR spectrum of the gas mixture leaving the wash bottle was used for the calibration corresponding to 303 ppm of nitric acid. The quantification of the HNO_3 concentration was carried out considering the absorbance in the spectral region of 836-917 cm^{-1} and using the spectrum at 303 ppm of HNO_3 for a single point calibration with zero intercept.

Formation of ammonium nitrate

5.3 Results and Discussion

5.3.1 Catalyst deactivation by deposition of ammonium nitrate

In order to evaluate the lowest possible operating temperature of the SCR process in the case of NO_x containing NO_2, the reactions of an equimolar mixture of $NO + NO_2$ with ammonia were investigated in the temperature range 140-200°C. The SCR catalyst used in these experiments was a powdered SCR catalyst (160 μm < d < 200 μm) containing 3.1 wt-% V_2O_5, 8 wt-% WO_3 on a TiO_2 support, as determined by ICP (ion coupled plasma) analysis. Table 5.1 reports the results of these experiments.

Table 5.1 Conversion of NO_2 due to the fast SCR reaction (4.4) and the ammonium nitrate route (5.1) on a powdered SCR catalyst sample (151 mg). Feed: NO=250 ppm, NO_2=250 ppm, NH_3=530 ppm, O_2=10%, H_2O=5%, balance N_2. V*=150 l_N/h.

T [°C]	NO out [ppm]	NO_2 out [ppm]	NH_3 out [ppm]	DeNOx due to fast SCR [%]	NH$_4$NO$_3$ route [%]	total DeNOx [%]
200	169	161	358	32.4	1.6	34
190	192	176	400	23.2	3.2	26.4
180	210	193	438	16	3.4	19.4
170	226	202	462	9.6	4.8	14.4
160	238	212	484	4.8	5.2	10
150	245	217	495	2	5.6	7.6
140	250	224	506	0	5.2	5.2

The equimolar mixture of NO and NO_2 reacts with ammonia on the SCR catalyst according to two different reaction pathways in the temperature range 140-200°C: the fast SCR reaction (4.4) and the ammonium nitrate route (5.1). The contribution of the fast

SCR reaction and of the ammonium nitrate route to the total removal of NO_x were evaluated with the following simplified equations:

Fast SCR reaction:

$$DeNOx\ (1) = \frac{NO_{IN} - NO_{OUT}}{NO_{IN}} \times 100 \qquad (5.12)$$

Ammonium nitrate route:

$$DeNOx\ (2) = \frac{NO_{OUT} - NO_{2,OUT}}{2 \cdot NO_{IN}} \times 100 \qquad (5.13)$$

Total DeNOx:

$$DeNOx\ (tot) = DeNOx\ (1) + DeNOx\ (2) \qquad (5.14)$$

The results reported in Table 5.1 show that the formation of ammonium nitrate has a negative temperature coefficient: it becomes increasingly important with decreasing temperature. The fast SCR reaction no longer contributes to the removal of NO_x at temperatures below 150°C; i.e. its rate becomes insignificant compared to the rate of reaction (5.1). On the other hand, the fast SCR reaction is dominating in the conversion of NO_x at 200°C: 32.4% of DeNOx are due to the fast SCR reaction, but only 1.6% are due to reaction (5.1). The negative dependence of the ammonium nitrate route is due to the fact that the equilibrium (5.2) shifts to the right side with decreasing temperature.

The reactions of an equimolar mixture of NO and NO_2 with ammonia were further investigated on a monolithic SCR catalyst at typical exhaust gas conditions (GHSV=52000 h^{-1}). Figure 5.1 reports the DeNOx as a function of time in the temperature range 150-200°C. It can be seen that above 180°C the DeNOx does not vary with time. On the other hand, below 180°C the removal of NO_x decreases with time, thus indicating a poisoning of the catalyst. At these low temperatures the ammonium nitrate

Formation of ammonium nitrate

formed in reaction (5.1) deposes on the catalyst, leading to a decrease of activity due to pore clogging.
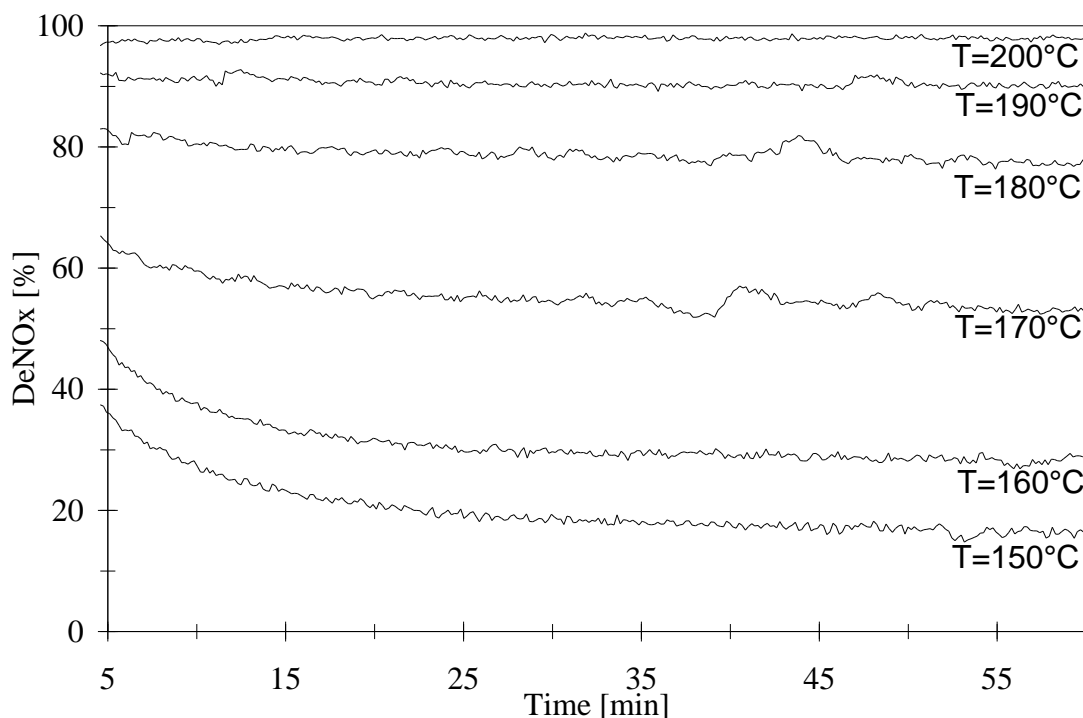
Figure 5.1   Poisoning of monolithic catalyst at various temperatures due to the formation of ammonium nitrate. $NO_{IN}=NO_{2,IN}=500$ ppm, $NH_{3,IN}=1000$ ppm, $GHSV=52000$ h^{-1}.

Figure 5.2 shows the behavior of the monolithic SCR catalyst as a function of time at 150°C. Both contributions from the fast SCR reaction and the ammonium nitrate route are much higher at the beginning of the experiment, and then decrease with time. This decrease may be ascribed to the deposition of ammonium nitrate within the pores of the catalyst. Practically stationary values are reached after some time because of the dependence of the condensation temperature on the pore size (small pore being filled first and larger pores only after or not at all). This capillary condensation effects could also explain the time dependence of DeNOx reported in Figure 5.2. The values reported in Table 5.1 correspond to the stationary values reached after ≈ 60 min.
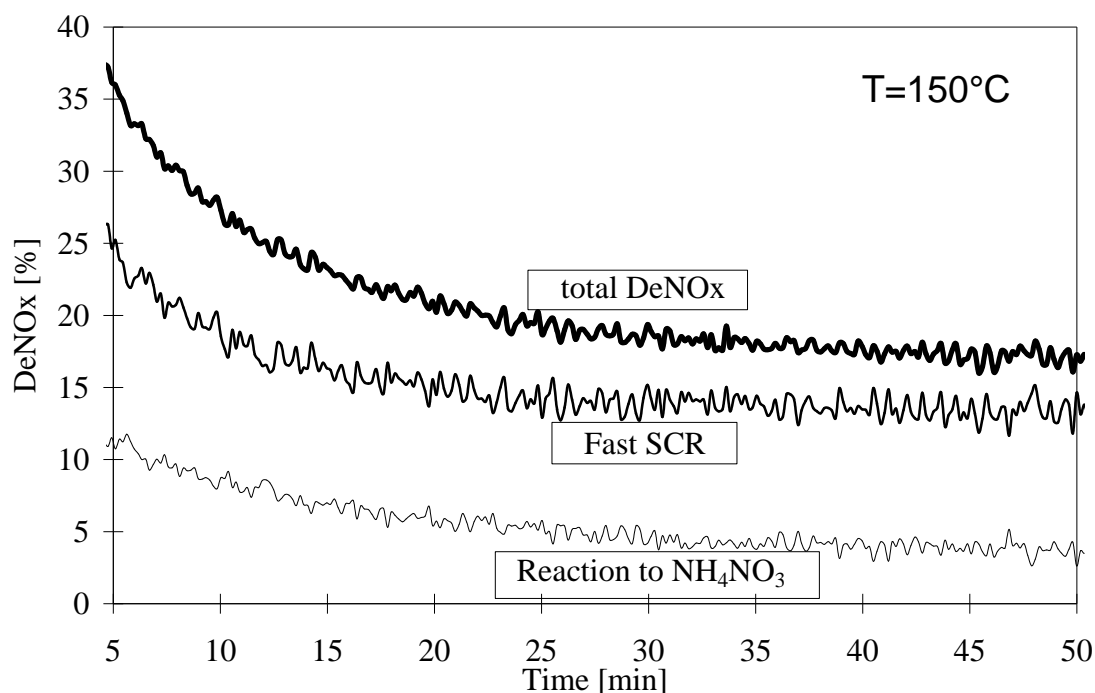
Figure 5.2 Contributions of the fast SCR reaction and of the ammonium nitrate route to the total DeNOx at 150°C. $NO_{IN}=NO_{2,IN}=500$ ppm, $NH_{3,IN}=1000$ ppm, GHSV=52000 h^{-1}.

Summarizing, the experiments demonstrate that the critical temperature for solid or liquid ammonium nitrate deposition (melting point = 170°C) is somewhere between 170 and 180°C under typical exhaust gas conditions. Higher temperatures are required if the condensation of ammonium nitrate is to be avoided.

Additional experiments have shown that the catalyst poisoning by ammonium nitrate is a reversible process due to the observation that the catalyst recovers its original activity when heated at temperatures above 200°C. This is in full analogy with the well-known deposition of ammonium sulfates ($(NH_4)_2SO_4$ and NH_4HSO_4) on SCR catalysts [11].

Formation of ammonium nitrate

5.3.2 Thermodynamic considerations

The thermodynamic condition for the formation of solid or liquid ammonium nitrate is given by:

$$p_{NH_3} \cdot p_{HNO_3} > K_p \tag{5.15}$$

The following equation for K_p has been derived from vapor pressure measurements of ammonium nitrate [5]:

$$K_p = 10^{15.0636-9340/T} \left[bar^2 \right] \tag{5.16}$$

Figure 5.3 reports the stability regions of solid ammonium nitrate calculated using equation (5.16). It can be seen that for an NH_3 concentration of 500 ppm the threshold partial pressure of HNO_3 amounts to ≈200 ppm at 150°C. This is a high value, and it is hardly present in the bulk gas phase of the monolithic channel. However, capillary condensation effects within the pores will further lower the partial pressures necessary for condensation.

Since the partial pressure of nitric acid within the catalyst is not really known, no safe prediction about the threshold temperature of ammonium nitrate deposition can be made. The prediction is further complicated by capillary condensation effects, which are dependent on the pore diameter. Practical experiments are, therefore, the only way to obtain information at which temperature ammonium nitrate starts to deposit. The results in Figure 5.1 suggest that ammonium nitrate will no longer deposit within the pores of the present monolithic SCR catalyst above 180°C. Therefore, 180°C can be suggested as a rough reference, although this value will depend on the experimental conditions, especially the ammonia concentration in the feed and the actual conversions of the two reactions.

Chapter 5
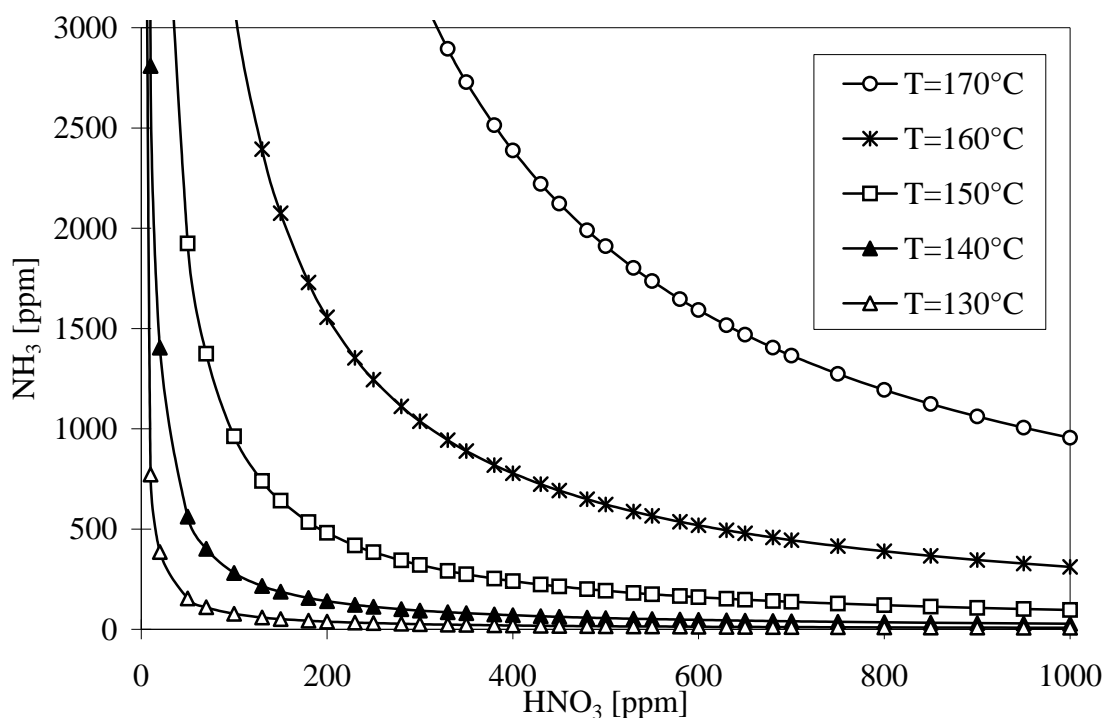
Figure 5.3   Thermodynamic stability region of solid ammonium nitrate (above and to the right of the limiting curves).

5.3.3   Formation and decomposition of ammonium nitrate

The formation and decomposition of ammonium nitrate were investigated in laboratory tests with a monolithic SCR catalyst containing 3.1 wt-% V_2O_5, 8 wt-% WO_3 on TiO_2. The results of a typical experiment are reported in Figure 5.4. At 150°C a gas mixture containing 1000 ppm NH_3 and 1000 ppm NO_2 was fed to the catalyst for $\approx$ 30 min. The concentrations of NO_2 and NH_3 detected at the catalyst outlet were practically equal, thus indicating that NO_2 and NH_3 reacted with a 1:1 stoichiometry. The amounts of NO_2 and NH_3 consumed in this reaction are given by the area between the line of the inlet concentration (1000 ppm) and the concentration curves at the catalyst outlet. After stopping the feeds of NH_3 and NO_2 at t$\approx$30 min, the catalyst was kept under a flow of O_2, H_2O and N_2 at 150°C for 30 min. During this period, no species were detected at the

catalyst outlet. At t $\approx$ 60 min, a heating ramp of 10K/min from 150 to 425°C was started and, upon heating the system, NH_3 and HNO_3 were detected at the catalyst outlet.

Figure 5.4   Formation and decomposition of ammonium nitrate in a humid feed. SCR catalyst M11 (600 cpsi). Heating rate = 10 K/min. Feed : $NO_{2,IN}=NH_{3,IN}=1000$ ppm (up to 30 min), 5% H_2O, 10% O_2, balance N_2. GHSV=52000 h^{-1}.

The amount of ammonia desorbed upon heating the system was much higher than the amount of ammonia physisorbed on the catalyst at the same temperature, which was determined in a separate experiment (reported as "blank NH_3" in Figure 5.4). The amount of NH_3 (or HNO_3) desorbed upon heating the system was evaluated by integrating the area below the curve of NH_3 (or HNO_3) concentration at t > 60 min. Appendix A1 (see paragraph 5.6.1) reports the mass balance for this experiment.

Chapter 5

The 1:1 stoichiometry of the reaction between NO_2 and NH_3 and the fact that the amount of NH_3 detected upon heating the system is about half the amount of the ammonia consumed in the reaction with NO_2 suggest that the following reactions occurred:

$$2\,NH_3 + 2\,NO_2 \rightarrow NH_4NO_3 + N_2 + H_2O \qquad (NH_4NO_3 \text{ formation}) \quad t < 30 \text{ min. (5.1)}$$

$$NH_4NO_3 \rightarrow NH_3 + HNO_3 \qquad\qquad (NH_4NO_3 \text{ decomposition}) \quad t > 60 \text{ min. (5.8)}$$

The decomposition reaction (5.8) is also confirmed by the fact that the differences between the concentrations of NH_3 and HNO_3 detected upon heating the system were within the experimental error. The amount of nitrous oxide detected upon heating the system was low, thus indicating a negligible contribution of reaction (5.10) in the present experiment.

The formation and decomposition of ammonium nitrate was also investigated on a V-free catalyst consisting of 8 wt-% WO_3 on TiO_2. The amount of ammonium nitrate formed on this catalyst was similar to the amount formed on the SCR catalyst, indicating that reaction (5.1) does not require a redox function, but only a surface where ammonia can adsorb.

Figure 5.5 reports the formation and decomposition of ammonium nitrate on a monolithic SCR catalyst in the case of a dry feed. The mass balance for this experiment is reported in Appendix A2 (see paragraph 5.6.2). The comparison of Figures 5.4 and 5.5 shows that the formation of ammonium nitrate is practically not influenced by the presence of water. Moreover, in the case of a dry feed, some nitrous oxide was detected upon heating the system, thus suggesting that part of the ammonium nitrate decomposed according to reaction (5.10). However, also in this case, the major part of ammonium nitrate decomposed into NH_3 and HNO_3.

The formation of ammonium nitrate was further investigated in a blank experiment carried out without catalyst. The amount of ammonium nitrate formed in the apparatus was about 15% of the amount observed in the experiments with the SCR catalyst.
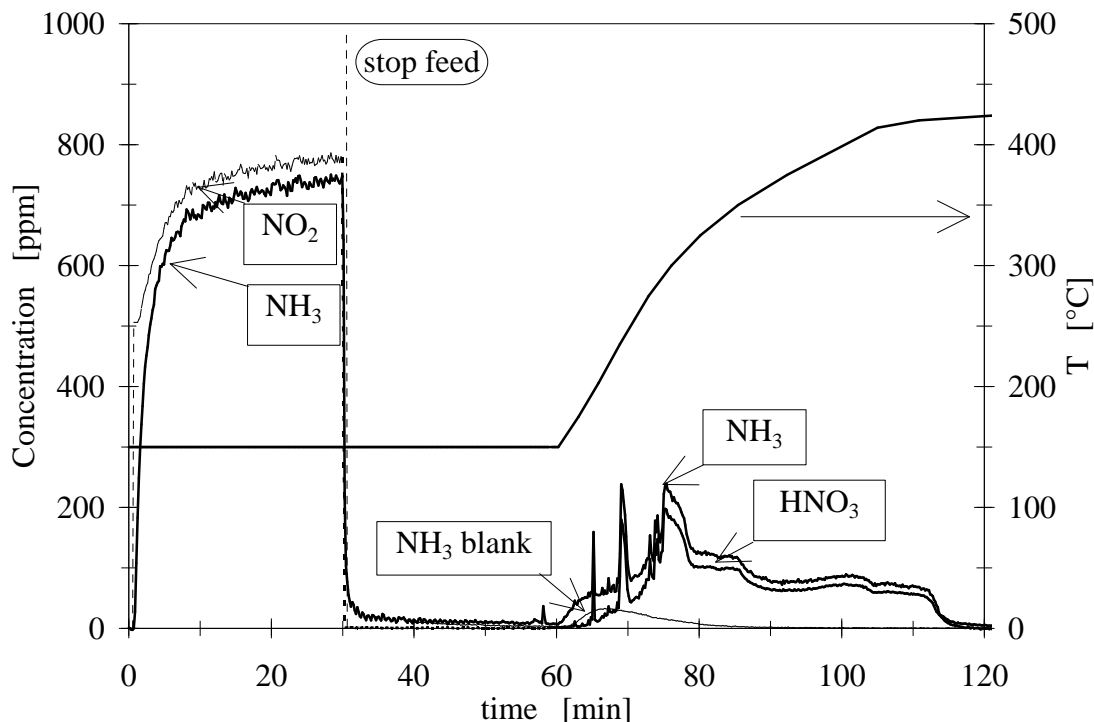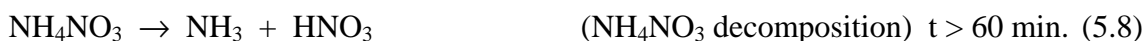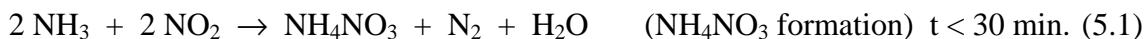
Formation of ammonium nitrate
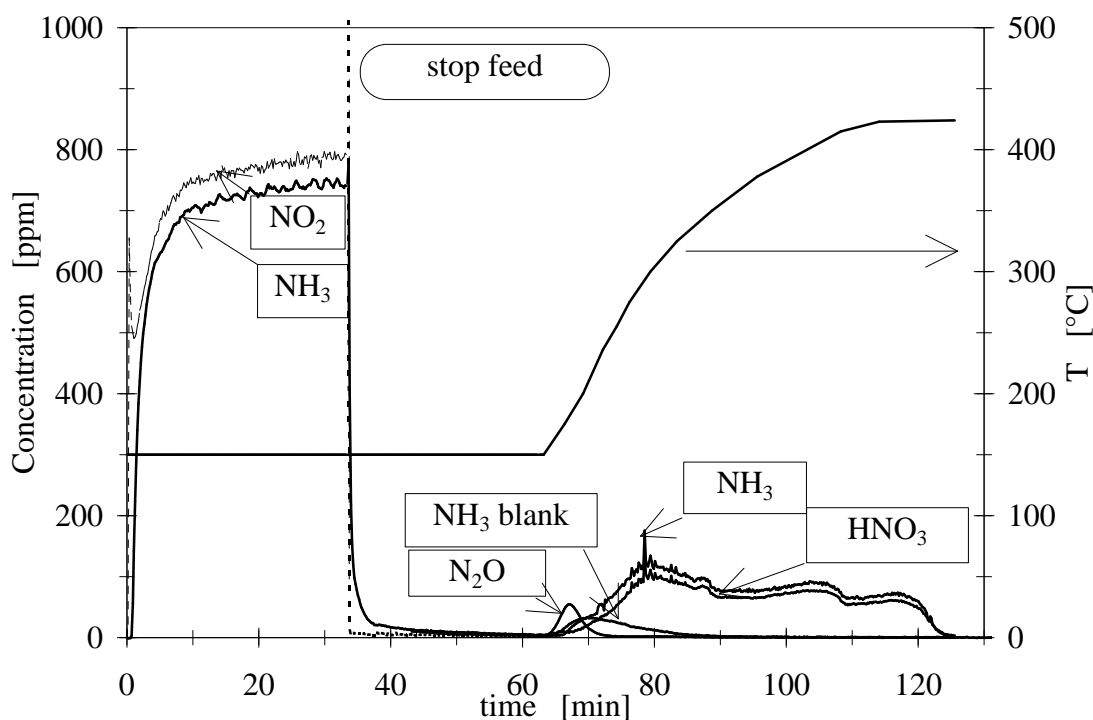
Figure 5.5   Formation and decomposition of ammonium nitrate in a dry feed. SCR
catalyst M11 (600 cpsi). Heating rate = 10 K/min. Feed: $NO_{2,IN}=$
$NH_{3,IN}=1000$ ppm (up to 30 min), 10% O_2, balance N_2. GHSV=52000h^{-1}.

The ammonium nitrate formed on the SCR catalyst may deposit on the catalyst itself or
on the tube and the reactor walls. The amount of ammonium nitrate deposed in the ex-
perimental apparatus was evaluated as follows. After loading the system with ammo-
nium nitrate, the catalyst was removed from the system before starting the heating pro-
cedure. Consequently, the species detected upon heating the system came from the am-
monium nitrate deposed in the experimental apparatus. The amount of ammonium ni-
trate deposed in the experimental apparatus was found to be ≈50% of the whole amount
of ammonium nitrate formed in the process.

Further experiments were made in order to investigate the influence of NO on the de-
composition of ammonium nitrate. 500 ppm NO were added to the feed at t≈30 min
after loading the system with ammonium nitrate. Figure 5.6 shows that, in the presence
of NO, the decomposition of ammonium nitrate occurs already at 150°C under the for-

mation of NO_2 and NH_3. We should mention here that, in the previous experiments, the decomposition of ammonium nitrate could only be observed when the reactor was heated up.

Figure 5.6 Formation and decomposition of ammonium nitrate in a humid feed. SCR catalyst M11 (600 cpsi). Heating rate = 25 K/min. Feed : $NO_{2,IN}=NH_{3,IN}=1000$ ppm (up to 30 min), $NO_{IN}=500$ ppm (after 30 min), 5% H_2O, 10% O_2, balance N_2. GHSV=52000 h^{-1}.

The following reaction explains the decomposition of ammonium nitrate in the presence of NO:

$$2\,NH_4NO_3\ +\ NO\ \rightarrow\ 3\,NO_2\ +\ 2\,NH_3\ +\ H_2O \tag{5.17}$$
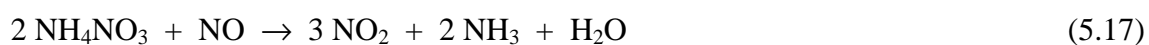
This reaction can be considered as the sum of the following two reactions:

Formation of ammonium nitrate

$$2 \, NH_4NO_3 \; \rightarrow \; 2 \, NH_3 \; + \; 2 \, HNO_3 \tag{5.8}$$

$$2 \, HNO_3 \; + \; NO \; \rightarrow \; 3 \, NO_2 \; + \; H_2O \tag{5.18}$$

When the temperature is increased (t > 75 min.), the remainder amount of ammonium nitrate decomposes into NH_3 and HNO_3. In our opinion, the ammonium nitrate deposed on the experimental apparatus decomposed into NH_3 and HNO_3. The amount of NH_3 detected during heating is lower than the value expected from the decomposition of ammonium nitrate. Therefore, part of the NO_2 formed in reaction (5.18) must have reacted with NO and NH_3 in the fast SCR reaction. Appendix A3 (see paragraph 5.6.3) reports the mass balance for this experiment, considering the contributions of the fast SCR reaction and of the reactions (5.1), (5.8) and (5.18). The mass balance closes quite well, suggesting that the proposed set of reactions is likely.

The influence of NO on the decomposition of ammonium nitrate was also investigated in an experiment with a V-free catalyst consisting of 8 wt-% WO_3 on TiO_2 support. The results reported in Figure 5.7 show that at 150°C ammonium nitrate is stable in the presence of NO. Conversely, on the SCR catalyst ammonium nitrate decomposes already at 150°C (Figure 5.6), thus suggesting that reaction (5.18) is favored by the V-sites. However, reaction (5.18) occurs also on the V-free catalyst upon heating the reactor. Probably the weak redox properties of WO_3 start to be active for this reaction only at higher temperatures.

The influence of 500 ppm CO or 500 ppm C1 as dodecane on the decomposition of ammonium nitrate was also investigated. These experiments showed that the decomposition of ammonium nitrate is not influenced by CO and HC at the investigated concentrations. This indicates that the nitrates have a much higher affinity to react with NO than with CO or hydrocarbons.

Chapter 5
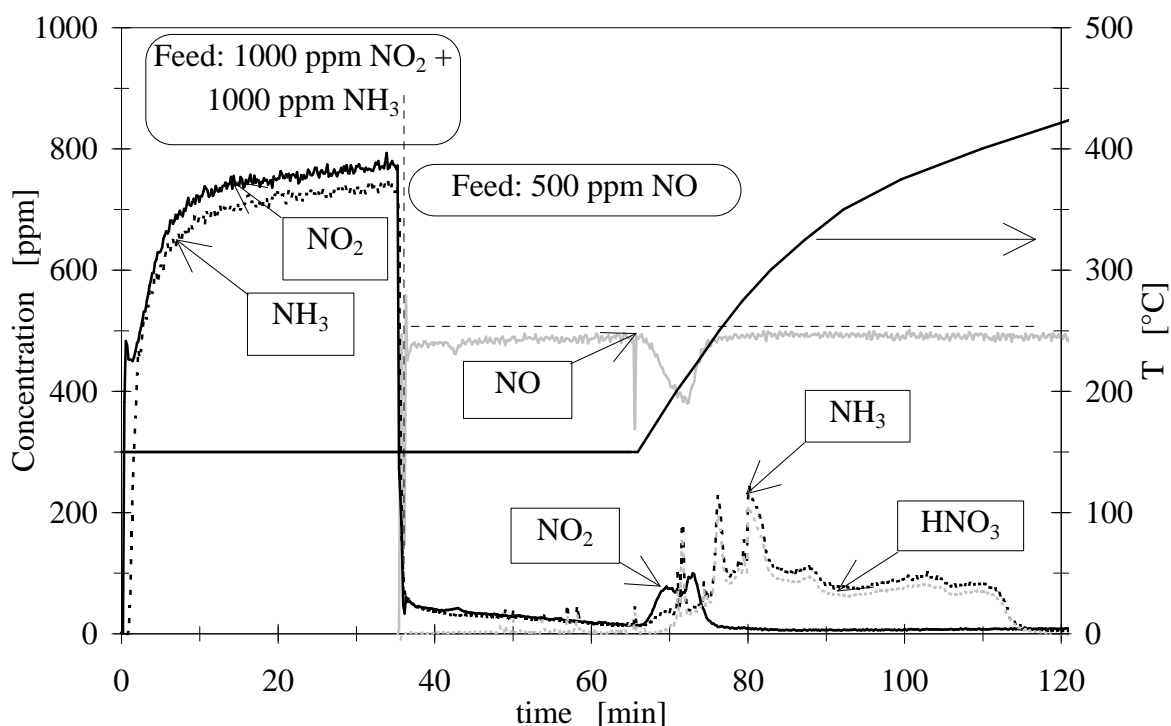
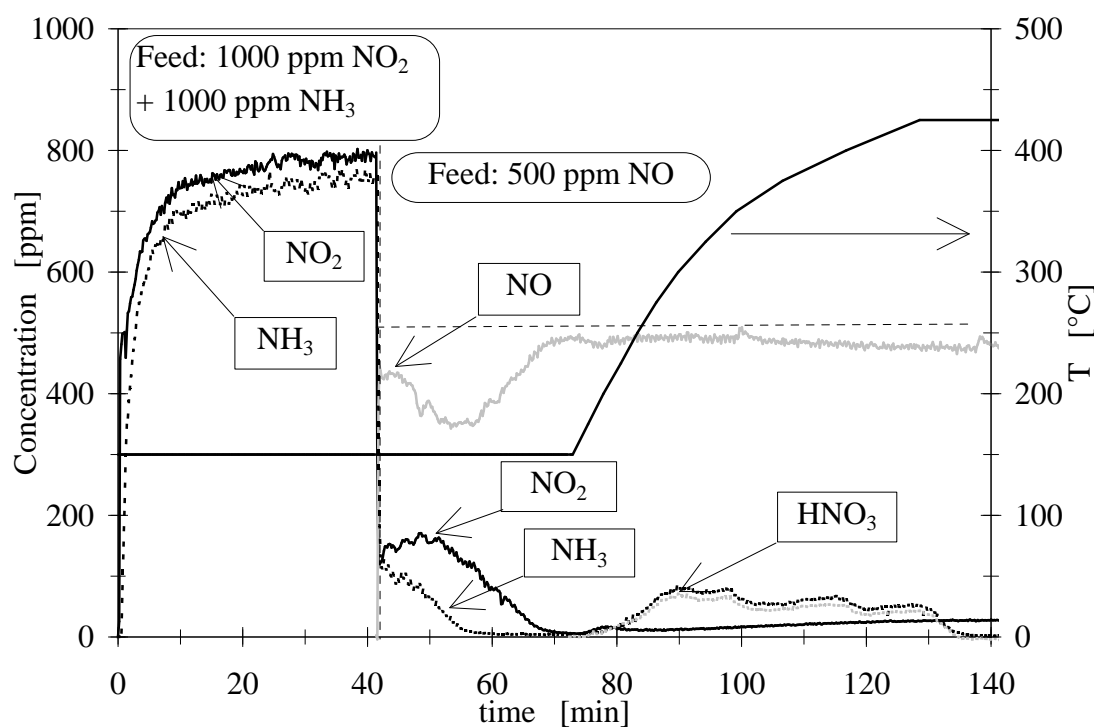**Figure 5.7** Formation and decomposition of ammonium nitrate in a humid feed. V-free catalyst. Heating rate = 25 K/min. Feed : $NO_{2,IN}$=$NH_{3,IN}$=1000 ppm (up to 30 min), NO_{IN}=500 ppm (after 30 min), 10% O_2, balance N_2. GHSV=52000 h^{-1}.

5.4 Conclusions

The simultaneous presence of NH_3 and NO_2 at temperatures below 200°C may lead to the formation of ammonium nitrate. This reaction occurs on the SCR catalyst and on the tube and reactor walls. The formation of ammonium nitrate has a negative temperature coefficient, thus becoming increasingly important with decreasing temperature. Experiments have shown that the formation of ammonium nitrate does virtually not depend on the redox properties of the catalyst, but simply requires a surface where ammonia can adsorb. The presence of water does virtually not influence the formation of ammonium nitrate. Depending on temperature and the partial pressures of ammonia and nitric acid, solid or liquid ammonium nitrate may deposit within the pores of the catalyst and thus cause its reversible deactivation. The ammonium nitrate deposed on the catalyst decomposes during a subsequent heating of the reactor and the catalyst will recover its original

Formation of ammonium nitrate

activity. The experiments suggested that a rough value of the threshold temperature where no disturbing solid deposits of ammonium nitrate form within the catalyst lies around 180°C under typical exhaust gas conditions.

The thermal decomposition of ammonium nitrate yields mainly ammonia and nitric acid. In a dry feed a small fraction of ammonium nitrate decomposes into nitrous oxide and water. NO (500 ppm) was found to lower the temperature of the decomposition of ammonium nitrate. At 150°C NO reacts with ammonium nitrate on the SCR catalyst leading to NO_2, ammonia and water. Conversely, the presence of 500 ppm CO or HC as dodecane did not influence the decomposition of ammonium nitrate, thus indicating the higher affinity of nitrates to react with NO than with CO or HC.

The ammonium nitrate route may be considered as the equivalent of the nitrate adsorption on an NSR (NO_x Storage Reduction) catalyst. In the case of the NSR catalyst, a basic oxide like, for example, BaO acts as the adsorbing site for HNO_3. In the case of the ammonium nitrate route, NH_3 represents the basic adsorbent and after reacting with HNO_3 leads to the formation of solid ammonium nitrate. Unlike with an NSR catalyst, adsorbed nitrate is not reduced in a subsequent cycle with rich reducing exhaust but decomposed when higher temperatures are again attained.

In conclusion, the ammonium nitrate route of NO_2 combines the features typical to the SCR and the NSR catalyst.

5.5   References

[1]   E. Jacob, G. Emmerling et al., *NO_x-Verminderung für Nutzfahrzeumotoren mit Harnstoff-SCR-Kompaktsystemen*, 19th Wiener Motorensymposium, May 7-8, 1998

[2]   S. Bröer and T. Hammer, *Appl. Catal. B* **28** (2000), 101

[3]   A. Kato, S. Matsuda, F. Nakajima, H. Kuroda and T. Narita, *J. Phys. Chem* **85** (1981), 4099

[4]   G. Tuenter, W. Leeuwen and L. Snepvangers, *Ind. Eng. Chem. Prod. Res. Dev.* **25** (1986), 233

[5]   A. Mearns and K. Ofosu-Asiedu, *J. Chem. Biotechnol.* **34 A** (1984), 350

[6]   A. Mearns and K. Ofosu-Asiedu, *J. Chem. Biotechnol.* **34 A** (1984), 341

[7]   C.U.I Odenbrand, L.A.H: Andersson, J.G.M. Brandin and S.T. Lundin, *Appl. Catal.* **27** (1986), 363

[8]   Gmelin, *Handbuch der Anorganischen Chemie*, Ammonium 8th Edition, Lieferung 1, 1936/69, 89

[9]   Gmelin, *Handbuch der Anorganischen Chemie*, Ammonium 8th Edition, Lieferung 1, 1936/69, 109

[10]   Perry's Chemical Engineer Handbook, 6th Edition, 3-70.

[11]   R. Kiyoura and K. Urano, *Ind. Eng. Chem. Process Des. Develop.* **9** (1970) 4, 489.

5.6 Appendix A

Reactions:

$$2\,NH_3 + 2\,NO_2 \rightarrow 2\,NH_4NO_3 + N_2 + H_2O \tag{I}$$

$$NH_4NO_3 \rightarrow NH_3 + HNO_3 \tag{II}$$

$$2\,HNO_3 + NO \rightarrow 3\,NO_2 + H_2O \tag{III}$$

$$2\,NH_3 + NO + NO_2 \rightarrow 2\,N_2 + 3\,H_2O \tag{IV}$$

$$NH_4NO_3 \rightarrow N_2O + 2\,H_2O \tag{V}$$
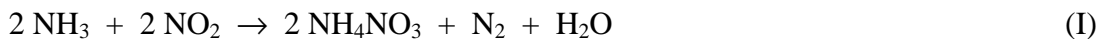
5.6.1 Appendix A1

Formation and decomposition of ammonium nitrate in wet conditions on an SCR catalyst coated on a metal monolith (Figure 5.4). The system was operated at atmospheric pressure and a gas hourly space velocity of 52000 h^{-1}. Feed: 1000 ppm NO_2, 1000 ppm NH_3, 5% H_2O, 10% O_2 and balance N_2. During the decomposition of ammonium nitrate, the addition of NO_2 and NH_3 to the feed was stopped.

Mass balance:

Experimentally measured values	
[1]	NH_3 consumed in react. (I) = 0.002925 mol
[2]	NH_3 desorbed = 0.001636 mol
[3]	HNO_3 desorbed = 0.00109 mol
[4]	NH_3 blank = 0.000306 mol
Calculated values	
[5]	NH_4NO_3 produced in (I) = 0.5 * ([1] - [4]) = 0.0013095 mol
[6]	NH_3 from NH_4NO_3 according to (II) = [5] = 0.0013095 mol
[7]	HNO_3 from NH_4NO_3 according to (II) = [5] = 0.0013095 mol
[8]	NH_3 desorbed = [6] + [4] = 0.001615 mol *compare to [2]*

5.6.2 Appendix A2

Formation and decomposition of ammonium nitrate in dry conditions on an SCR catalyst coated on a metal monolith (Figure 5.5). The system was operated at atmospheric pressure and a gas hourly space velocity of 52000 h^{-1}. Feed: 1000 ppm NO_2, 1000 ppm NH_3, 10% O_2 and balance N_2. During the decomposition of ammonium nitrate, the addition of NO_2 and NH_3 to the feed was stopped.

Mass balance:

Experimentally measured values	
[1]	NH_3 consumed in react. (I) = 0.003114 mol
[2]	NH_3 desorbed = 0.001461 mol
[3]	HNO_3 desorbed = 0.001036 mol
[4]	N_2O produced = 0.0000758 mol
[5]	NH_3 blank = 0.000306 mol
Calculated values	
[6]	NH_4NO_3 produced in (I) = 0.5 * ([1] - [5]) = 0.001404 mol
[7]	NH_3 from NH_4NO_3 according to (II) = [6] - [4] = 0.001328 mol
[8]	HNO_3 from NH_4NO_3 according to (II) = [6] - [4] = 0.001328 mol
[9]	NH_3 desorbed = [7] + [5] = 0.001634 mol *compare to [2]*

5.6.3 Appendix A3

Formation and decomposition of ammonium nitrate in wet conditions on an SCR catalyst coated on a metal monolith (Figure 5.6). The system was operated at atmospheric pressure and a gas hourly space velocity of 52000 h^{-1}. Feed: 1000 ppm NO_2, 1000 ppm

NH$_3$, 10% O$_2$, 5% H$_2$O and balance N$_2$. During the decomposition of ammonium nitrate, the addition of NO$_2$ and NH$_3$ to the feed was stopped and the addition of 500 ppm NO was started.

Mass balance:

	Experimentally measured values	
[1]	NH$_3$ consumed in react. (I) = 0.003693 mol	
[2]	NO consumed = 0.000826 mol	
[3]	NO$_2$ produced = 0.001288 mol	
[4]	HNO$_3$ desorbed = 0.000715 mol	
[5]	NH$_3$ desorbed = 0.001257 mol	
[6]	NH$_3$ blank = 0.000306 mol	
	Calculated values	
[7]	NH$_4$NO$_3$ produced in (I) = 0.5*([1] - [6]) = 0.001694 mol	
[8]	NH$_3$ from NH$_4$NO$_3$ according to (II) = [7] = 0.001694 mol	
[9]	HNO$_3$ from NH$_4$NO$_3$ according to (II) = [7] = 0.001694 mol	
[10]	HNO$_3$ reacted in (III) = [9] - [4] = 0.000979 mol	
[11]	NO consumed in (III) = [10] / 2 = 0.0004895 mol	
[12]	NO$_2$ produced in (III) = 3 * [10] / 2 = 0.0014685 mol	
[13]	NO reacted in (IV) = [2] - [11] = 0.0003365 mol	
[14]	NO$_2$ reacted in (IV) = [13] = 0.0003365 mol	
[15]	NO$_2$ produced тот= [12] - [14] = 0.001135 mol *compare to [3]*	
[16]	NH$_3$ reacted in (IV) = 2 * [13] = 0.000673	
[17]	NH$_3$ desorbed = [8] + [6] - [16] = 0.001327 *compare to [5]*	

Chapter 5

<div align="right">

6

</div>

The probable role of NO$_2$ in the
fast SCR reaction

6.1   Introduction

The interest for the fast SCR reaction has considerably increased during the last years due to its higher DeNOx potential at low temperatures:

$$4\,NH_3 \;+\; 2\,NO \;+\; 2\,NO_2 \quad\rightarrow\quad 4\,N_2 \;+\; 6\,H_2O \qquad \text{(fast SCR reaction)} \tag{6.1}$$

$$4\,NH_3 \;+\; 4\,NO \;+\; O_2 \quad\rightarrow\quad 4\,N_2 \;+\; 6\,H_2O \qquad \text{(standard SCR reaction)} \tag{6.2}$$
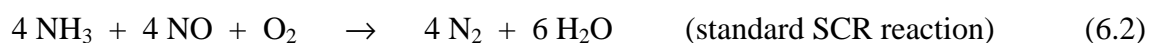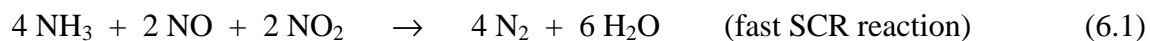
The beneficial effect of the fast SCR reaction on the overall NO$_x$ conversion has been reported by various authors [1-6]. However, not all aspects of the fast SCR reaction have been understood in the past.

This chapter reports on results of transient experiments in a test reactor and in-situ Raman spectroscopy investigating the role of NO$_2$ in the fast SCR reaction (6.1).

6.2   Experimental

6.2.1   Reactor and catalysts

The transient catalytic tests were carried out in the experimental apparatus described in chapter 2. Two different monolithic catalyst samples based on TiO$_2$-WO$_3$-V$_2$O$_5$ were used. One was a commercial extruded catalyst (D42B) and the other was a catalyst

coated on a metallic substrate (M11) prepared in house according to the procedure reported in chapter 3. Further specifications are given in Table 6.1.

Table 6.1   Catalyst specifications and operating conditions

	units	D42B	M11
cell density	cells/inch^2	300	600
V_2O_5	wt-%	≈ 3	≈ 3
WO_3	wt-%	≈ 8	≈ 8
sample volume	cm^3	8.3	7.3
gas stream in test	l_N/h	432	380
GHSV	1/h	52000	52000

6.2.2   Influence of oxygen

The influence of oxygen on the NO_x conversion was tested in a steady state type experiment with catalyst M11 at three temperatures (200, 250, 300°C). The steady state NO_x conversion was measured for various oxygen concentrations in the feed. The feed contained 0-20 % O_2, 5 % H_2O, 1000 ppm NH_3, 1000 ppm NO_x with balance nitrogen. NO_x consisted of 1000 ppm NO in the case of standard SCR and of 500 ppm each NO and NO_2 in the case of fast SCR.

6.2.3   Transient experiments

The catalyst sample (D42B) was pretreated in the reactor at 450°C in a flow of 10% O_2 + 5% H_2O with balance N_2 for 1 hour. Subsequently, it was reduced at 300°C in a feed gas consisting of 1000 ppm NO, 1000 ppm NH_3, 5 % H_2O, balance N_2 for 30 minutes. Due to the absence of oxygen in the feed and considering reaction (6.2), the catalyst

will be reduced ($V^{+5} \rightarrow V^{+4}$), i.e. the required oxygen will be taken from the V_2O_5 lattice. In the next step, adsorbed NH_3 was removed by heating the catalyst to 450°C in a stream of 5% $H_2O + N_2$. A first re-oxidation experiment was then performed at 300°C with a feed containing 345 ppm of NO_2, 5 % H_2O, balance N_2. A second re-oxidation experiment was made with a feed containing also 350 ppm NH_3. This experiment was repeated with a catalyst which had not been reduced previously.

6.2.4   In-situ Raman experiments

Raman spectra were collected using a confocal Raman microscope (Labram, DILOR) equipped with a 50x magnification objective (laser spot size ≈ 5 μm) and a thermoelectrically cooled CCD detector (1152 x 300 pixels). The Raman spectra were obtained in a backscattering geometry with the yellow line (λ = 568.2 nm) of a Kr-ion laser (Coherent Innova 302). The power at the sample was kept at 2.0±0.1 mW. No sample degradation occurred after prolonged exposure to this laser power, as shown by the constancy of the Raman spectra with acquisition time. Raman spectra were routinely acquired in the range from 250 to 1500 cm^{-1} using a 1800 grooves/mm grating. The catalyst treatments were carried out in a Linkam T1500 heated stage equipped with a quartz window for the collection of in-situ Raman spectra.

The formation of V^{+5} species by oxidation of V^{+4} centers can be monitored directly by in-situ Raman spectroscopy, since the V^{+5}=O groups associated with V^{+5} ions in the vanadia lattice give rise to strong Raman bands in the range between 850 and 1030 cm^{-1}. In order to avoid the interference of the Raman bands corresponding to the W=O stretching, the in-situ Raman spectroscopy experiments were carried out on a W-free TiO_2-V_2O_5 based catalyst.

A fraction of 160-200 μm particle size was used after calcination at 500°C for 4 hours. After positioning into the Raman cell, the sample was heated to 500°C (30 °C/min) in a flow of 900 ppm NH_3/N_2 (30 ml$_N$/min, atmospheric pressure) and kept at this temperature for 20 minutes. Then the cell was flushed with N_2 for 10 minutes in order to desorb NH_3 from the catalyst and cooled down to ambient temperature. The result of this reducing treatment was a drop of the intensity of the V^{+5}=O stretching bands in the region

850-1030 cm^{-1} to 0.65 times its original value, due to the partial conversion of V^{+5}=O groups to V^{+4}-OH groups. The residual intensity of the V^{+5}=O stretching bands after reduction indicates that not all V^{+5} centers present in the catalyst can be reduced to V^{+4} by the applied treatment. Finally, the oxidizing mixture (synthetic air or 900 ppm NO$_2$ in N$_2$) was fed to the cell at a flow of 30 ml$_N$/minute and after 15 minutes a 4 °C/min heating ramp up to 500°C was started. While heating, one Raman spectrum every two minutes was acquired. In order to follow the re-oxidation of V^{+4}-OH groups to V^{+5}=O groups in a quantitative manner, the Raman spectra were baseline corrected, by subtracting the 2nd order polynomial that fitted the 1200-1500 cm^{-1} region best, and deconvoluted using Gaussian-Lorentzian curves. The positions of the peaks used in the fitting procedure and their assignment are listed in Table 6.2. The sum of the area of the V^{+5}=O stretching peaks was calculated and its variation with temperature during re-oxidation was considered.

Table 6.2   Spectral components used to fit the baseline corrected Raman spectra.

Peak position [cm^{-1}]	Assignment	Reference
397	Anatase	[7]
512	Anatase	[7]
519	Anatase	[7]
636	Anatase	[7]
645	Anatase	[7]
799	Anatase	[8]
857	V-O-V stretch	[9]
921	V=O stretch	[10]
990	V=O stretch	[10]
1020	V=O stretch	[10]

6.3 Results and Discussion

6.3.1 Influence of oxygen

Figure 6.1 shows the stationary NO_x conversion ("DeNOx") of the standard SCR reaction (NO_x in the feed = pure NO) as a function of oxygen in the feed. If the feed contains no oxygen, the DeNOx is zero at all three temperatures. It can be seen that oxygen accelerates the reaction at all three temperatures. However, the influence of oxygen concentration is different for the three temperatures. At the lower temperatures of 200 and 250°C, the DeNOx is still depending on oxygen concentration at 20 % oxygen. This is no longer true at 300°C, where the DeNOx is virtually independent of oxygen concentration above ≈ 4% oxygen.
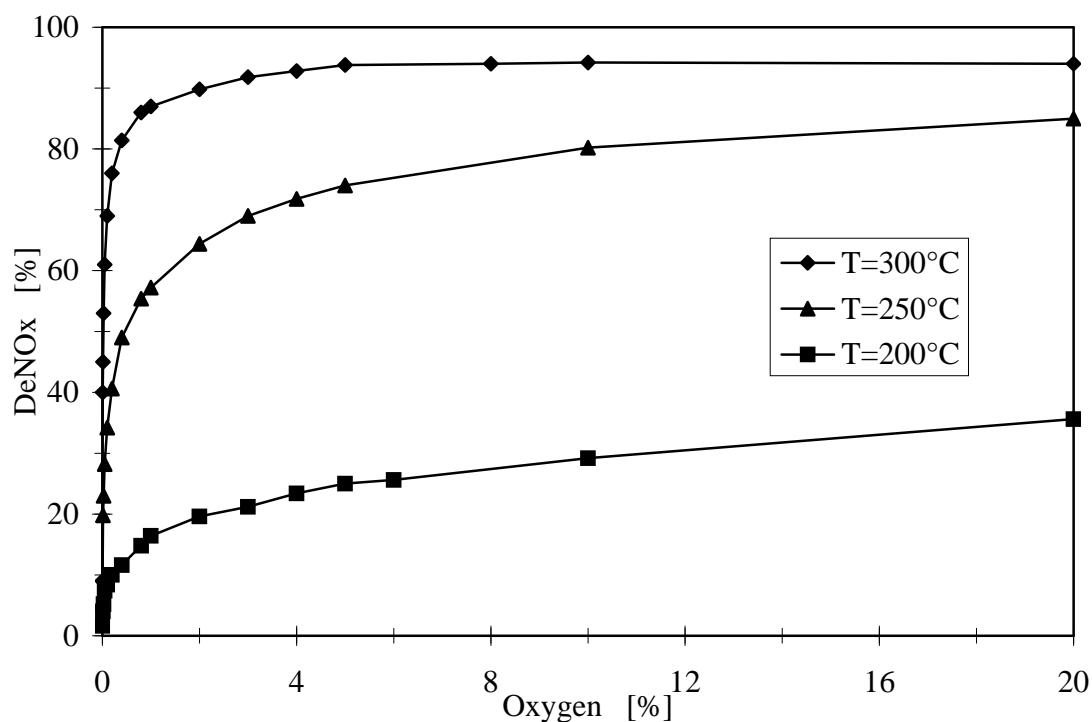

Figure 6.1   DeNOx vs. O_2 concentration. Catalyst M11. Feed: 1000 ppm NO, 1000 ppm NH_3, 5% H_2O, O_2 varied, balance N_2.

These results suggest that oxygen is rate limiting for the standard SCR reaction only at temperatures below 300°C and this may well be due to depletion of lattice oxygen or

The probable role of NO_2 in the fast SCR reaction

reduction of V. Other researchers have also found evidence that the re-oxidation of V may be rate limiting at low temperatures [11-13].

Analogous experiments have been carried out to test the influence of oxygen on the fast SCR reaction. In this case, NO_x in the feed consisted of 500 ppm NO + 500 ppm NO_2. At all three temperatures, no influence of oxygen concentration on DeNOx could be found. The conversion was 91 % at 200°C, and practically 100% at both 250 and 300°C. This proves that the fast SCR reaction does not involve gaseous oxygen.

6.3.2 Transient experiments

Figure 6.2 shows the concentrations of NO and NH_3 at the reactor outlet during the reduction of the catalyst in a feed without oxygen. The rise in ammonia concentration shows a delay of about one minute due to its adsorption on the catalyst. The concentrations of both NH_3 and NO rise slowly up to their values in the feed. This implies that initially the SCR reaction takes place at an appreciable rate, consuming oxygen from the V_2O_5 lattice, and thereby reducing steadily the V^{+5} sites to V^{+4}. After consumption of all available lattice oxygen the SCR reaction ceases.

The amount of V-sites on the catalyst can be evaluated from the amount of NO reacted in the process if the rate of the following reaction without oxygen is practically zero at the actual conditions (T=300°C, GHSV =52000 h^{-1}):

$$4 \, NH_3 \; + \; 6 \, NO \quad \rightarrow \quad 5 \, N_2 \; + 6 \, H_2O \qquad\qquad (6.3)$$

The fact that the outlet concentrations of NO and NH_3 approach their inlet values when the catalyst is completely reduced proves that this assumption is correct. From a quantitative analysis of the curve of NO concentration in Figure 6.2, the amount of the reduced V-sites can be calculated to be 0.84 mmol - one V-site is reduced in each SCR cycle. The amount of reduced V-sites corresponds to about 40% of the total amount of V-sites of the catalyst.

Chapter 6
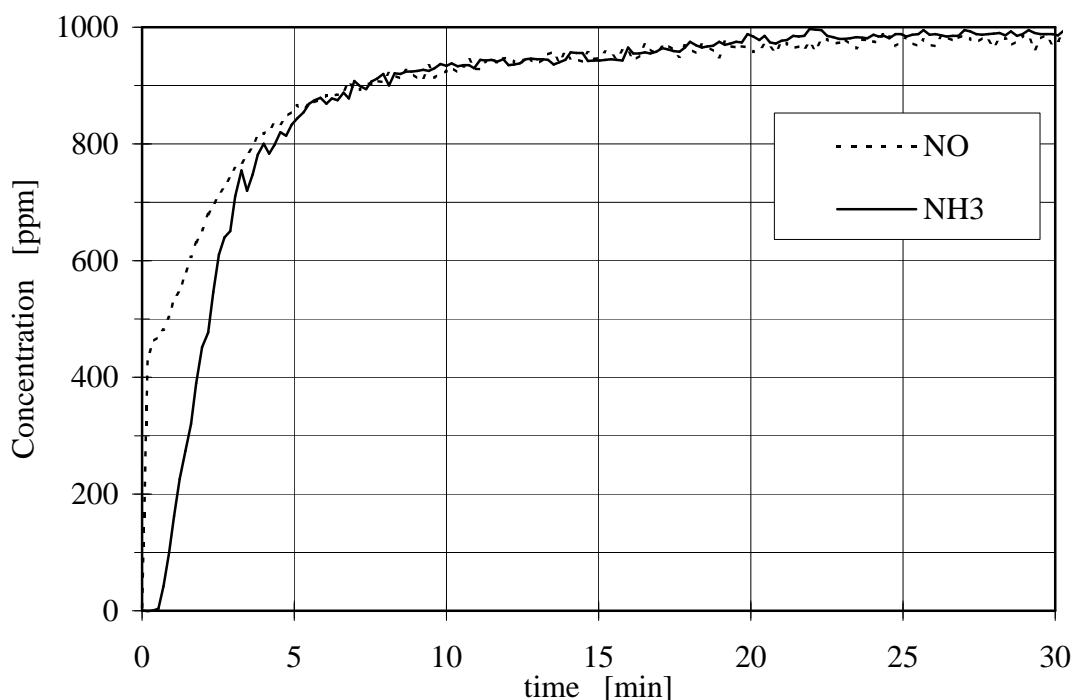
Figure 6.2   Reduction of catalyst D42B. Feed: 1000 ppm NO, 1000 ppm NH$_3$, 5% H$_2$O, balance N$_2$.

Figure 6.3 shows the results of the re-oxidation of the catalyst by NO$_2$ in terms of concentrations of NO and NO$_2$ at the reactor outlet vs. time (after the reported thermal stripping of adsorbed ammonia). The re-oxidation of the V^{+4} sites by NO$_2$ leads to the formation of NO which is detected at the reactor outlet.

The quantitative analysis of the curves in Figure 6.3 shows that the amount of NO detected at the reactor outlet corresponds to the amount of NO$_2$ consumed in the process (0.35 mmol). From these considerations, we propose the following scheme for the re-oxidation of the V^{+4} sites by NO$_2$:

$$2\ V^{+4}OH\ +\ NO_2\quad \rightarrow \quad 2\ V^{+5}{=}O\ +\ NO\ +\ H_2O \tag{6.4}$$
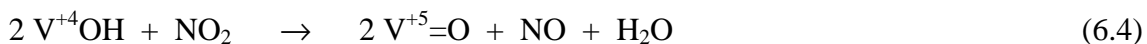
According to this reaction the number of the V-sites is twice the amount of NO produced in the re-oxidation: $2 \cdot 0.35 = 0.7$ mmol. This value is close to the value of 0.84

The probable role of NO$_2$ in the fast SCR reaction

mmol obtained previously considering the amount of NO consumed during the reduction of the catalyst.
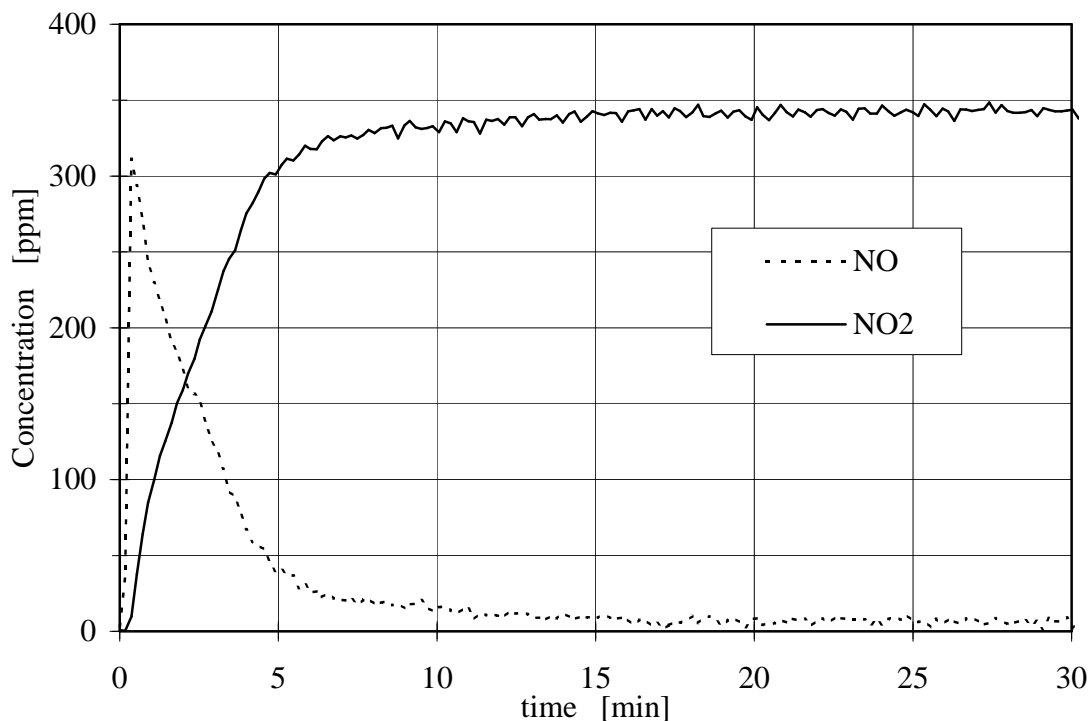
Figure 6.3   Re-oxidation of catalyst D42B. Feed: 345 ppm NO_2, 5% H_2O, balance N_2.

If ammonia is present together with NO_2 during the re-oxidation phase, the situation becomes more complex. NO formed in reaction (6.4) will react with NO_2 and NH_3 on the catalyst according to the fast SCR reaction (6.1). Therefore, the amount of NO detected at the reactor outlet is much lower than the amount formed according to (6.4) and additional NO_2 is consumed in the fast SCR reaction. Figure 6.4 reports the re-oxidation of the catalyst with a stream containing NH_3 and NO_2. After $\approx$ 15 minutes, the concentration of NO_2 approaches a stationary value. The difference between the NO_2 concentration in the feed and the stationary value is the amount consumed according to the SCR reaction involving NO_2 only:

$$4\,NH_3 \; + \; 3\,NO_2 \quad \rightarrow \quad 3.5\,N_2 \; + \; 6\,H_2O \tag{6.5}$$

Chapter 6

Figure 6.4 reports also the DeNOx vs. time for this experiment. The DeNOx vs. time curve falls gradually to a stationary value which is reached after about 15 minutes. The stationary value is due to the SCR reaction (6.5) with pure NO_2. The decrease of $DeNO_x$ with time can be explained as follows: At the beginning, NO_2 reacts not only with NH_3 but also reoxidizes the V^{+4} sites thereby forming NO. This NO reacts with NH_3 and NO_2 according to the fast SCR reaction (6.1). Consequently, the DeNOx is initially high, then decreases with time as the V^{+4} sites are oxidized. In the steady-state only reaction (6.5) occurs, and the DeNOx corresponds to the conversion of NO_2 in this reaction. The amount of NO formed in the re-oxidation of the V^{+4} sites corresponds to the amount of NO_2 that reacts in reaction (6.1). An exact quantitative evaluation of Figure 6.4 is not possible. However, it shows that the re-oxidation of the V^{+4} sites occurs according to reaction (6.4) also when NH_3 is present in the system.
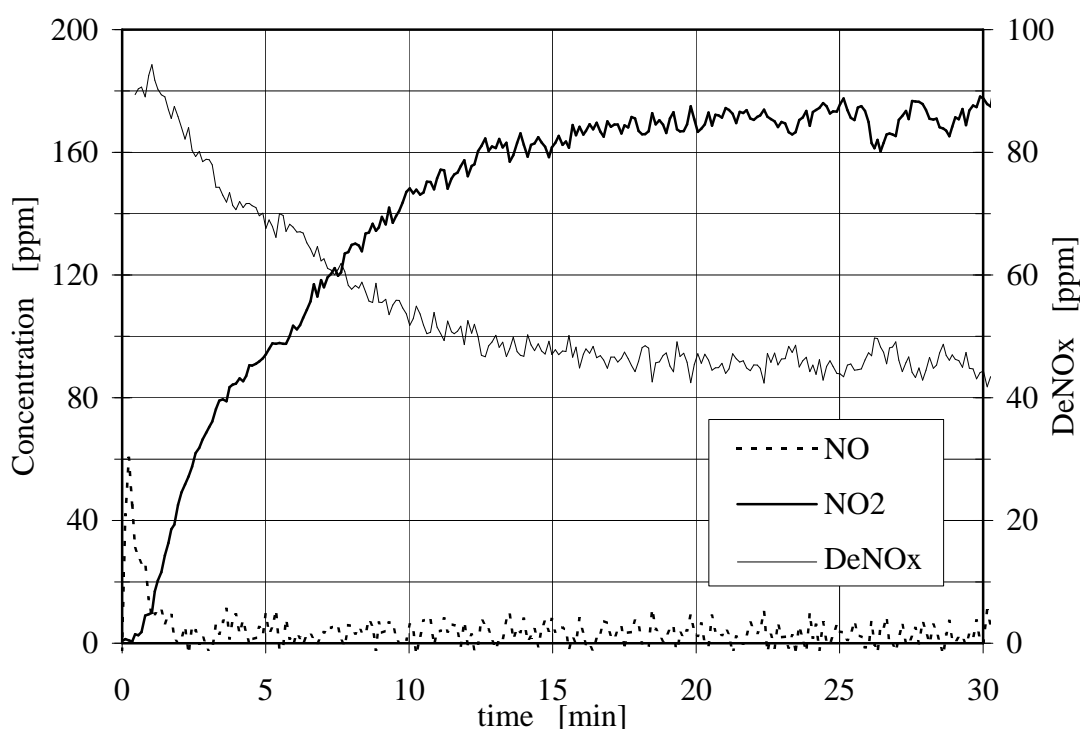
Figure 6.4   Re-oxidation of catalyst D42B. Feed: 320 ppm NO_2, 350 ppm NH_3, 5% H_2O, balance N_2.

The probable role of NO_2 in the fast SCR reaction

The above experiment was repeated with an oxidized SCR catalyst. In this case the concentration of NO_2 at the reactor outlet and the DeNOx approach the steady-state values much faster (Figure 6.5). This confirms that the transient in the values of $DeNO_x$ and in the outlet concentration of NO_2 reported in Figure 6.4 are due to reaction (6.4).
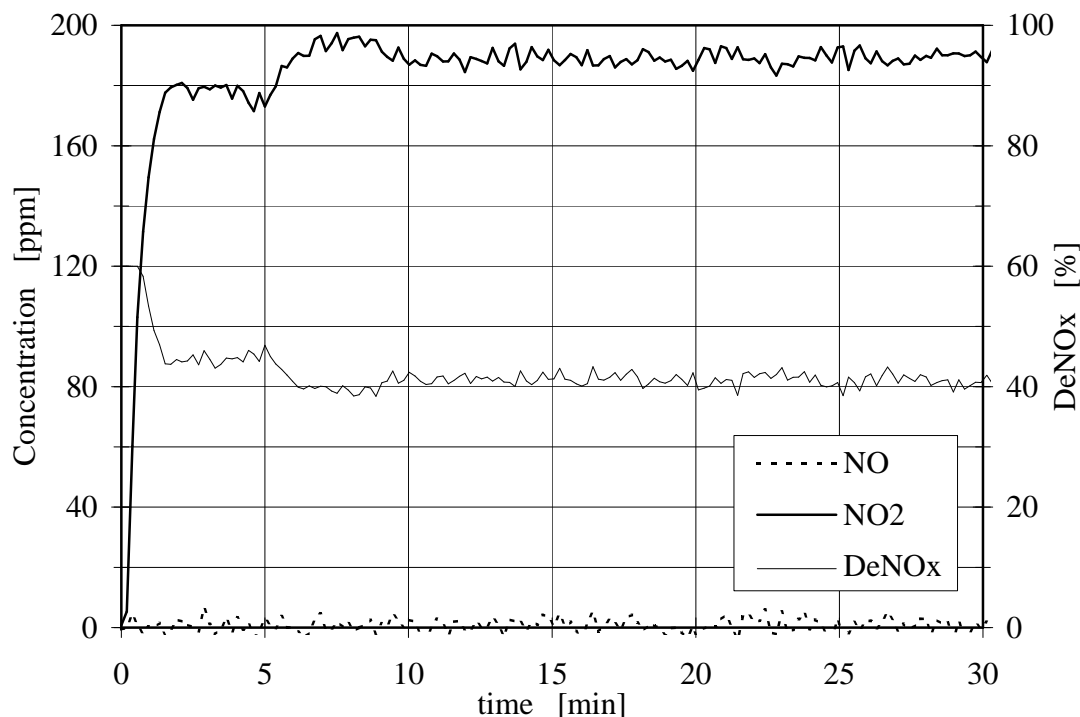
Figure 6.5 Experiment on catalyst D42B not previously reduced. Feed: 320 ppm NO_2, 350 ppm NH_3, 5% H_2O, balance N_2.

6.3.3 In-situ Raman experiments

The Raman spectra of the calcined catalyst before and after data treatment are shown in Figure 6.6. The sum of the area of the $V^{+5}=O$ stretching peaks (dark gray in Figure 6.6b) was calculated and its variation with temperature during re-oxidation was considered.

Figure 6.7 shows the variation of the total area of the $V^{+5}=O$ stretching bands with temperature during the oxidation of a TiO_2-V_2O_5 catalyst, previously reduced with NH_3.

Two different oxidation treatments were carried out, one with synthetic air, the other with 900 ppm NO_2/N_2. With both oxidizing mixtures the intensity of the $V^{+5}=O$ increases with increasing temperature indicating that new $V^{+5}=O$ groups are formed by oxidation of V^{+4} centers. The slope of the I (V=O) vs. T curve corresponding to re-oxidation with the NO_2-containing mixture is higher, suggesting that the oxidation of V^{+4} centers with 900 ppm NO_2/N_2 is faster than the corresponding reaction with air.

It is theoretically possible to extract from the I (V=O) vs. T plots in Figure 6.7 the kinetic parameters of the oxidation of V^{+4} centers with NO_2 and air. However, this operation is complicated by two facts. First, the temperature of the area of the catalyst generating the detected Raman signal might be significantly different from the one of the surrounding material, due to the heat developed by the absorption of the laser beam. Second, the relation between the intensity of the sum of the $V^{+5}=O$ stretching bands and the amount of V^{+5} centers in the catalyst is of a complex nature. As a matter of fact it is well known that the intensity of the $V^{+5}=O$ stretching bands is strongly influenced by a number of structural properties, e.g. the degree of polymerization of the V^{+5} centers, as well as the degree of hydration and the crystallinity of the vanadium oxide phase [10,14].

However these complications do not prevent a qualitative use of the plots in Figure 6.7. Since all experimental parameters (e.g. laser power, heating rate, grain-size) were the same during the re-oxidation treatments with 900 ppm NO_2/N_2 and with air, it can be safely assumed that the temperature deviation of the laser-irradiated spot was the same for both experiments. In other words, the temperature scale in Figure 6.7 might not reflect the actual temperature of the laser-irradiated spot during the re-oxidation ramp, but is surely the same for both curves. Similarly, a significant influence of a different evolution of the structural properties listed above on the shape of the I (V=O) vs. T curves for the two oxidizing agents is not likely. This is supported by the fact that the $V^{+5}=O$ intensity at the end of both re-oxidation treatments is the same, indicating that the chosen oxidizing agent has no influence on the structural properties of the completely oxidized vanadium oxide obtained at the end of the heating ramps.

The probable role of NO₂ in the fast SCR reaction
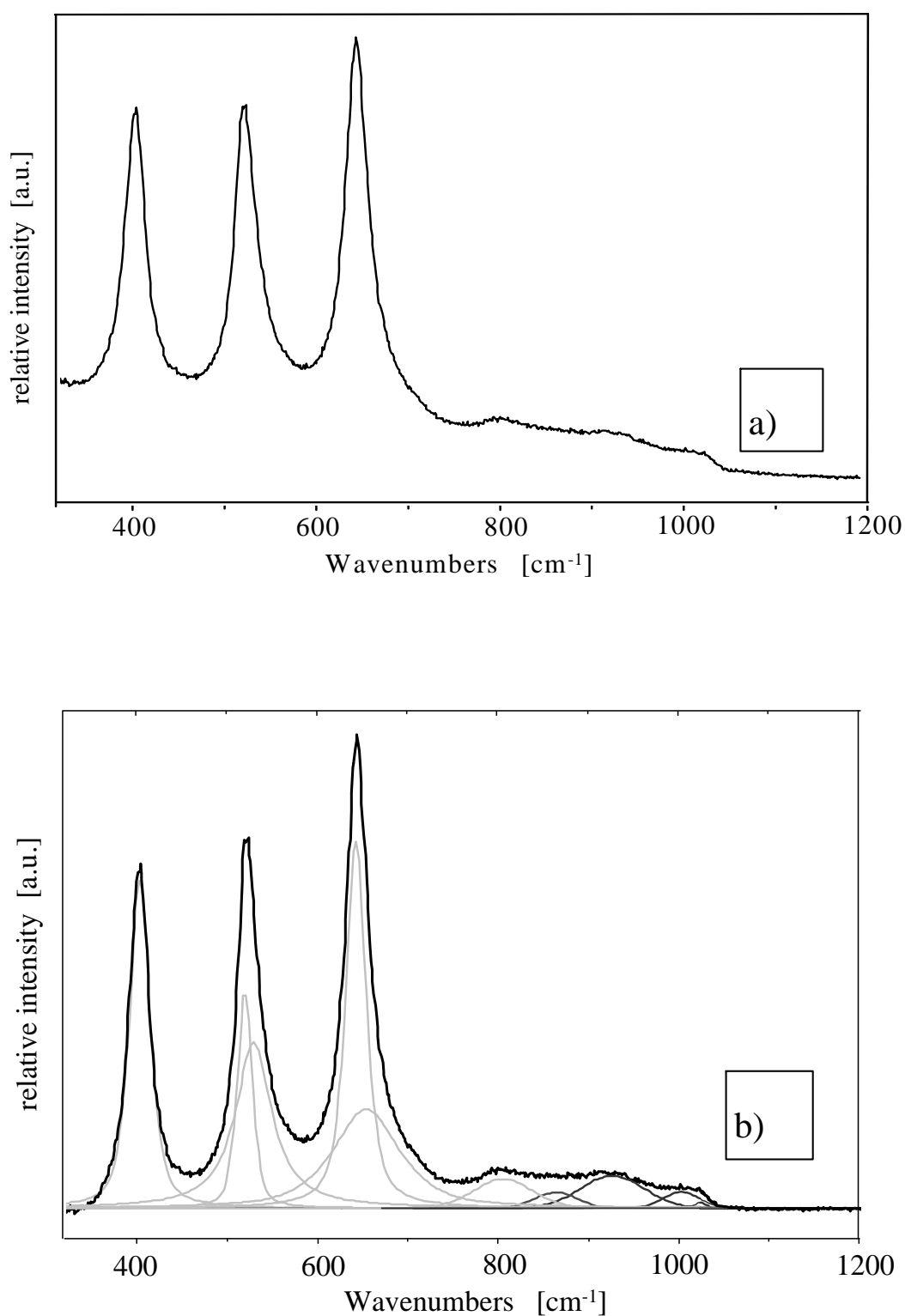
Figure 6.6 Raman spectra of the calcined catalyst. a) as measured; b) after baseline correction and band deconvolution (see text). Pale gray lines indicate anatase peaks, dark gray lines V=O stretching bands.
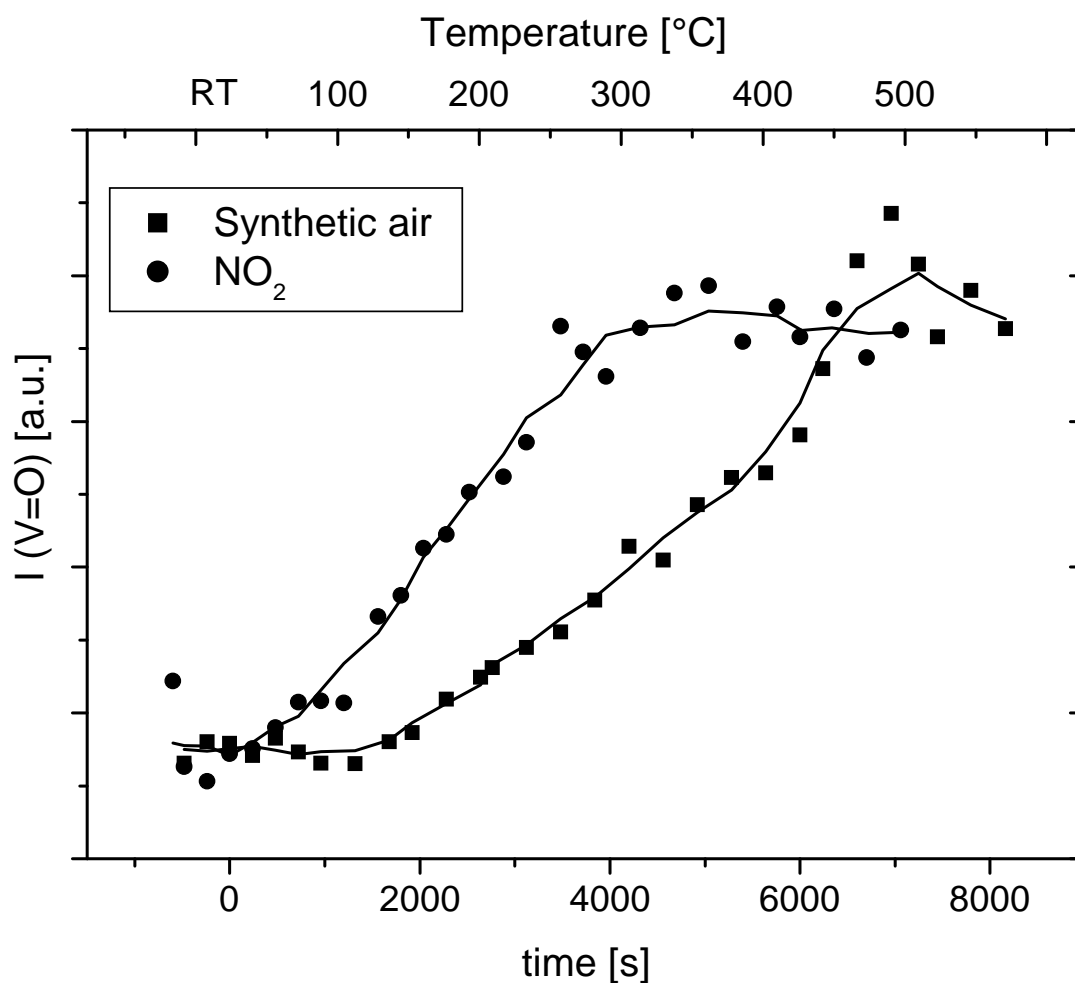
Figure 6.7   Variation of the V=O stretching bands (sum of all areas) with tempera-
ture in a) synthetic air (squares) and b) 900 ppm NO_2/N_2 (circles). The
black lines are obtained by adjacent point smoothing of the data. Heating
rate = 4 °C/min. The ramp was started at t = 0 s (T = 22°C) and was
stopped after 7080 s (T = 500°C). Negative times refer to spectra ac-
quired before the beginning of the heating ramp.

The probable role of NO_2 in the fast SCR reaction

It is plausible that such a lack of influence of the specific oxidizing agent on the structural properties of the catalyst is valid at any stage of the oxidation treatment and that the intensity of the $V^{+5}=O$ stretching bands is related to the amount of V^{+5} present in the catalyst in the same way for both oxidizing agents. Therefore, it can be concluded that the steeper increase of I (V=O) observed during treatment with the NO_2/N_2 mixture is a direct indication of a faster oxidation of V^{+4} sites with 900 ppm NO_2/N_2 than with air.

6.3.4 Proposed reaction mechanism

The rate of NO_x conversion of the standard SCR reaction is influenced by the presence of oxygen at temperatures below 300°C. This implies that oxygen is involved in the rate determining step of this reaction under these conditions. On the other hand, the fast SCR reaction does not depend on oxygen concentration and even proceeds in the absence of oxygen, indicating that oxygen is not involved in the mechanism of this reaction. At temperatures below 300°C the fast SCR reaction is faster than the standard SCR reaction, whereas the rates of both reactions converge at higher temperatures. These observations can be accounted for assuming that in the fast SCR reaction NO_2 plays the role of oxygen, speeding up the rate limiting step at low temperatures. The mechanisms proposed for the standard SCR reaction [15,16] postulate that oxygen is essential for the re-oxidation of the vanadium sites of the catalyst. In the case of the fast SCR reaction this role is played by NO_2 in a much more efficient way. The Raman experiments have confirmed that NO_2 re-oxidizes the vanadium sites faster than oxygen thus explaining the higher rate of the fast SCR reaction at low temperatures. Furthermore, transient experiments have shown that one molecule of NO is formed for each molecule of NO_2 consumed in the re-oxidation of the vanadium sites (equation 6.4). From these observations, we propose a mechanism for the fast SCR reaction similar to the one suggested by Ramis et al. [15] for the standard SCR reaction:

$$V^{+5}=O \ + \ NH_3 \quad \rightarrow \quad HO\text{-}V^{+4}\text{-}N^\bullet H_2 \tag{I}$$

$$HO\text{-}V^{+4}\text{-}N^\bullet H_2 \ + \ {}^\bullet NO \quad \rightarrow \quad HO\text{-}V^{+4}\text{-}(NH_2)\text{-}NO \tag{II}$$

$$HO\text{-}V^{+4}\text{-}(NH_2)\text{-}NO \quad \rightarrow \quad HO\text{-}V^{+4} \ + \ N_2 \ + \ H_2O \tag{III}$$

$$2\,HO\text{-}V^{+4} \ + \ NO_2 \quad \rightarrow \quad 2\,V^{+5}=O \ + \ {}^\bullet NO' \ + H_2O \tag{IV}$$

$$V^{+5}=O \ + \ NH_3 \quad \rightarrow \quad HO\text{-}V^{+4}\text{-}N^\bullet H_2 \tag{I'}$$

$$HO\text{-}V^{+4}\text{-}N^\bullet H_2 \ + \ {}^\bullet NO' \quad \rightarrow \quad HO\text{-}V^{+4}\text{-}(NH_2)\text{-}NO' \tag{II'}$$

$$HO\text{-}V^{+4}\text{-}(NH_2)\text{-}NO' \quad \rightarrow \quad HO\text{-}V^{+4} \ + \ N_2 \ + \ H_2O \tag{III'}$$

$$2\,NH_3 \ + \ NO \ + \ NO_2 \quad \rightarrow \quad 2\,N_2 \ + \ 3\,H_2O \tag{1}$$
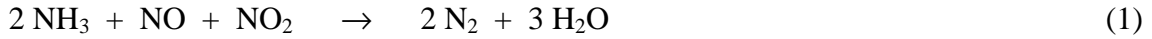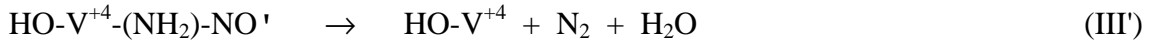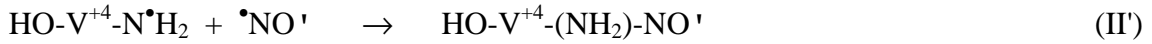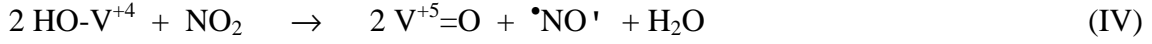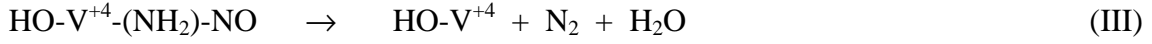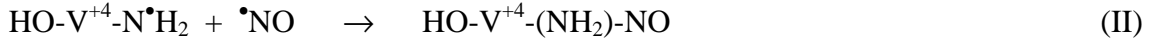
$${}^\bullet NO' \ = \ {}^\bullet NO \text{ formed from } NO_2 \text{ in (IV)}$$

This reaction mechanism differs only in the re-oxidation step (IV) from the mechanism proposed by Ramis et al. [15] for the standard SCR reaction. Therefore, the fast SCR reaction can be considered as a standard SCR reaction in which NO_2 plays the role of supplying more reactive oxygen for the re-oxidation of the catalyst.

6.5   Conclusions

The re-oxidation of the vanadium sites is the rate limiting step in the standard SCR reaction at temperatures below 300°C. In the fast SCR reaction NO_2 is very effective in speeding up this critical step. The faster re-oxidation of the vanadium sites by NO_2 allows to increase the reaction rate of the SCR process at low temperatures. The fast SCR reaction can be considered as a standard SCR reaction in which NO_2 plays the role of a more efficient oxidizer for the vanadium sites.

6.5   References

[1]   E. Jacob, G. Emmerling et al., *NOx-Verminderung für Nutzfahrzeugmotoren mit Harnstoff-SCR-Kompaktsystemen (GD-KAT)*, Fortschritt-Berichte VDI Reihe 12, Nr. 348, Bd. 1, 19th Int. Vienna Motor Symposium, May 7-8 1998, p. 366

[2]   J. Gieshoff, A. Schäfer-Sindlinger, P. C. Spurk, J. A. A. van der Tillaart and G. Garr, *SAE Paper* N. 2000-01-0189.

[3]   G. R. Chandler, B. J. Cooper, J. P. Harris, J. E. Thoss, A. Uusimäki, A. P. Walker and J. P. Warren, *SAE Paper* N. 2000-01-0188.

[4]   L. Hofmann, W. Mathes and S. Fischer, *Die Entwicklung des SINOx-Systems für Nutzfahrzeuge zur Serienreife*, 20th Int. Vienna Motor Symposium, May 6-7 1999.

[5]   M. Koebel, M. Elsener and M. Kleemann, *Catal. Today* **59** (2000), 335

[6]   M. Koebel, M. Elsener and G. Madia, *Ind. Chem. Eng. Res.* **40** (2001), 52

[7]   D. Bersani, P. P. Lottici, M. Braghini and A. Montenero*, Phys. Stat. Sol. (b)* **K5** (1992), 170

[8]   S.S. Chan, I.E. Wachs, L.L. Murrel, L. Wang and W. Keith Hall, *J. Phys. Chem.* **88** (1984), 5831

[9]   L.J. Alemany, L. Lietti, N. Ferlazzo, G. Busca, E. Giamello and F. Bregani, *J. Catal.* **155** (1995), 117

[10]   G.T. Went, L.J. Leu, R.R. Rosin and A.T. Bell, *J. Catal.* **134** (1992), 492

[11]   L. Lietti, P. Forzatti and F. Bregani, *Ind. Eng. Chem. Res.* **35** (1996), 3884

[12]   L. Casagrande, L. Lietti, I. Nova, P. Forzatti and A. Baiker, *Appl. Catal. B* **22** (1999), 63

[13]   J.M Hermann and J. Disdier, *Catal. Today* **56** (2000), 389

[14]   G. T. Went, S. Ted Oyama and A. T. Bell, *J. Phys. Chem.* **94** (1990), 4246

[15]   G. Ramis, G. Busca, F. Bregani and P. Forzatti, *Appl. Catal.* **64** (1990), 259

[16]   N. Y. Topsoe, *Science* **265** (1994), 1217

The probable role of NO$_2$ in the fast SCR reaction

7

Side reactions of the SCR process

7.1   Introduction

The reduction of nitric oxide with ammonia or other N-containing reducing agents by SCR is generally considered to be highly selective. The term "selective" refers primarily to the oxidizing educts of the reduction: NO shall be reduced in preference to O_2 which is present in lean exhaust gases in much higher amounts. This means that the standard SCR reaction (7.1) should proceed at a much higher rate than reaction (7.2), usually designated as Selective Catalytic Oxidation (SCO):

$$4\,NH_3 \;+\; 4\,NO \;+\; O_2 \;\rightarrow\; 4\,N_2 \;+\; 6\,H_2O \tag{7.1}$$

$$4\,NH_3 \;+\; 3\,O_2 \;\rightarrow\; 2\,N_2 \;+\; 6\,H_2O \tag{7.2}$$

However, the term "selective" also refers to the products. Elementary nitrogen (and water) is the desired product of the DeNOx process, but the formation of higher oxidized nitrogen species like N_2O, NO and NO_2 cannot be excluded. N_2O is undesired due to its potential for depleting stratospheric ozone and its strong greenhouse warming effect [1]. Additionally, the formation of N_2O, NO and NO_2 leads to a deterioration of the DeNOx effect and to an unnecessary consumption of reducing agent.

It should be mentioned that, according to this definition, the selectivity of the SCR reaction (7.1) is not 100 % for NO, because four NO molecules are reduced together with one oxygen molecule. Making the balance in terms of electrons transferred to NO

and O_2, the ratio is 2:1 resulting in a selectivity of 2/3 for the reduction of NO and 1/3 for the reduction of O_2. Nevertheless, SCR with N-containing reducing agents is about two orders of magnitude more selective than so-called HC-SCR using hydrocarbons. Evaluating published results on HC-SCR in terms of NO-selectivity yields typical values of the order of a percent.

Much work on the SCR reaction and its selectivity has been done on "model" catalysts applying "pure" operating conditions (catalysts with high V-content and no W, absence of water in the feed). However, these investigations were focused on special aspects and suffered from a lack of realistic catalysts and realistic operating conditions.

This chapter reports investigations on the selectivity of SCR reactions obtained with "real" catalysts under operating conditions matching those of diesel exhaust. The experiments were carried out with a monolithic SCR catalyst (M11) prepared in house according to the procedure described in chapter 3. The subject will be discussed not only for the "standard SCR" reaction but also for the "fast SCR" and the "NO_2-SCR" reaction, i.e. for the cases where the gas contains NO_2 in addition to NO.

7.2   Chemistry and known facts

7.2.1   Side reactions of the standard SCR reaction (only NO present)

The standard SCR reaction is the sole possible DeNOx reaction if the feed gas contains NO_x only in the form of NO. The most evident byproduct of the standard SCR reaction (7.1) is nitrous oxide N_2O. On typical commercial catalysts based on TiO_2-WO_3-V_2O_5 its formation gets perceptible at temperatures above $\approx 380°C$. Other possible byproducts like NO, NO_2 and N_2 from the SCO reaction (7.2) are not detectable by the usual analytical techniques. On the other hand, a consumption of reducing agent (NH_3) exceeding the theoretical value according to (7.1) is often observed at temperatures above 380°C.

Considering the formation of these byproducts at higher temperatures under standard SCR conditions the following reactions of ammonia with oxygen are possible:

$$4\,NH_3 \;+\; 3\,O_2 \;\rightarrow\; 2\,N_2 \;+\; 6\,H_2O \tag{7.2}$$

$$4\,NH_3 \;+\; 4\,O_2 \;\rightarrow\; 2\,N_2O \;+\; 6\,H_2O \tag{7.3}$$

$$4\,NH_3 \;+\; 5\,O_2 \;\rightarrow\; 4\,NO \;+\; 6\,H_2O \tag{7.4}$$

$$4\,NH_3 \;+\; 7\,O_2 \;\rightarrow\; 4\,NO_2 \;+\; 6\,H_2O \tag{7.5}$$

$$4\,NH_3 \;+\; 4\,NO \;+\; 3\,O_2 \;\rightarrow\; 4\,N_2O \;+\; 6\,H_2O \tag{7.6}$$
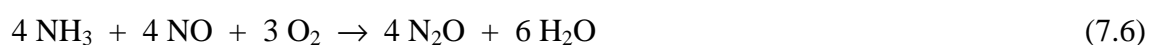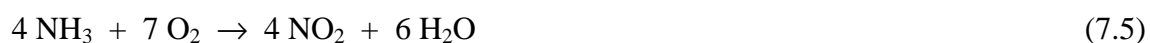
Considering first reactions (7.2) to (7.5) we can see that the degree of ammonia oxidation increases in a systematic way. This is evident from the increasing amount of oxygen consumed and from the increasing oxidation number of nitrogen in the product (Table 7.1).

Table 7.1   Oxidation of ammonia with oxygen according to reactions (7.2) - (7.5)

reaction Nr.	product	electrons transferred $NH_3 \rightarrow$ product	oxidation number of N in product
(7.2)	N_2	3	0
(7.3)	N_2O	4	+1
(7.4)	NO	5	+2
(7.5)	NO_2	7	+4

Il'Chenko and Golodets [2] have investigated the basic phenomena of ammonia oxidation with oxygen over metal oxide catalysts. They have shown that the catalytic activity and the product selectivity depend on the bond energy of surface oxygen in a very general way. Oxides with low surface oxygen bond energy show high activity and favor

Side reactions of the SCR process

the formation of products of deep oxidation (NO, NO_2). The inverse is observed for oxides with high surface oxygen bond energy: low catalytic activity and the preferential formation of products of mild oxidation (N_2, N_2O). In addition, increasing temperature shifts the product distribution towards deep oxidation. V_2O_5 catalysts were reported to be very selective for N_2 formation at low temperatures. On the other hand, noble metal catalysts like Pt and Pd are very effective in promoting deep oxidation, i.e. formation of NO/NO_2.

Li et al. [3] investigated the SCO of ammonia on TiO_2-V_2O_5 catalysts. Water was found to inhibit the activity and to increase the selectivity for the oxidation of ammonia to N_2. Ramis et al. [4] suggested that hydrazine (N_2H_4) is an intermediate species in the mechanism of the SCO of ammonia.

Let us now look at the special case of nitrous oxide formation under the conditions of standard SCR (presence of O_2, NO, NH_3,). Considering the equations above it is clear that N_2O may be formed from oxidation of ammonia by O_2 (reaction 7.3) or from oxidation by NO + O_2 (reaction 7.6). The key question is which reaction is prevailing under typical SCR conditions. Isotopic labeling experiments over TiO_2-V_2O_5 catalysts performed by various groups [5-10] have shown that, under SCR conditions, one of the two N-atoms originates from ammonia and the other from NO. This suggests that nitrous oxide is formed mainly according to reaction (7.6) over these catalysts.

Odenbrand et al. [11] and Kotter et al. [12] investigated the formation of N_2O over TiO_2-V_2O_5 catalysts with a V_2O_5-content higher than 20 %, i.e. more than a monolayer. They found that the formation of nitrous oxide is catalyzed by crystalline V_2O_5. Topsoe et al. [13] investigated the influence of water on the reactivity of TiO_2-V_2O_5 catalysts for the reduction of nitric oxide and observed that water inhibits the activity for SCR at temperatures lower than 663 K, while preventing the formation of N_2O.

7.2.2   Side reactions in the presence of NO_2

An improved SCR process relies on the fact that the SCR reaction is much faster with an equimolar mixture of NO and NO_2 than with pure NO [14,15]:
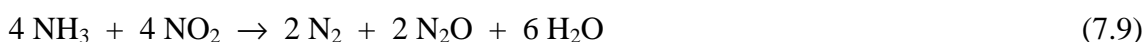
$$4\,NH_3 + 2\,NO + 2\,NO_2 \rightarrow 4\,N_2 + 6\,H_2O \qquad \text{(fast SCR reaction)} \qquad (7.7)$$
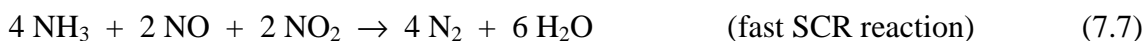
The effect of NO_2 is most pronounced at low temperatures where an increase in reaction rate is most essential. However, if NO_x downstream of the oxidation catalyst contains more than 50% NO_2, excessive NO_2 can only react according to the reaction equation of NO_2-SCR:

$$4\,NH_3 + 3\,NO_2 \rightarrow 3.5\,N_2 + 6\,H_2O \qquad (7.8)$$

This reaction is even slower than the standard SCR reaction, what may favor the contribution of other side reactions, and consequently change the order of selectivities.

In exhaust gases containing NO_2, a formation of N_2O may also be observed at low temperatures, especially if the concentration of NO_2 in the feed exceeds that of NO. In a recent paper Blanco et al. [16] report an enhanced formation of nitrous oxide on a TiO_2-V_2O_5 catalyst for a NO_x feed containing NO_2. The experiments were performed at low temperatures (180-230°C) and in the absence of water. The following reactions should be considered for the formation of nitrous oxide in exhaust gases containing NO_2:

$$4\,NH_3 + 4\,NO_2 \rightarrow 2\,N_2 + 2\,N_2O + 6\,H_2O \qquad (7.9)$$

$$6\,NH_3 + 8\,NO_2 \rightarrow 7\,N_2O + 9\,H_2O \qquad (7.10)$$

$$4\,NH_3 + 4\,NO_2 + O_2 \rightarrow 4\,N_2O + 6\,H_2O \qquad (7.11)$$

This chapter will also consider the enhanced formation of nitrous oxide at lower temperatures due to the presence of NO_2.

7.3   Selectivities

The common notion of selectivity refers to the formation of different products. Usually, a species is involved in two or more reactions leading to the formation of several products, e.g. :

$$\nu_A\, A \;\rightarrow\; \nu_B\, B \tag{7.12}$$

$$\nu_A\, A \;\rightarrow\; \nu_C\, C \tag{7.13}$$

The selectivity for product B is then defined as:

$$S_B = \frac{B\ produced}{B\ produced\ +\ C\ produced}\quad \left[\frac{mol}{mol}\right] \tag{7.14}$$

In the case of SCR such a definition based on the product distribution is not very useful. In this case, the primary interest is the selective reduction of NO_x in the presence of oxygen. This calls for an appropriate definition referring to the selective reduction of NO_x. The definition should also take into account that the desired product (N_2) can be formed not only by SCR reactions, but also by the selective catalytic oxidation of ammonia (SCO), thus leading to an increased consumption of reducing agent. Therefore, high product selectivity to nitrogen may also be observed with a catalyst showing high SCO activity for ammonia (7.2). In the evaluation of the experiments, we will use the following definition of selectivity for the standard SCR and the fast SCR reaction:

$$S_{NOx} = \frac{NO_x\ converted}{NH_3\ consumed}\quad \left[\frac{mol}{mol}\right] \tag{7.15}$$

According to this definition the selectivity is 100% if all ammonia consumed in the process has reacted with NO_x in the standard SCR reaction (7.1) and the fast SCR reaction (7.7). Due to the fact that the stoichiometric coefficients ν_{NH3} and ν_{NOx} are not equal for the NO_2-SCR reaction (7.8), the corresponding equation would be:

$$S_{NO2} = \frac{4}{3}\cdot\frac{NO_2\ converted}{NH_3\ consumed}\quad \left[\frac{mol}{mol}\right] \tag{7.16}$$

Chapter 7

In the case that side reactions take place, additional ammonia will be consumed by these reactions. This will become evident if S_{NOx} or S_{NO2} are lower than 1. However, due to the fact that N_2 and NO/NO_2 cannot be distinguished experimentally from N_2 formed in DeNOx reactions and from NO/NO_2 present in the original feed, the corresponding selectivities cannot be determined. The only detectable new product is N_2O, so the following selectivity definition will be used in the discussion of the results:

$$S_{N_2O} = \frac{\nu_{NH_3} \cdot N_2O \text{ formed}}{\nu_{N_2O} \cdot NH_3 \text{ consumed}} \left[\frac{mol}{mol} \right] \qquad (7.17)$$

where ν_{NH3} and ν_{N2O} are the stoichiometric coefficients of ammonia and nitrous oxide of the respective reaction equation.

For the special case where the feed contains no nitrogen oxides, but only ammonia and oxygen, the amounts of N_2O, NO and NO_2 formed on the catalyst can be measured, N_2 may be obtained by difference. Selectivities referring to the total amount of ammonia consumed may thus be obtained as:

$$S_i = \frac{\nu_{NH_3} \cdot \text{Product (i) formed}}{\nu_i \cdot NH_3 \text{consumed}} \left[\frac{mol}{mol} \right] \qquad (7.18)$$

where ν_{NH3} and ν_i are again the stoichiometric coefficients of ammonia and product i of the respective reaction equation.

7.4   Experimental

The description of the experimental apparatus used in these investigations has been reported in chapter 2. The SCR catalyst was prepared in house according to the recipe described in chapter 3. The monolithic SCR catalyst M11 was used in these investigations; its specifications are reported in Table 3.1. The investigations were performed at gas hourly space velocity (GHSV) of 52000 h^{-1}. The base feed is composed of 5% H_2O (if present), 10% O_2 with balance N_2.

Side reactions of the SCR process

7.5   Results

7.5.1   Direct oxidation of ammonia

Figure 7.1 reports the overall conversion of NH_3 in the presence of oxygen over a TiO_2-WO_3-V_2O_5 catalyst with dry and humid feeds. The conversion of ammonia increases with temperature and is strongly inhibited by the presence of water. E.g., at 350°C, the conversion of ammonia is 85% with a dry feed, but is below 2% when water is present.
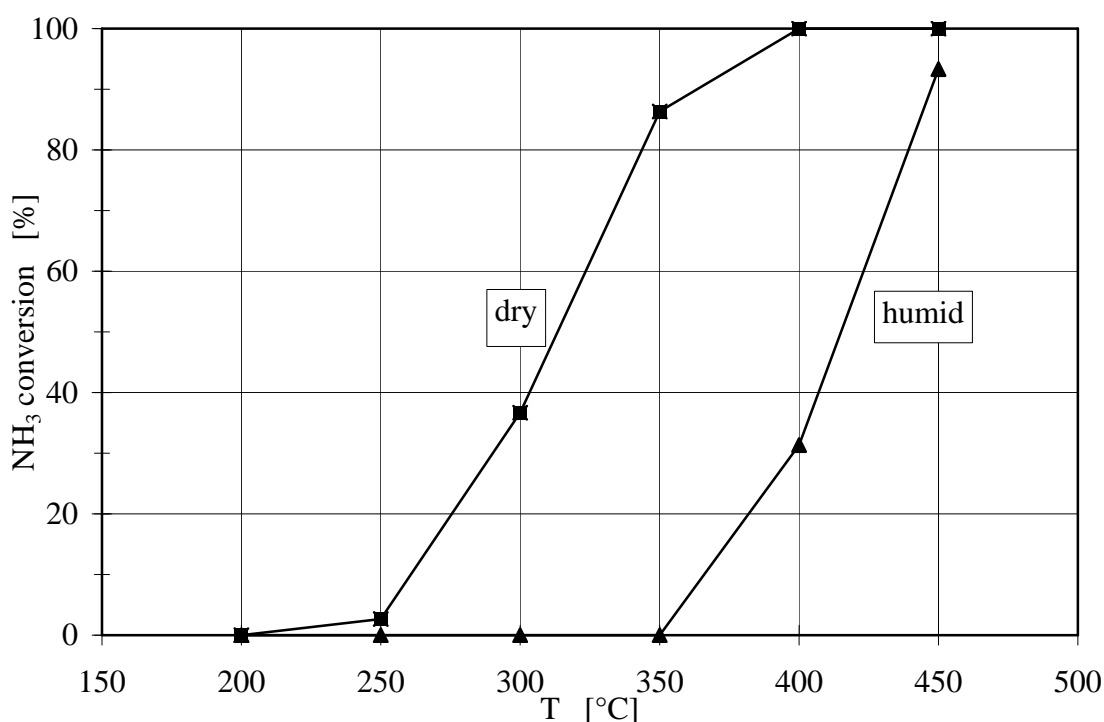
Figure 7.1   Oxidation of ammonia as a function of temperature. Feed: 1000 ppm NH_3, 10% O_2, 5% H_2O (case "humid"), balance N_2.

The amount of ammonia reacted in reactions (7.3), (7.4) and (7.5) is determined indirectly from the amounts of N_2O, NO and NO_2 measured at the catalyst outlet. The remaining amount of ammonia consumed in the process must have been oxidized to nitrogen according to the SCO reaction (7.2). The selectivities for the reactions (7.2), (7.3), (7.4) and (7.5) were evaluated according to equation (7.18) and the results are plotted in Figure 7.2 and 7.3 as a function of temperature for dry and humid feeds. At low temperatures the selectivity for the selective catalytic oxidation (SCO) of ammonia is high,

but decreases with rising temperature. In a dry feed the oxidation of ammonia forms a relevant amount of N_2O above 250°C. Moreover, at 450°C, significant amounts of NO and NO_2 are produced (Figure 7.2). According to Figure 7.3 the presence of water strongly inhibits all reactions but enhances considerably the selectivity for the SCO reaction (7.2). Only at temperatures above 350°C, N_2O formation according to reaction (7.3) becomes noticeable and leads to a loss in the selectivity for the SCO reaction. The amounts of NO and NO_2 formed by direct oxidation of ammonia in a humid feed remain negligible up to 450°C.

7.5.2   Selectivity and DeNOx under SCR conditions

NO$_x$ consisting of pure NO: Under conditions prevailing in a typical exhaust gas, NO is consumed either in the standard SCR reaction (7.1) or in reaction (7.6) forming N_2O. As shown in the previous paragraph, the formation of NO by direct oxidation of ammonia may be neglected in a humid feed. However, SCO of ammonia may occur at very high temperatures.

Table 7.2 reports the gas concentrations at the reactor outlet for a feed containing 300 ppm NO and 300 ppm NH_3 in the humid base feed as well as the selectivities for SCR and N_2O formation. The selectivity for the standard SCR reaction was evaluated according to equation (7.15). The selectivity for the formation of N_2O was evaluated according to equation (7.17), using the stoichiometric coefficients of reaction (7.6). At temperatures below 400°C the amount of N_2O produced is negligible, thus resulting in a very high selectivity for the standard SCR reaction. At temperatures above 350°C the selectivity for the standard SCR reaction decreases with increasing temperature.

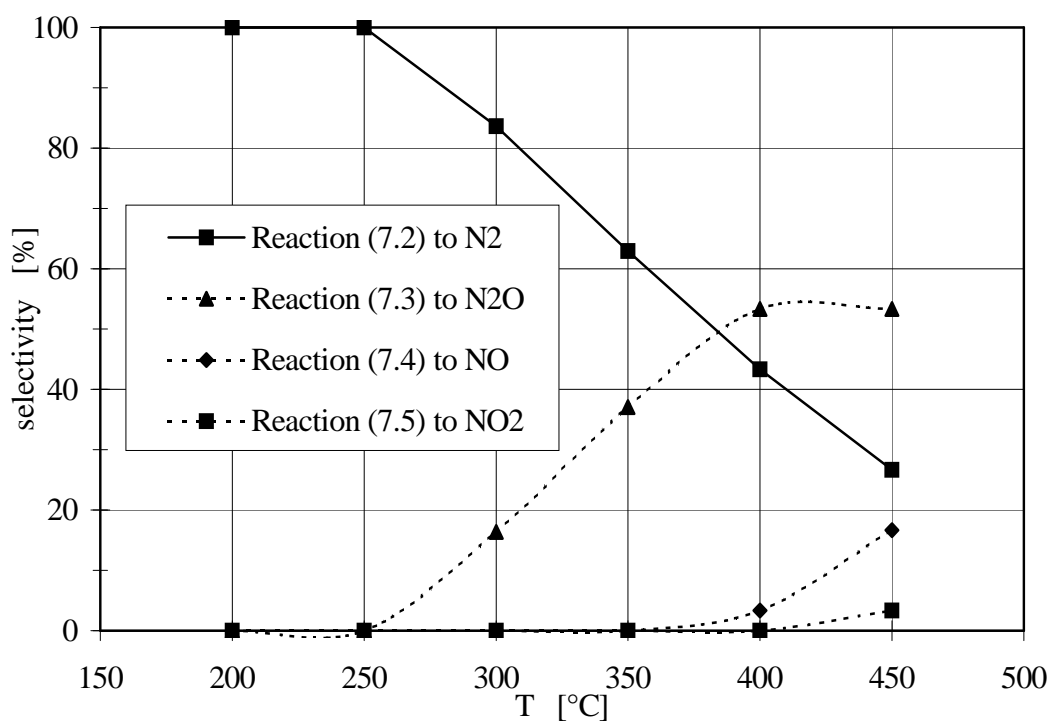*Side reactions of the SCR process*

Figure 7.2 Selectivity for the ammonia oxidation reactions (7.2) to (7.5) in the absence of water. Feed: 1000 ppm NH_3, 10% O_2, balance N_2.
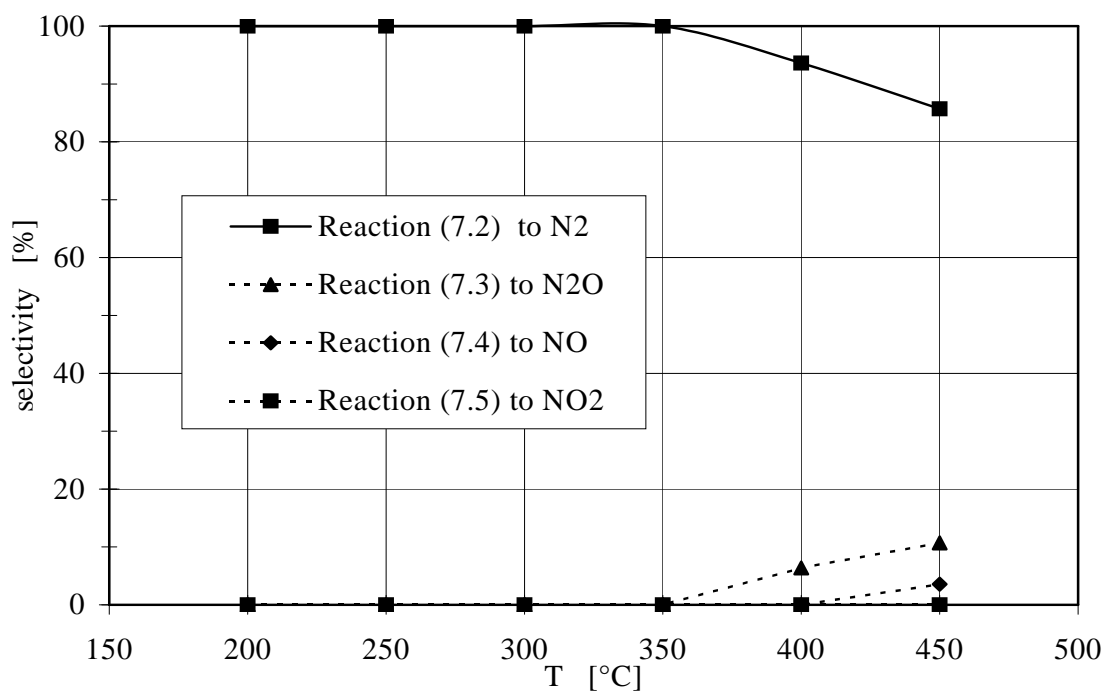

Figure 7.3 Selectivity for the ammonia oxidation reactions (7.2) to (7.5) in the presence of water. Feed: 1000 ppm NH_3, 10% O_2, 5% H_2O, balance N_2.

Chapter 7

At 450°C the sum of the selectivities for the standard SCR reaction and for N$_2$O formation is lower than 100%. The missing difference must be attributed to selective catalytic oxidation of ammonia (reaction 7.2).

Table 7.2   Selectivities for a feed containing pure NO. Feed: 300 ppm NO, 300 ppm NH$_3$, 5% H$_2$O, 10% O$_2$, balance N$_2$.

T [°C]	NO$_{OUT}$ [ppm]	N$_2$O$_{OUT}$ [ppm]	NH$_{3,OUT}$ [ppm]	SCR selectivity [%]	N$_2$O selectivity [%]
200	173	0	180	100	0
250	46	0	44	100	0
300	10	0	13	100	0
350	4	1	7	100	0.3
400	16	5	3	96	1.7
450	81	16	2	73	5.4

NO$_x$ consisting of an equimolar mixture of NO and NO$_2$: The selectivity of the fast SCR reaction was investigated with 150 ppm NO, 150 ppm NO$_2$ and 300 ppm NH$_3$ added to the humid base feed. Table 7.3 reports the concentrations of the gases at the reactor outlet and the selectivities for SCR and N$_2$O formation. The selectivity for the fast SCR reaction was evaluated according to equation (7.15). The selectivity for the formation of N$_2$O was evaluated according to equation (7.17), using the stoichiometric coefficients of reaction (7.6). As in the case of the standard SCR, the selectivity for the fast SCR reaction is very high at temperatures below 400°C, then it decreases with increasing temperature. Vice versa, the selectivity for the formation of N$_2$O, increases with increasing temperature. Again, at 450°C, the sum of the two selectivities is lower than 100%. The missing difference must be attributed to SCO of ammonia (reaction 7.2).

Table 7.3   Selectivities for a feed containing an equimolar mixture of NO and NO_2. Feed: 150 ppm NO, 150 ppm NO_2, 300 ppm NH_3, 5% H_2O, 10% O_2, balance N_2.

T [°C]	NO_{OUT} [ppm]	$NO_{2,OUT}$ [ppm]	N_2O_{OUT} [ppm]	$NH_{3,OUT}$ [ppm]	SCR selectivity [%]	N_2O selectivity [%]
200	4	4	0	8	100	0
250	2	0	0	0	100	0
300	0	0	0	0	100	0
350	2	0	0	0	100	0
400	14	2	4	0	95	1.3
450	83	10	16	0	69	5.3

NO_x consisting of pure NO_2: The SCR reaction with NO_2 according to (7.8) is much slower than the fast SCR reaction and still slower than the standard SCR reaction [17]. Table 7.4 resumes the results of experiments with a humid base feed containing 300 ppm NO_2 and 300 ppm NH_3. The SCR selectivity was calculated using equation (7.16). The N_2O selectivity was evaluated according to equation (7.17), using the stoichiometric coefficients of reaction (7.10).

It can be seen that the SCR selectivity is 100 % only at medium temperatures of 300 – 350°C, but may easily reach values above 100% at lower and higher temperatures. This means that the NO_2-SCR reaction (7.8) is observed as the sole reaction only at medium temperatures. Selectivities above 100 % must be interpreted as a stoichiometry ν_{NH3}/ν_{NO2} differing from reaction for pure NO_2 SCR ($\nu_{NH3}/\nu_{NO2} = 4/3$). At high temperatures the conversion of NO_2 to NO, favored by the thermodynamic equilibrium $NO_2 \Leftrightarrow NO + \frac{1}{2}O_2$, allows for the fast SCR reaction (7.7) with $\nu_{NH3}/\nu_{NO2} = 1$. At low temperatures the NO_2-SCR reaction competes with reaction (7.19), which has also $\nu_{NH3}/\nu_{NO2} = 1$ and may lead to the formation of ammonium nitrate [17]:

Chapter 7

$$4\,NH_3 \,+\, 4\,\ NO_2 \,\rightarrow\, 2\,NH_4NO_3 \,+\, 2\,N_2 \,+\, 2\,H_2O \qquad\qquad (7.19)$$
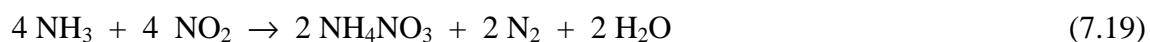
Reaction (7.19) has a negative temperature coefficient and thus becomes important at low temperatures. Looking at the N_2O selectivity it can be seen that the trend is completely different from the first two cases, where the N_2O formation was restricted to the highest temperatures. In the case of pure NO_2 in the feed, a moderate N_2O selectivity is observed over the whole temperature range 250-450°C.

Table 7.4 Selectivities for a feed containing NO_2 only. Feed: 300 ppm NO_2, 300 ppm NH_3, 5% H_2O, 10% O_2, balance N_2.

T [°C]	NO_{OUT} [ppm]	$NO_{2,OUT}$ [ppm]	N_2O_{OUT} [ppm]	$NH_{3,OUT}$ [ppm]	SCR Selectivity [%]	N_2O Selectivity [%]
200	0	235	0	233	129	0
250	0	257	4	252	119	7.1
300	1	187	7	149	100	4
350	4	87	9	16	100	2.7
400	6	64	11	3	106	3.2
450	21	54	13	3	110	3.8

Influence of water on the selectivities: Table 7.5 compares calculated SCR selectivities for humid and dry feeds at various temperatures. It can be seen that the presence of water increases the selectivity of both the standard SCR and the fast SCR reaction. The beneficial effect of water leads to a widening of the temperature window towards higher temperatures at which high SCR selectivities are observed.

For the case of NO_2 in the feed, it appears that the selectivities are higher in the case of the dry feed. Selectivities above 100 % must again be interpreted as a stoichiometry

ν_{NH3}/ν_{NO2} differing from reaction for pure NO_2 SCR ($\nu_{NH3}/\nu_{NO2} = 4/3$), i.e. contribution from standard and fast SCR ($\nu_{NH3}/\nu_{NO2} = 1$). This means that the apparent higher selectivities in the case of dry feed are due to a higher formation of intermediate NO from NO_2 thus leading to an increased contribution of fast SCR to the total NO_x conversion. The higher redox activity of the catalyst with dry feed thus speeds up the reaction of the thermal equilibrium $NO + \frac{1}{2}O_2 \Leftrightarrow NO_2$.

Table 7.5 Selectivities for the standard, the fast and the NO_2-SCR reaction in dry and humid feeds. Feed: 300 ppm NO_x, 300 ppm NH_3, 5% H_2O, 10% O_2, balance N_2.

	Selectivity standard SCR		Selectivity fast SCR		Selectivity NO_2-SCR	
T [°C]	dry feed [%]	humid feed [%]	dry feed [%]	humid feed [%]	dry feed [%]	humid feed [%]
200	100	100	100	100	139	129
250	100	100	100	100	119	119
300	98	100	100	100	103	100
350	95	100	96	100	105	100
400	70	96	69	95	111	106
450	29	73	28	69	128	110

Dependence of DeNOx on temperature: Figure 7.4 reports the NO_x conversion ("DeNOx") as a function of temperature for a humid feed with 1000 ppm of NO_x for the three cases: pure NO, equimolar mixture of NO and NO_2, pure NO_2. The rest of the feed consists of 1000 ppm NH_3, 5% H_2O, 10% O_2 with balance N_2.

In the case of pure NO, the activity of the catalyst at 200°C is low, resulting in low values of DeNOx. On increasing temperature, the catalyst becomes more active, re-

Chapter 7

sulting in a rising DeNOx. Similar to the values shown in Table 7.2, ammonia is almost fully consumed at temperatures of 350°C and higher. However, a decreasing DeNOx is observed above 350°C. Therefore, at high temperatures, part of the ammonia must be consumed in side reactions leaving less ammonia to react in the standard SCR reaction. This leads to a maximum of DeNOx at about 350°C (Figure 7.4).
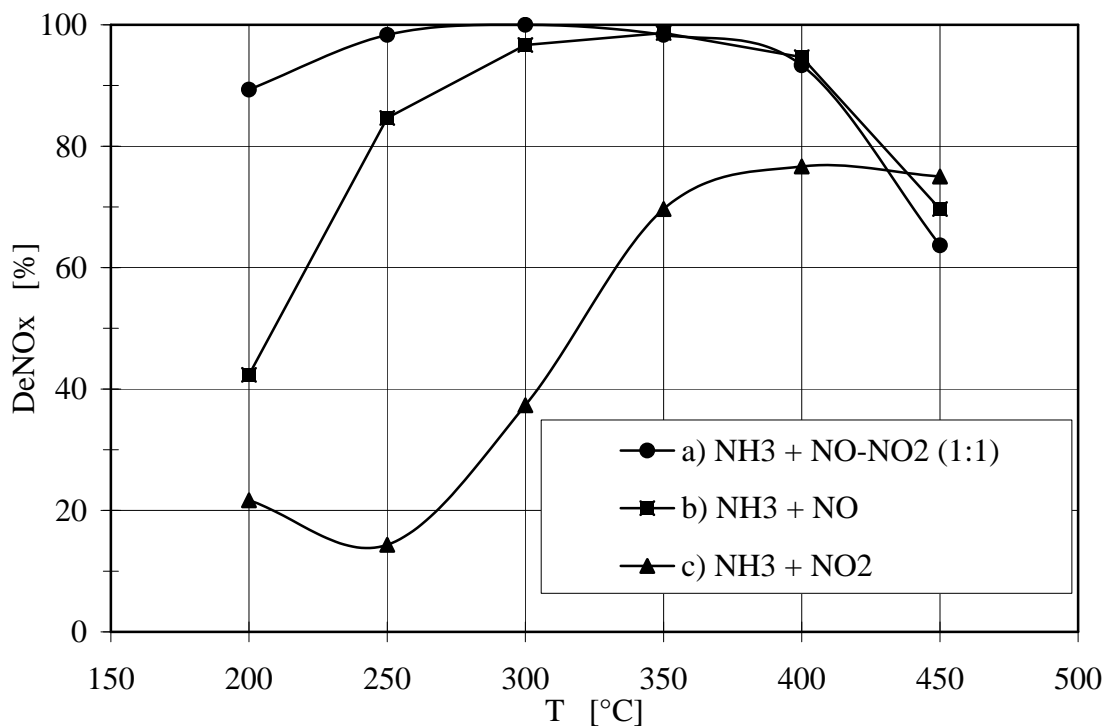

Figure 7.4   DeNOx as a function of temperature for various humid feeds: a) 150 ppm NO + 150 ppm NO_2; b) 300 ppm NO; c) 300 ppm NO_2. The rest of the feed consists in all cases of 300 ppm NH_3, 10% O_2, 5% H_2O, balance N_2.

Similar results were obtained for feeds with NO_x consisting of pure NO_2 or equimolar mixture of NO and NO_2. In the case of a feed with pure NO_2, the negative temperature coefficient of reaction (7.19) leads to the minimum in the curve of DeNOx vs. temperature at about 250°C [17].

Influence of water on DeNOx: In a similar way, Figure 7.5 compares the temperature dependence of DeNOx for a dry feed with NO_x consisting of pure NO, equimolar

Side reactions of the SCR process

mixture of NO and NO_2, pure NO_2. Comparing Figure 7.4 and 7.5 leads to the conclusion that the presence of water influences both activity and selectivity of the three SCR reactions. Generally, the presence of water inhibits all SCR reactions. However, for a feed containing the equimolar mixture of NO and NO_2, the influence of water is very small due to the high rate of the fast SCR reaction even in the presence of water. A second general conclusion is that the presence of water enhances the selectivity for all three SCR reactions at high temperatures as already shown in the selectivity tests.
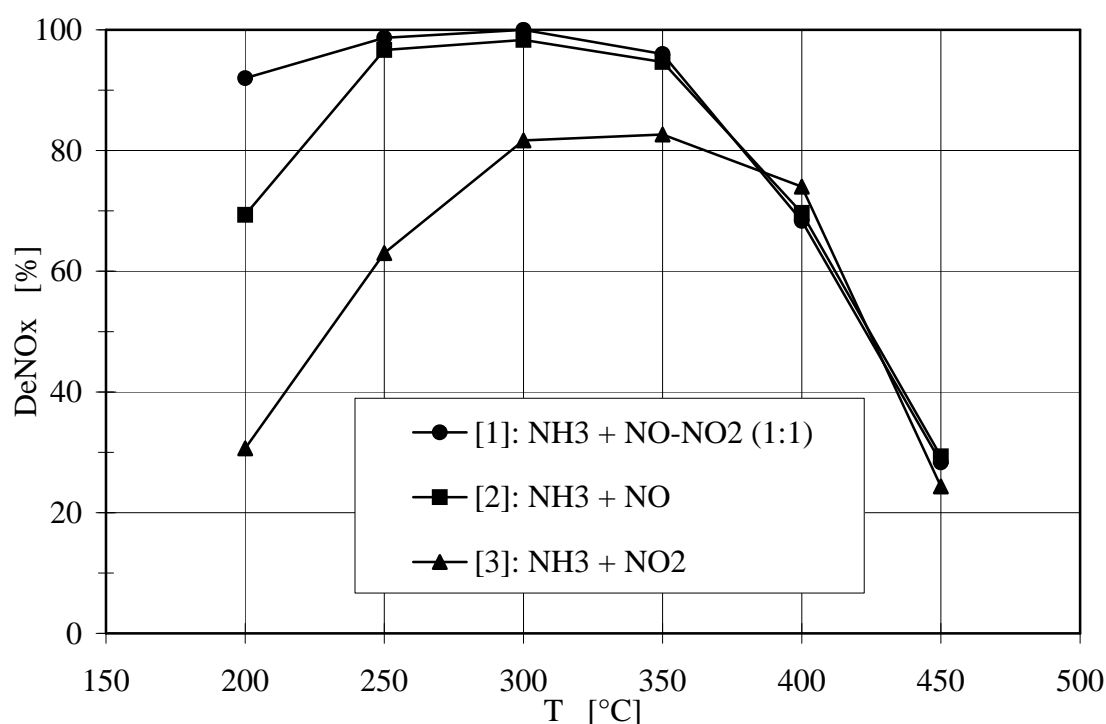

Figure 7.5   DeNOx as a function of temperature for various dry feeds: a) 150 ppm NO + 150 ppm NO_2; b) 300 ppm NO; c) 300 ppm NO_2. The rest of the feed consists in all cases of 300 ppm NH_3, 10% O_2, balance N_2.

7.5.3   Formation of N_2O

Figure 7.6 reports the formation of N_2O for dry feeds with different ratios of NO_2/NO_x. It can be seen that the formation of N_2O for feeds containing either pure NO or equimolar NO-NO_2 increases with temperature. N_2O can be formed by direct oxidation of ammonia and by the reaction between NH_3 and NO_x. Comparing experiments carried

Chapter 7

out with and without NO_x in the feed have shown that most of the N_2O is formed in the reactions between NH_3 and NO_x. If the feed contains pure NO_2, the amount of nitrous oxide formed exhibits a maximum at low temperatures ($\approx 250°C$). On the other hand, this feed leads to the lowest formation of N_2O at high temperatures.
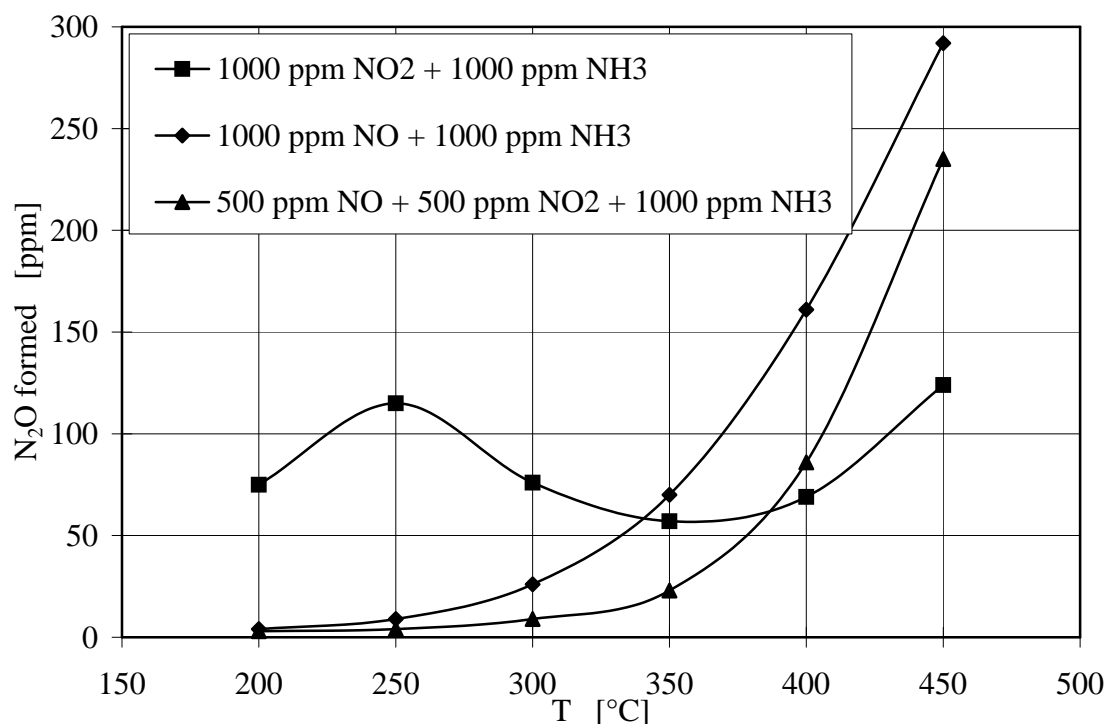

Figure 7.6 N_2O formation as a function of temperature in a dry feed of 1000 ppm NO_x, 1000 ppm NH_3, 10% O_2, balance N_2.

Figure 7.7 reports the formation of N_2O for humid feeds with different ratios of NO_2/NO_x. The N_2O concentrations are much lower in the presence of water meaning that the formation of N_2O is strongly inhibited by water for all three feeds. For feeds containing either pure NO or equimolar $NO-NO_2$, the amount of N_2O formed at temperatures below 400°C is low (some ppm). In the case of a feed containing pure NO_2, a considerable formation of N_2O is observed already at 250°C with a flat maximum at $\approx 350°C$.

Side reactions of the SCR process
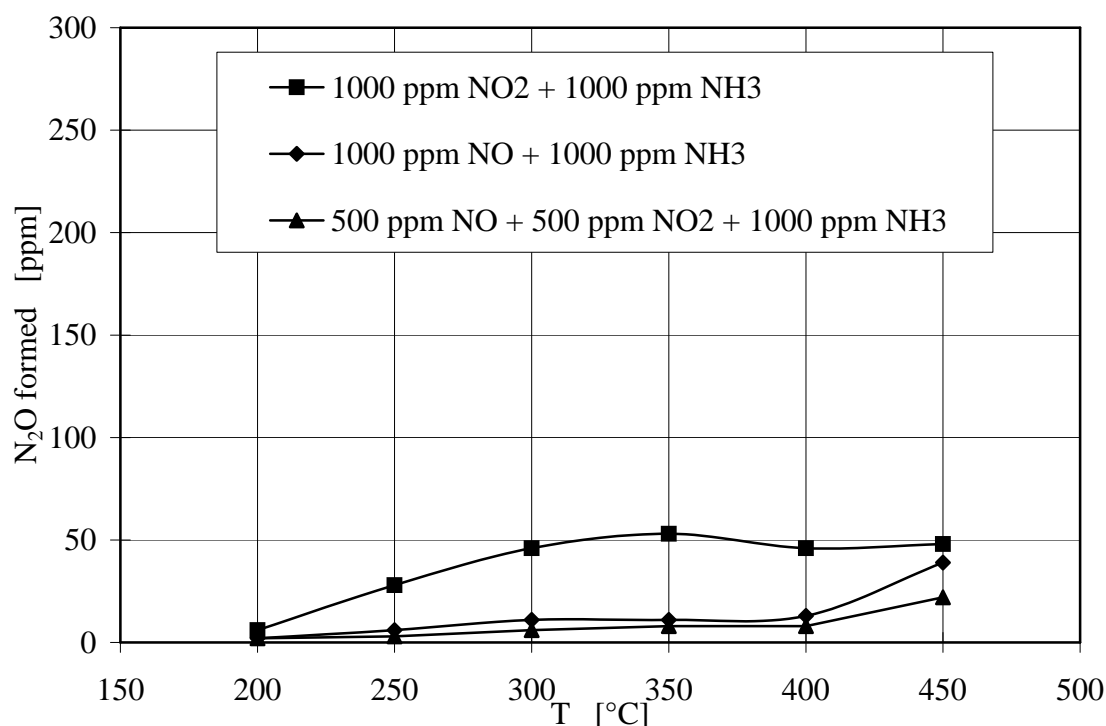
Figure 7.7 N_2O formation as a function of temperature in the presence of water. Feed: 1000 ppm NO_x, 1000 ppm NH_3, 10% O_2, 5% H_2O, balance N_2.

In another series of experiments, the influence of the ratio NO_2/NO_x on the formation of nitrous oxide for humid feeds was tested. Figure 7.8 shows that the formation of N_2O increases with the fraction of NO_2 in the feed if the ratio of NO_2/NO_x is higher than 50%.

The influence of oxygen on the formation of N_2O was investigated for both dry and humid feeds. These experiments have shown that the formation of N_2O is not influenced by the presence of oxygen for feeds containing pure NO_2. This proves that the reaction (7.11) can be neglected.

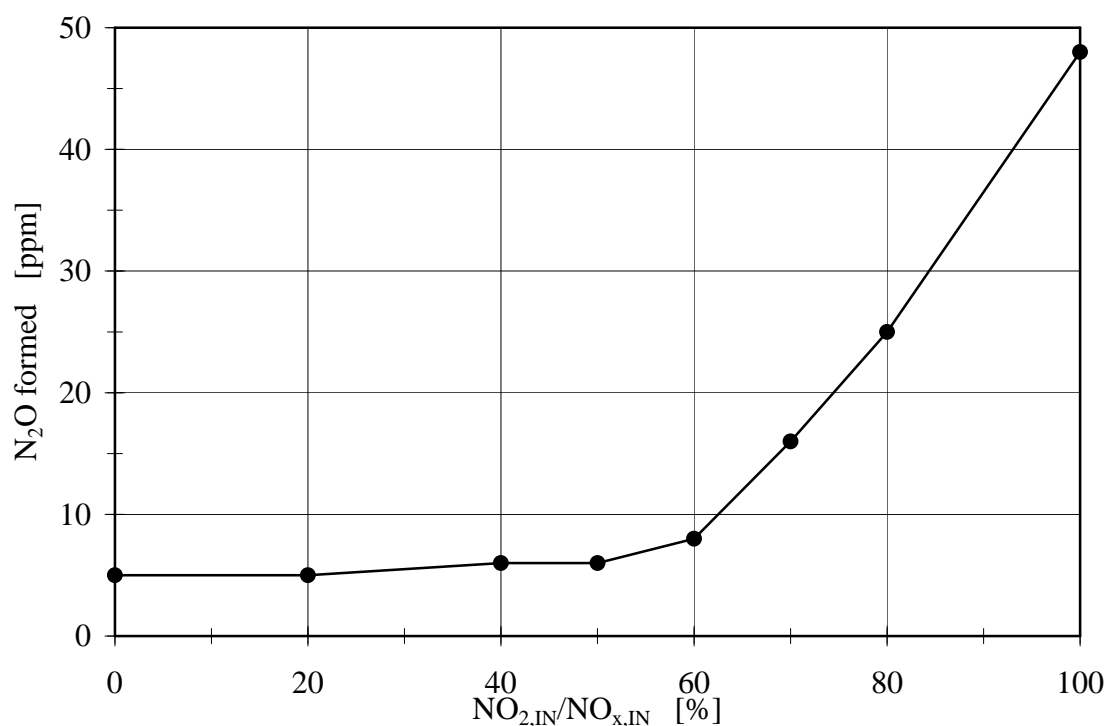**Figure 7.8**   N$_2$O formation as a function of NO$_{2,IN}$/NO$_{x,IN}$ in the presence of water at T = 300°C. Feed: 1000 ppm NO$_x$, 1000 ppm NH$_3$, 10% O$_2$, 5% H$_2$O, balance N$_2$.

7.6   Discussion

The selectivity of the standard and the fast SCR reaction over "real" SCR catalysts under "real" operating conditions (= presence of water) is very high at temperatures below 400°C (Table 7.5). However, a decrease in SCR selectivity is observed at temperatures above 350°C. The experiments have shown that the decrease in SCR selectivity of the standard and the fast SCR reaction is mainly due to the SCO of ammonia and to the formation of nitrous oxide. Other hypothetical reactions do not significantly contribute to the loss of SCR selectivity under real exhaust gas conditions. The presence of water inhibits the SCR activity of all three reactions and increases the selectivity in the case of the standard and the fast SCR reaction. In the following, we

propose an explanation for the influence of water on the standard and the fast SCR reaction considering some published reaction mechanisms.

Many authors [12,18,19] agree on the fact that the presence of water converts part of the Lewis acid sites of the catalyst into Brownsted acid sites. Ramis et al. [18] proposed that the activation of ammonia on a Lewis acid site is the fundamental step in the mechanism of the standard SCR reaction. Therefore, the inhibiting effect of water at low temperatures could be due to a decrease of the surface concentration of Lewis acid sites. In a later paper Ramis et al. [4] proposed hydrazine (N_2H_4) as an intermediate in the SCO of ammonia. They suggested that N_2H_4 is formed by dimerization of two NH_2 species originating from the dissociative adsorption of ammonia on two adjacent Lewis acid sites. At high temperatures the adsorption of water is weakened and this should lead to a high amount of (adjacent) Lewis acid sites. This should favor the SCO of ammonia and consequently cause a loss of selectivity for the SCR reactions. This effect is even more pronounced in dry conditions resulting in the very low SCR selectivities observed at high temperatures (Table 7.5).

The mechanism of N_2O formation by reaction between NH_3 and NO has not been fully explained. Topsoe et al. [13] proposed that the active sites for the N_2O formation and the SCR reactions are the same and suggested a nitrosamidic species as intermediate in the formation of nitrous oxide. The presence of water influences the decomposition of this intermediate either to nitrogen or to nitrous oxide according to:

$$N_2O \xleftarrow{\text{dry: dehydrogenation}} NH_xNO \xrightarrow{\text{wet: dehydration}} N_2$$

Topsoe et al. [13] proposed that the surface hydroxylation by water promotes dehydration leading to the formation of nitrogen. This could explain the strong inhibiting effect of water on the formation of N_2O.

Under typical exhaust gas conditions, the formation of N_2O at low temperatures is negligible for NO_x consisting of pure NO or NO_2 fractions below 50%. On the other hand, remarkable amounts of N_2O are formed at low temperatures if the NO_x contains more than 50% NO_2. The amount of N_2O formed at low temperatures increases with the

Chapter 7

NO_2 fraction. At temperatures above 400°C the formation of N_2O does virtually not depend on the NO_2 content.

If the feed contains pure NO_2, the amount of N_2O formed in a dry feed exhibits a pronounced maximum at about 250°C. This suggests that two reactions with different temperature dependence are responsible for the formation of N_2O:

$$4 \, NH_3 \, + \, 4 \, NO_2 \, \rightarrow \, 2 \, N_2 \, + \, 2 \, N_2O \, + \, 6 \, H_2O \qquad \text{(at low temperatures)} \qquad (7.9)$$

$$6 \, NH_3 \, + \, 8 \, NO_2 \, \rightarrow \, 7 \, N_2O \, + \, 9 \, H_2O \qquad \text{(at high temperatures)} \qquad (7.10)$$
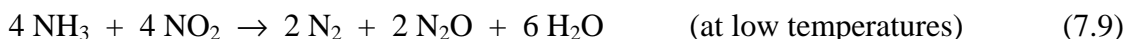
Previous investigations have shown that at low temperatures (T<200°C) reaction (7.19) involving NO_2 and NH_3 may lead to the formation of ammonium nitrate on these catalysts [15,17]. Because ammonium nitrate is not stable at temperatures above 200°C it can decompose into nitrous oxide and water according to:

$$NH_4NO_3 \, \rightarrow \, N_2O \, + \, 2 \, H_2O \qquad\qquad (7.20)$$

High concentrations of water will shift the equilibrium of this reaction to the left hand side and thus reduce the formation of nitrous oxide, what may be interpreted as an inhibition by water. We suggest that ammonium nitrate is an intermediate species in reaction (7.9), this reaction being a combination of reactions (7.19) and (7.20):

$$4 \, NH_3 \, + \, 4 \, NO_2 \rightarrow 2 \, N_2 \, + \, 2 \, H_2O \, + \, 2 \, NH_4NO_3 \rightarrow 2 \, N_2 \, + \, 2 \, N_2O \, + \, 6 \, H_2O \quad (7.9a)$$

The negative temperature dependence of reaction (7.19) leading to ammonium nitrate would explain the maximum of N_2O formation at ≈250°C reported in Figure 7.6. An ammonium nitrate intermediate species has also been proposed by Centi et al. [20-22] in the formation of N_2O by the SCR process on Cu/Al_2O_3 catalysts.

7.7 Conclusions

Under typical exhaust gas conditions, the selectivity for both the standard and the fast SCR reaction is high at temperatures below 400°C. The presence of water favors the

SCR selectivity, whereas it inhibits the SCR activity. Selective catalytic oxidation of ammonia and the formation of nitrous oxide are the main side reactions, which lower the SCR selectivity above 350°C. For feeds with NO_x consisting of pure NO or equimolar NO and NO_2, the formation of N_2O is negligible at temperatures below 400°C. An additional strong formation of N_2O at low temperatures is observed for feeds with a ratio of NO_2/NO_x above 50%. The reaction responsible for N_2O formation at low temperatures probably involves ammonium nitrate as an intermediate species.

7.8   References

[1]   R.F. Weiss, *J. Geophys. Res.* **86** (1981), 7185

[2]   N.I. Il'Chenko, G.I. Golodets, *J. Catal.* **39** (1975), 57

[3]   Y. Li and J.N. Armor, *Appl. Catal. B* **13** (1997), 131

[4]   G. Ramis, L. Yi and G. Busca, *Catal. Today* **28** (1996), 373

[5]   F. Janssen, F. Van der Kerkhof, H. Bosch and J.J. Ross, *Phys. Chem.* **91** (1987), 5931

[6]   F. Janssen, F. Van der Kerkhof, H. Bosch and J.J. Ross, *Phys. Chem.* **91** (1987), 6633

[7]   B.L.D. Duffy, H.E. Curry Hyde, N.W. Cant and P.F. Nelson, *J. Phys. Chem.* **98** (1994), 7153

[8]   U.S. Okzan, Y. Cai and M.W. Kumthekar, *J. Catal.* **149** (1994), 375

[9]   U.S. Okzan, Y. Cai and M.W. Kumthekar, *J. Catal.* **149** (1994), 390

[10]   U.S. Okzan, Y. Cai and M.W. Kumthekar, *J. Phys. Chem.* **99** (1995), 2363

[11] C.U.I. Odenbrand, P.L.T. Gabrielsson, J.G.M. Brandin and L.A.H. Andersson, *Appl. Catal.* **78** (1991), 109

[12] M. Kotter, H.G. Lintz, T. Turek and D.L. Trimm, *Appl. Catal.* **52** (1989), 225

[13] N.Y. Tospoe, T. Slabiak, B.S. Clausen, T.Z. Srnak and J.A. Dumesic, *J. Catal.* **134** (1992), 742

[14] E. Jacob, G. Emmerling et al. *NOx-Verminderung für Nutzfahrzeugmotoren mit Harnstoff-SCR-Kompaktsystemen (GD-KAT),* 19th International Wiener Motorensymposium, Vienna, 7-8 May 1998

[15] M. Koebel, M. Elsener and G. Madia, *Ind. Chem. Eng. Res.* **40** (2001), 52

[16] J. Blanco, P. Avila, S. Suarez, J.A. Martin and C. Knapp, *Appl. Catal. B* **28** (2000), 235

[17] M. Koebel, G. Madia and M. Elsener, *Catal. Today* (to be published).

[18] G. Ramis, G. Busca, F. Bregani and P. Forzatti, *Appl. Catal. B* **64** (1990), 259

[19] N.Y. Topsoe, *J. Catal.* **128** (1991), 499

[20] G. Centi and S. Perathoner, *Appl. Catal. A* **132** (1995), 179

[21] G. Centi, S. Perathoner, P. Biglino and E. Giamiello, *J. Catal.* **152** (1995), 75

[22] G. Centi and S. Perathoner, *J. Catal.* **152** (1995), 93

Effects of an oxidation pre-catalyst on the removal of NO_x

8.1 Introduction

Beside measures aiming at increasing the volumetric activity of the SCR catalyst itself, utilizing the fast SCR reaction is another method to enhance the SCR efficiency especially at low temperatures [1-3]. The practical application of this method calls for enhancing the NO_2 content in the exhaust upstream of the SCR catalyst. NO_2 can be produced by oxidizing part of the exhaust NO either on a Pt-based catalyst or by using plasma techniques [4-6]. Figure 8.1 depicts such a combined system for the removal of nitrogen oxides. The reducing agent, i.e. NH_3 or urea, is introduced downstream of the NO oxidation device in order to avoid its direct oxidation.
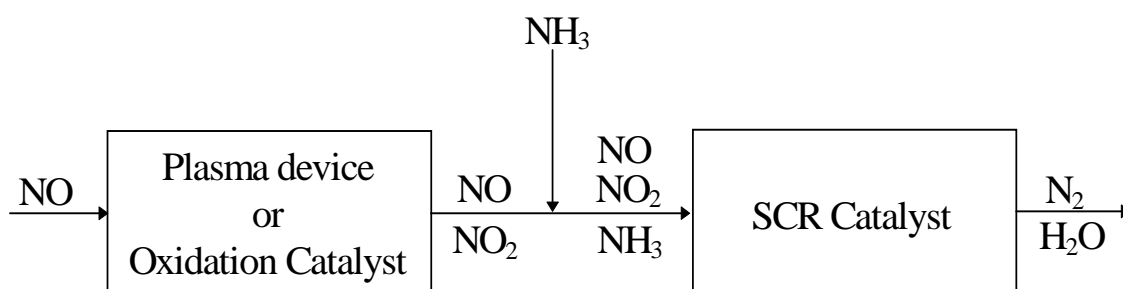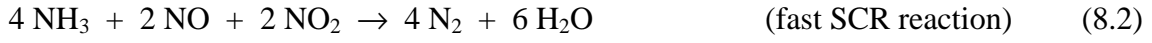

Figure 8.1   Scheme of a combined system for the removal of NO_x.

As already reported in previous chapters, the use of mixtures of $NO + NO_2$ allows other reactions to occur in addition to the standard SCR reaction:

$$4\,NH_3 \;+\; 4\,NO \;+\; O_2 \;\rightarrow\; 4\,N_2 \;+\; 6\,H_2O \qquad\qquad \text{(standard SCR reaction)} \;(8.1)$$

$$4\,NH_3 \;+\; 2\,NO \;+\; 2\,NO_2 \;\rightarrow\; 4\,N_2 \;+\; 6\,H_2O \qquad\qquad \text{(fast SCR reaction)} \qquad (8.2)$$

$$4\,NH_3 \;+\; 3\,NO_2 \;\rightarrow\; 3.5\,N_2 \;+\; 6\,H_2O \qquad\qquad \text{(NO}_2\text{-SCR reaction)} \qquad (8.3)$$

At temperatures below 300°C, the fast SCR reaction (8.2) is much faster than the standard SCR reaction (8.1). Conversely, the NO_2-SCR reaction (8.3) is much slower than the fast SCR reaction (8.2) and still slower than the standard SCR reaction (8.1) [3,7].

The increase of the reaction rate has long been known [8,9], but has only recently been rediscovered as a practical means for automotive SCR systems. At the 19th International Vienna Motor Symposium, Jacob et al. [2] presented the so-called "GD-Kat" system comprising a Pt-based oxidation pre-catalyst for the partial oxidation of NO to NO_2, thus enhancing the DeNOx performance of the SCR catalyst. Gieshoff et al. [10] investigated the removal of NO_x in both model gas experiments and engine bench tests using a combined system of oxidation (Pt-based) and SCR (TiO_2-WO_3-V_2O_5) catalysts. The addition of an oxidation catalyst significantly improved the removal of NO_x in the low temperature region of the engine. An integrated CRT (Continuously Regenerating Trap) and SCR system has been described by Chandler et al. [11] for the simultaneous reduction of nitrogen oxides and particulate matter. The CRT, composed of a Pt-based oxidation catalyst upstream of a diesel particulate filter [12], increased the NO_2 fraction upstream of the SCR catalyst, thus leading to an improved NO_x removal at low temperatures. Kim et al. [13] investigated the removal of NO_x using a combined system consisting of a pulse corona discharge and a Co-ZSM-5 catalyst. They found that the removal of NO_x was enhanced by the oxidation of NO to NO_2 in the plasma device. Similar results were obtained by Bröer et al. [14] using a combined system of non-thermal plasma and a TiO_2-WO_3-V_2O_5 catalyst.

This chapter reports the individual performances of an oxidation catalyst (Pt-based) and an SCR catalyst (TiO_2-WO_3-V_2O_5) as well as their combination. The effects of temperature, presence of hydrocarbons, NO_2 content and volume of the oxidation catalyst on the NO_x removal have been investigated in laboratory tests.

Chapter 8

8.2 Experimental

8.2.1 Catalyst samples

The oxidation catalyst was a commercial catalyst from Degussa (V09) with a Pt loading of 90 g/ft^3. This is a coated type supported on a cordierite monolith of 400 cpsi (cells per square inch) and with a volume of 2.1 cm^3.

The SCR catalyst was prepared in house according to the recipe reported in chapter 3. The monolithic SCR catalyst M11 was used in these investigations; its specifications have been reported in Table 3.1.

8.2.2 Experimental setup

The description of the experimental set-up has been reported in chapter 2. In order to test the effect of hydrocarbons, dodecane was added as a typical representative of diesel exhaust. A concentration of $\approx$ 200 ppm C1 was obtained by bubbling a partial stream of N_2 ($\approx$2.5% of the total feed to the reactor) through a wash bottle containing dodecane (>98%, Fluka) thermostated at 37°C.

The SCR performances of two combined systems comprising an oxidation and an SCR catalyst were compared with the behavior of the SCR catalyst alone. In a first experiment, the extent of NO oxidation was investigated on the oxidation catalyst. The composition of the resulting product gas was then used to compose a comparable model gas which was used as the feed in a successive experiment for testing the SCR catalyst. The reducing agent, i.e. NH_3, was added in variable amounts in order to determine the NO_x conversion at a slip of 10 ppm ammonia. Using this procedure, the removal of NO_x on the SCR catalyst yields the SCR performance of the combined system.

In a combined system, the volume ratio of oxidation and SCR catalysts is correlated to the ratio of the gas hourly space velocities (GHSV):

$$\frac{\text{Volume SCR - Cat}}{\text{Volume Oxi - Cat}} = \frac{\text{GHSV Oxi - Cat}}{\text{GHSV SCR - Cat}} \tag{8.4}$$

The SCR performances of two combined systems with $V_{OXI}:V_{SCR} = 1:5$ (system A) and $V_{OXI}:V_{SCR} = 2:5$ (system B) were investigated. The experiments on the SCR catalyst were performed at a fixed space velocity of 54000 h^{-1}, resulting in a total gas flow rate of 394 l_N/h using a catalyst volume of 7.3 cm^3.

According to equation (8.4), the required GHSV in the oxidation catalyst is 270000 h^{-1} for system A and 135000 h^{-1} for system B. Therefore, the NO oxidation was tested at a gas flow rate of 567 and 284 l_N/h over the oxidation catalyst ($V_{OXI} = 2.1$ cm^3).

8.3 Results and Discussion

8.3.1 Oxidation catalyst

Figure 8.2 depicts the conversion of NO to NO_2 on the oxidation catalyst as well as the ratio NO_2/NO_x according to the thermodynamic equilibrium of the reaction:

$$2\,NO\ +\ O_2\ \Leftrightarrow\ 2\,NO_2 \qquad\qquad (\text{oxidation of NO}) \qquad\qquad (8.5)$$

The thermodynamic equilibrium curve exhibits a sigmoid pattern, with the NO_2 content starting to decrease significantly at temperatures above 200°C.

At typical exhaust gas conditions and temperatures below 150°C the conversion of NO to NO_2 on Pt-based oxidation catalysts is negligible - above it increases with temperature. At high temperatures the oxidation of NO is limited by the thermodynamic equilibrium resulting in a maximum conversion of NO on the oxidation catalyst. With increasing space velocity, the maximum conversion of NO is shifted to higher temperatures and the maximum conversion is lower. It can also be seen in Figure 8.2 that the oxidation of NO is inhibited by hydrocarbons. This may be due to HC competing with NO on the active sites of the catalyst or to the reduction of previously formed NO_2 by hydrocarbons.
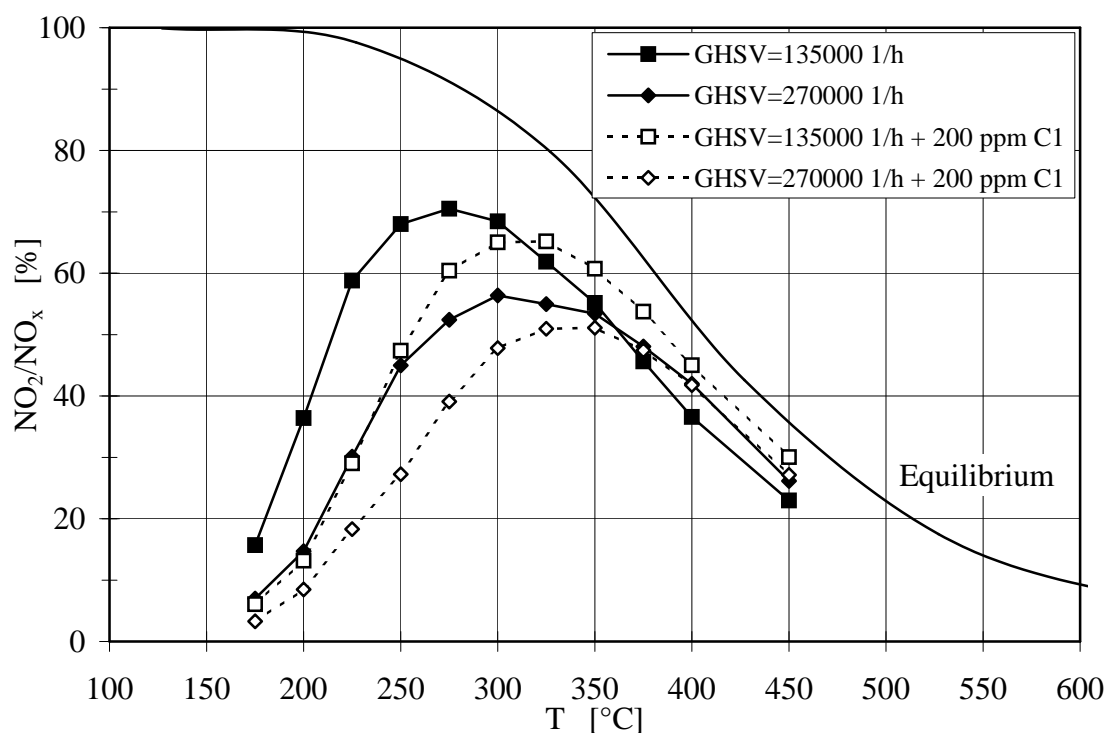
Chapter 8

Figure 8.2 NO oxidation on an oxidation catalyst at different space velocities with and without hydrocarbons in the feed. Feed: 1000 ppm NO, 5% H_2O, 10% O_2, 200 ppm C1 as dodecane (if present), balance N_2.

8.3.2 SCR catalyst

Figure 8.3 shows the NO_x conversion (DeNOx) at 10 ppm NH_3 slip as a function of temperature for a feed with NO_x = pure NO. The DeNOx increases with temperature and reaches values higher than 90% above 300°C. Hydrocarbons in the feed inhibit the removal of NO_x at temperatures up to 300°C, but have virtually no effect at higher temperatures. When ammonia was omitted in the feed, no NO_x removal could be seen in the presence of hydrocarbons, indicating that hydrocarbons are not involved in the NO_x reduction on this catalyst.
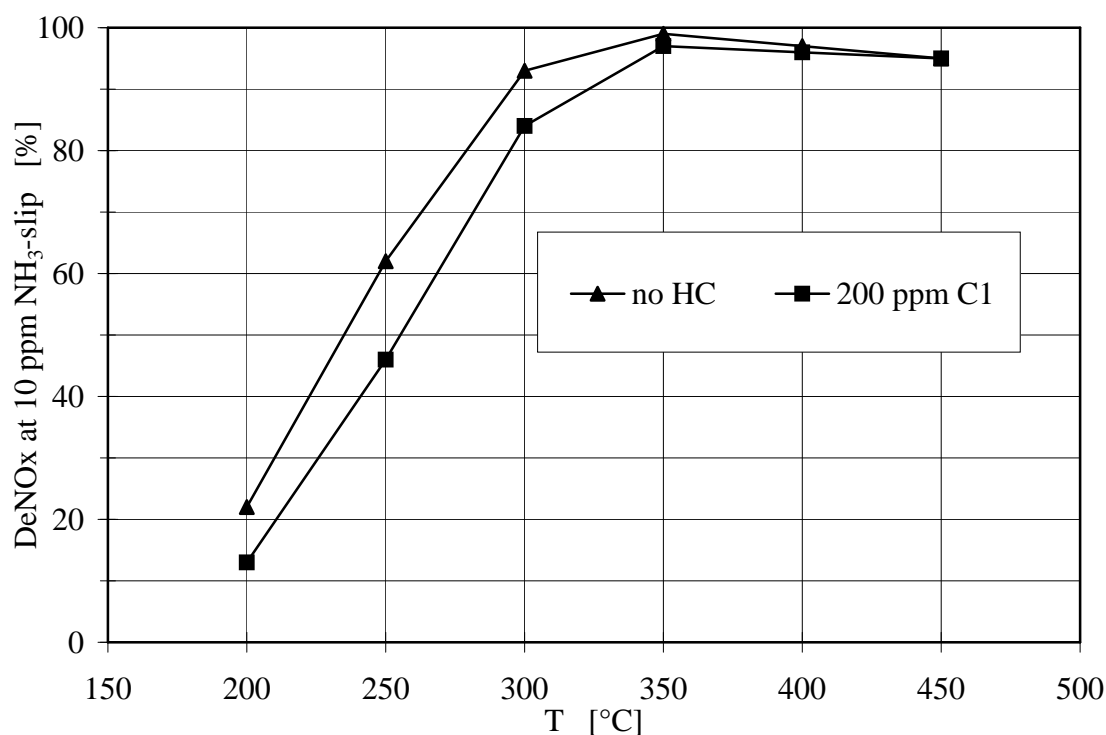
Figure 8.3 DeNOx at 10 ppm NH_3-slip vs. temperature on an SCR catalyst. Feed: 1000 ppm NO, NH_3 (variable), 5% H_2O, 10% O_2, balance N_2.

The high selectivity of TiO_2-WO_3-V_2O_5 catalysts for the SCR reactions (8.1), (8.2) and (8.3) below 380°C is well known [15]. Figure 8.4 shows the influence of the feed ratio NO_2/NO_x on DeNOx in the temperature range 200-350°C. Higher temperatures were not considered due to the occurrence of side reactions like the selective oxidation of ammonia to nitrogen and the formation of nitrous oxide. These reactions become increasingly important at temperatures above 380°C.

At temperatures below 300°C the DeNOx increases linearly for NO_2 fractions from 0% to 50% of total NO_x. The highest DeNOx was observed when NO and NO_2 were fed in equimolar amounts. This behavior must be attributed to the fast SCR reaction (8.2) with a reaction rate about ten times higher than the standard SCR reaction (8.1) at temperatures below 250°C. The remaining NO or NO_2 reacts with ammonia according to the standard or NO_2-SCR reaction, yielding the DeNOx of these reactions at the actual conditions of temperature and space velocity. For NO_2 fractions between 50% and 100%

Chapter 8

the DeNOx decreases linearly with a steep slope. The stronger decline compared to the incline is due to the different reaction rates of standard and NO_2-SCR. At NO_2 fractions from 0% to 50% of total NO_x, the residual NO after quantitative reaction of NO_2 is depleted according to the standard SCR reaction. At NO_2 fractions from 50% to 100% of total NO_x, the residual NO_2 must react by the slow NO_2-SCR reaction.

At 300°C, the DeNOx is only slightly enhanced by increasing the NO_2 fraction. In addition, NO_2 above 50% has a strong negative effect on DeNOx, because at this temperature NO_2 reacts slowly with ammonia according to the NO_2-SCR reaction (8.3).

Above 350°C, the rate of NO_x conversion does virtually not depend on the NO_2 content in the feed. This is due to the approximation of the rate constants of reactions (8.1) and (8.3).
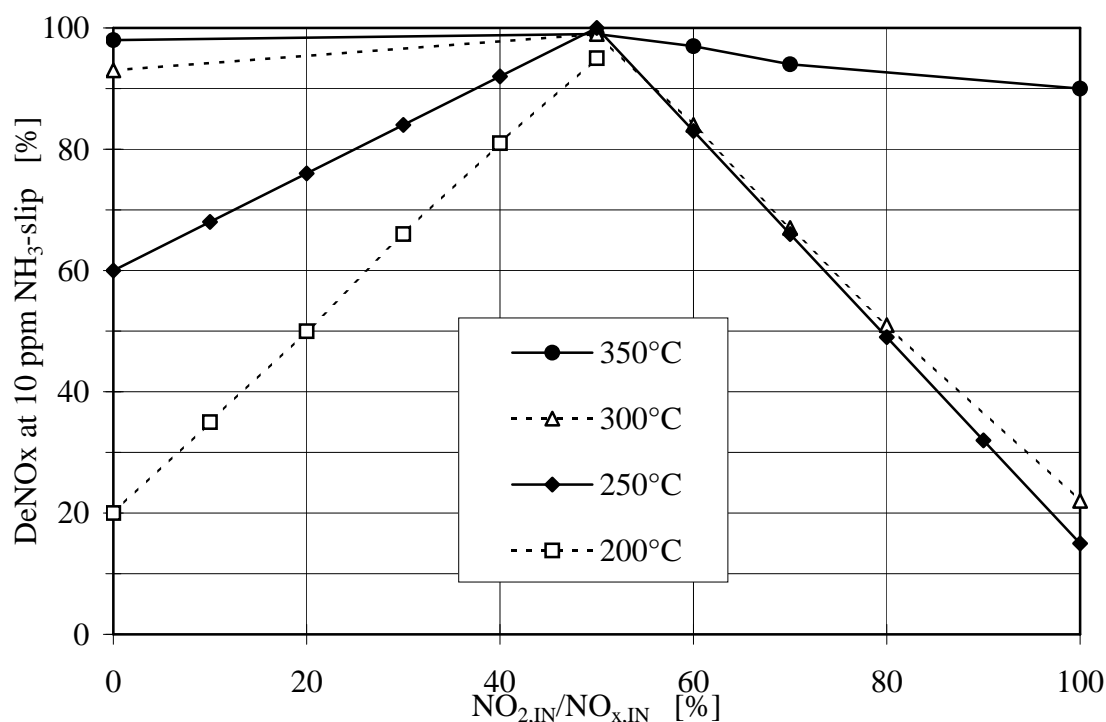

Figure 8.4   DeNOx at 10 ppm NH_3-slip vs. temperature on an SCR catalyst. Feed: 1000 ppm NO_x, NH_3 (variable), 5% H_2O, 10% O_2, balance N_2.

Effects of an oxidation pre-catalyst on the removal of NO_x

8.3.3 Calculations

Based on these experiments, the removal of NO_x (NO and NO_2) from exhaust gases on an SCR catalyst may be calculated distinguishing two cases:

Case 1) $NO_{2,IN}/NO_{x,IN} < 50\%$: fast SCR and standard SCR reaction

The amount of NO_x abated in the fast SCR reaction is

$$NO_x \text{ abated in fast SCR reaction} = 2 \cdot NO_{2,IN}.$$

The remaining NO

$$NO = NO_{x,IN} - 2 \cdot NO_{2,IN}$$

reacts according to the standard SCR reaction exhibiting the DeNOx (in %) of this reaction at the actual conditions of temperature and space velocity:

$$NO_x \text{ abated in standard SCR} = \left(NO_{x,IN} - 2 \cdot NO_{2,IN}\right) \cdot \frac{DeNOx_{standard}}{100}$$

The total amount of NO_x abated on the SCR catalyst is the sum of NO_x converted in the fast and standard SCR reactions:

$$\text{total } NO_x \text{ converted} = 2 \cdot NO_{2,IN} + \left(NO_{x,IN} - 2 \cdot NO_{2,IN}\right) \cdot \frac{DeNOx_{standard}}{100}$$

Thus, the overall DeNOx can be calculated as follows:

$$DeNOx = 100 \cdot \frac{\text{total } NO_x \text{ conv.}}{NO_{x,IN}} = DeNOx_{standard} + 2 \cdot \left(100 - DeNOx_{standard}\right) \cdot \frac{NO_{2,IN}}{NO_{x,IN}} \quad (8.6)$$

Case 2) $NO_{2,IN}/NO_{x,IN} > 50\%$: fast SCR reaction and NO_2-SCR reaction

The amount of NO_x abated in the fast SCR reaction is

$$NO_x \text{ abated in fast SCR} = 2 \cdot NO_{IN} = 2 \cdot \left(NO_{x,IN} - NO_{2,IN}\right).$$

Chapter 8

The remaining NO_2

$$NO_2 = NO_{x,IN} - 2 \cdot \left(NO_{x,IN} - NO_{2,IN} \right) = 2 \cdot NO_{2,IN} - NO_{x,IN}$$

reacts according to the NO_2-SCR exhibiting the DeNOx (in %) of this reaction at the actual temperature and space velocity:

$$NO_x \text{ abated in } NO_2\text{-SCR} = \left(2 \cdot NO_{2,IN} - NO_{x,IN} \right) \cdot \frac{DeNOx_{NO2}}{100}$$

The total amount of NO_x abated on the SCR catalyst is the sum of NO_x converted in the fast and NO_2-SCR reactions:

$$\text{total } NO_x \text{ converted} = NO_{x,IN} - \left(2 \cdot NO_{2,IN} - NO_{x,IN} \right) \cdot \left(1 - \frac{DeNOx_{NO2}}{100} \right)$$

The overall DeNOx may then be calculated:

$$DeNOx = 100 \cdot \frac{\text{total } NO_x \text{ converted}}{NO_{x,IN}} = 100 - \left(2 \cdot \frac{NO_{2,IN}}{NO_{x,IN}} - 1 \right) \cdot \left(100 - DeNOx_{NO2} \right) \qquad (8.7)$$

Example: A gas mixture containing 1000 ppm NO_x with 40% NO_2 is fed to the SCR catalyst at T=250°C, GHSV=52000 h^{-1}. The rest of the feed consists of 1000 ppm NH_3, 10% O_2, 5% H_2O and balance N_2. As long as NO and NO_2 are present they react quantitatively in equimolar amounts (400 ppm NO + 400 ppm NO_2) in the fast SCR reaction according to (8.2). The remaining 200 ppm NO will react according to the standard SCR reaction, which showed a DeNOx of 60 % at these operative conditions. Therefore, 120 ppm NO are abated in the standard SCR reaction, whereas 80 ppm NO remain unconverted. Totally 920 ppm NO_x are abated on the catalyst resulting in a DeNOx of 92%. The experimentally measured DeNOx value is 93%.

Table 8.1 compares measured with calculated values of DeNOx using equations (8.6) and (8.7). The agreement between calculations and experimental results is very good. The results prove the adequacy of the concept of sequential reactions on TiO_2-WO_3-V_2O_5 catalysts. Thus, it can be stated that:

- if $NO_{2,IN}/NO_{x,IN} < 50\%$, the main reactions occurring on the SCR catalyst below 350°C are the standard and fast SCR reactions; the positive effect of increasing the NO_2 fraction from 0% to 50% is due to the increasing amount of NO_x abated in the fast SCR reaction.

- if $NO_{2,IN}/NO_{x,IN} > 50\%$, the main reactions occurring on the SCR catalyst below 350°C are the fast and NO_2-SCR reactions; the negative effect of increasing the NO_2 fraction from 50% to 100% is due to the increasing amount of NO_x which must react in the slower NO_2-SCR reaction.

- the removal of NO_x on the SCR catalyst is virtually independent of the NO_2 content of the feed above 350°C, as both the standard and the NO_2-SCR reaction show very high DeNOx (>90%) at these temperatures.

8.3.4 Combined system of oxidation and SCR catalysts

Figure 8.5a compares the NO_x conversion of the SCR catalyst alone and of two combined systems having different volume ratios $V_{OXI}:V_{SCR}$ of 1:5 (system A) and 2:5 (system B). The volume of the oxidation catalyst determines the degree of NO oxidation and therefore also the NO_2 content in the feed to the SCR catalyst. Due to the larger volume of the oxidation catalyst in system B, more NO_2 is produced than in system A (Figure 8.2). Figure 8.5a reveals that the combined systems exhibit generally a higher NO_x removal at temperatures below 250°C than the SCR catalyst alone. At 200°C the highest NO_x removal was obtained with system B that produced the highest NO_2 concentrations ($NO_{2,IN}/NO_{x,IN} \approx 40\%$) in the feed. In contrast, at 250°C system A exhibited the highest removal of NO_x. At 250°C the oxidation of NO in system B exceeded 50% resulting in a decreased DeNOx due to NO_2-SCR. Similar results were obtained with system B at 300°C, where the degree of NO oxidation was so high ($\approx 70\%$) that the DeNOx was even lower than on the SCR catalyst alone.

The experiments reported above were carried out also with gas mixtures containing hydrocarbons. Figure 8.5b shows that also in this case the combined systems A and B

achieve higher NO_x conversions than the SCR catalyst alone at temperatures below 250°C. As already shown above in Figure 8.2, the presence of hydrocarbons inhibits the conversion of NO to NO_2 on the oxidation catalyst, lowering the NO_2 content in the feed to the SCR catalyst.

Table 8.1   DeNOx at 10 ppm NH_3 over an SCR catalyst as a function of the ratio NO_2/NO_x in the feed. Comparison of experimental results and mathe-matical calculations. Feed: 1000 ppm NO_x, NH_3 variable, 5% H_2O, 10% O_2 balance N_2. Bold face: experimental values for pure NO and NO_2 used in the calculations.

T	200°C		250°C		300°C		350°C	
NO_2/NO_x [%]	DeNOx meas. [%]	DeNOx calc. [%]	DeNOx meas. [%]	DeNOx calc. [%]	DeNOx meas. [%]	DeNOx calc. [%]	DeNOx meas. [%]	DeNOx calc. [%]
0	**20**	20	**60**	60	**93**	93	**98**	98
10	35	36	67	68				
20	50	52	76	76				
30	66	68	85	84				
40	81	84	93	92				
50	95	100	100	100	99	100	99	100
60			84	83	84	84	97	98
70			68	66	69	69	94	96
80			50	49	53	53		
90			33	32				
100			**15**	15	**22**	22	**90**	90

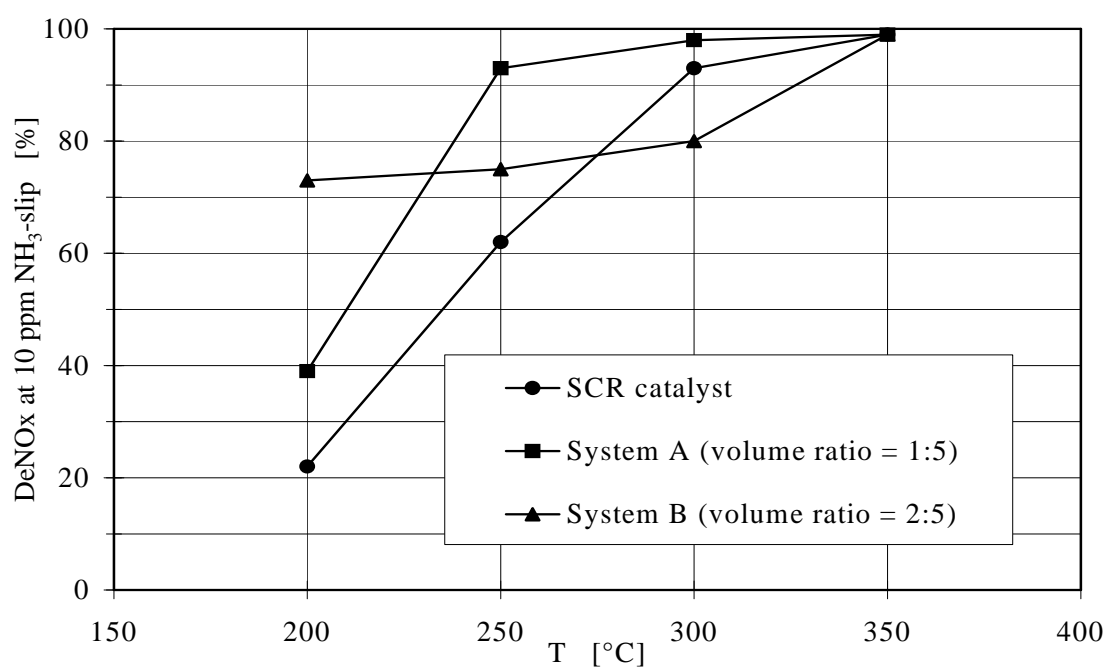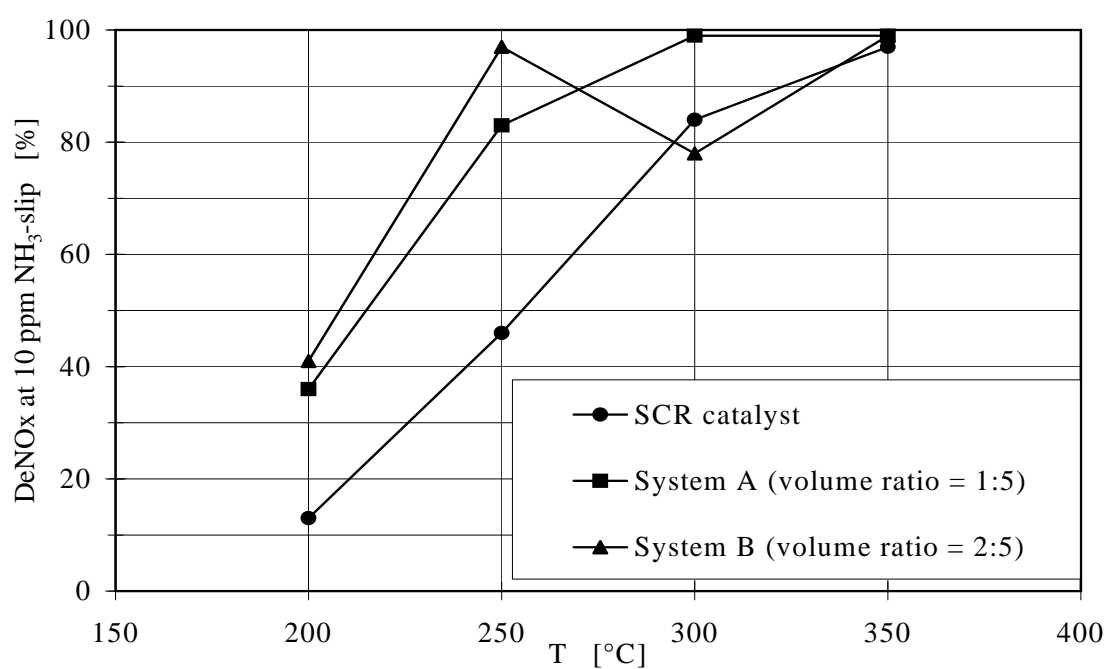*Effects of an oxidation pre-catalyst on the removal of NO_x*

Figure 8.5a

Figure 8.5b

DeNOx at 10 ppm NH_3-slip vs. temperature for the combined systems A and B and for the SCR catalyst alone with (Figure 8.5a) and without (Figure 8.5b) hydrocarbons (200 ppm C1 as dodecane). Feed: 1000 ppm NO, NH_3 (variable), 5% H_2O, 10% O_2, balance N_2.

Therefore, the presence of hydrocarbons is favorable for the removal of NO_x in system B above 200°C – a temperature region where more than 50% of NO is converted to NO_2 in the absence of hydrocarbons (Figure 8.5b). On the other hand, at 200°C, the presence of hydrocarbons inhibited the NO_x conversion of system B, since the NO oxidation was below 50% in the gas mixture without hydrocarbons. The NO_2 fraction in the SCR feed is further reduced by the presence of hydrocarbons, lowering the contribution from the fast SCR reaction. Similarly, the inhibiting effects of hydrocarbons on the NO oxidation lowered the removal of NO_x in system A which generally exhibited a low conversion of NO to NO_2 in the absence of hydrocarbons, due to the smaller volume of the catalyst (Figure 8.5b).

These experiments have shown that the volume of the oxidation catalyst strongly influences the SCR performance of a system comprising of an oxidation and an SCR catalyst. The optimum conditions would be a 50% conversion of NO to NO_2 at all operative conditions, allowing for NO_x to react only in the fast SCR reaction. However, the conversion of NO to NO_2 on the oxidation catalyst depends on several parameters such as temperature, space velocity, presence of hydrocarbons and partial pressure of NO. Consequently, the ratio NO_2/NO_x upstream of the SCR catalyst changes according to the operative conditions, resulting in a varying performance of the combined system.

Generally, a small oxidation catalyst yields a low degree of NO oxidation at 200°C and therefore only a slight enhancement of NO_x removal compared to the SCR catalyst alone. However, the oxidation of NO increases with temperature, thus leading to a pronounced enhancement of NO_x removal at 250°C. On the other hand, a generously sized oxidation catalyst yields a high fraction of oxidized NO already at 200°C, thus enhancing remarkably the DeNOx in comparison to the SCR catalyst alone. However, if the fraction of generated NO_2 exceeds 50% at 250 and 300°C, negative effects on DeNOx will result.

For each mobile source of nitrogen oxides, an optimum volume ratio of oxidation and SCR catalysts can be found allowing for a maximum DeNOx performance. This optimum can be determined considering the overall amount of NO_x abated in a test cycle. For instance, if the system will be operated for a longer time at ≈ 200°C than at ≈

250°C, system B would be preferred. On the other hand, system A would be a better choice if the temperature of the exhaust gases decreases down to 200°C only for short periods of time.

8.4   Conclusions

The combination of an oxidation and an SCR catalyst allows to enhance the NO_x conversion in comparison to the SCR catalyst alone at temperatures below 350°C. Both the oxidation of unburned hydrocarbons and the conversion of NO to NO_2 on the oxidation catalyst have beneficial effects on the conversion of NO_x on the SCR catalyst. The highest removal of NO_x is obtained if the oxidation catalyst yields a feed gas with NO_2/NO_x=50%.

For NO_x with NO_2 fractions below 50% and temperature below 350°C, the main reactions occurring on the SCR catalyst are the standard and the fast SCR reaction. The enhancement of NO_x removal with increasing NO_2 fractions up to 50% is due to the increasing amount of NO_x abated in the fast SCR reaction. For $NO_2/NO_x>50\%$ and temperature below 350°C, the main reactions occurring on the SCR catalyst are the fast and the NO_2-SCR reaction. In this case, the NO_x conversion decreases because an increasing amount of NO_x reacts in the slower NO_2-SCR reaction.

The SCR performance of a combined system is strongly influenced by the volume ratio between oxidation and SCR catalysts. The volume of the oxidation catalyst determines the NO_2 content in the feed to the SCR catalyst, resulting in positive or negative effects on DeNOx.

Therefore, the optimum volume ratio between oxidation and SCR catalysts remains a compromise between the antagonistic effects described. Nevertheless, an increased NO_x conversion can always be achieved by a skilled combination of oxidation and SCR catalysts.

8.5 References

[1]   M. Koebel, M. Elsener and M. Kleemann, *Catal. Today* **59** (2000), 335

[2]   E. Jacob, G. Emmerling et al. *NO$_x$-Verminderung für Nutzfahrzeugmotoren mit Harnstoff-SCR-Kompaktsystemen*, 19th Intern. Wiener Motorensymposium, May 7-8 1998

[3]   M. Koebel, M. Elsener and G. Madia, *Ind. Chem. Eng. Res.* **40** (2001), 52

[4]   S. Bröer, *Plasmainduzierte Entstickung dieselmotorischer Abgase - Der Einfluss gasförmiger Additive sowie die Kombination mit katalytischen und reaktiven Materialen*, Thesis TU, Siemens AG, Munich 1998

[5]   B.M. Penetrante, R.M. Brusasco, B.T. Merritt and G.E. Vogtlin, *SAE Paper* N. 1999-01-3687

[6]   B.M. Penetrante, R.M. Brusasco, B.T. Merritt and G.E. Vogtlin*, Pure Appl. Chem.* **71**, (199), 1829

[7]   M. Koebel, G. Madia and M. Elsener, submitted to *Catal. Today*

[8]   A. Kato, S. Matsuda, F. Nakajima, H. Kuroda and T. Narita *J. Phys. Chem.* **85** (1981), 4099

[9]   G. Tuenter, W. Leeuwen and L. Snepvangers *Ind. Eng. Chem. Prod. Res. Dev*. **25** (1986), 633

[10] J. Gieshoff, A. Schäfer-Sindlinger, P.C. Spurk and J.A.A. v.d.Tillaart, *SAE Paper* N. 2000-01-0189

[11] G.R. Chandler, B.J. Cooper, J.P. Harris, J.E. Thoss, A. Uusumaki, A.P. Walker and J.P. Warren, *SAE Paper* N. 2000-01-0188

[12] B.J. Cooper, H.J. Jung and J.E. Thoss, *US Patent* 4,902,487 (1990)

[13]   M. Kim, K. Takashima, S. Katasura and A. Mizuno, *J. of Phys. D. Appl. Phys*. **3**4 (2001), 604

[14]   S. Bröer and T. Hammer, *Appl. Catal. B* **28** (2001), 101

[15]   G. Madia, M. Koebel, M. Elsener and A. Wokaun, submitted *to Ind. Chem. Eng. Res.*

Chapter 8

9

Experiments on the diesel test stand

9.1 Introduction

In order to investigate the SCR process under realistic conditions, additional experiments on a diesel engine test stand have been performed. The main limitations of laboratory tests are the following:

1. The investigation of the behavior of urea under laboratory conditions is not possible. The problems encountered here are the very small quantities of urea solution to be injected which may be partly overcome by using less concentrated solutions. However, this will lead to higher relative amounts of water in the feed than in the real exhaust and consequently lower temperatures and slower rates of urea decomposition. In addition, the residence times will usually be much higher in the lab experiment than on the test stand thus yielding completely different concentrations of decomposition products at the catalyst entrance (mainly NH_3, HNCO, urea).

2. The influence of minor components present in real exhaust is neglected in the lab test. This pertains especially to hydrocarbons and soot. In some of the lab tests dodecane was added as a typical hydrocarbon. However, this is only a rough approximation of reality.

3. We should also mention that carbon dioxide is completely omitted in the lab tests due to analytical problems of the FTIR-technique used. However, various lab experiments suggest that this effect is really neglectable.

4. The effect of load changes leading to sudden changes of temperature and adsorbed ammonia cannot be investigated realistically in the lab tests.

9.2   Experimental

9.2.1   Description of the test stand

Figure 9.1 depicts the scheme of the diesel test stand HARDI ("**HAR**nstoff-**DI**esel" = "urea-diesel"). The technical data of the diesel engine are the following:

Engine	Liebherr D924TI-E
Properties	4 cylinders, direct injection, turbo charged with intercooler
Cylinder volume	6.596 liters
rpm in tests	1500 min^{-1}
Maximum power in tests	116 kW

An aqueous urea solution containing 32.5 wt-% urea was used in the experiments. The urea solution is injected in the exhaust upstream of the SCR catalyst. The urea dosage system comprises a magnetic injection valve whose on/off frequency can be varied in order to control the amount of injected reducing agent. Additional experiments were carried out using an ammonia solution of 24 wt-% NH_3.

9.2.2   Test program

Investigations both in steady state and unsteady state conditions were carried out in the range of engine operating points generating electrical powers of 10-100 kW. These investigations were performed using an SCR catalyst alone and a combined system of
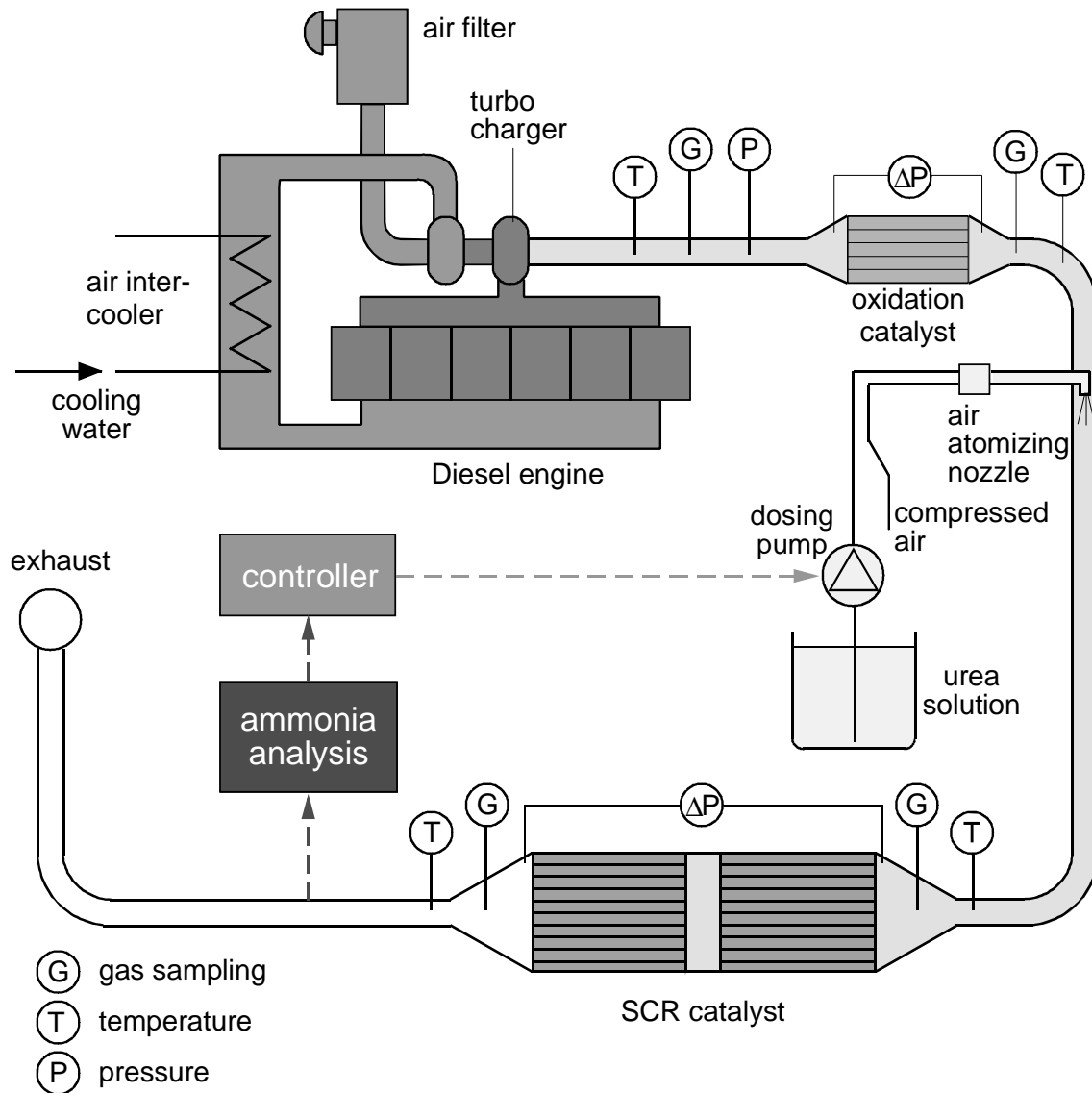
Figure 9.1 Scheme of the test stand. The oxidation catalyst was only used in the investigations of the combined system oxidation catalyst + SCR catalyst.

oxidation and SCR catalysts. Table 9.1 reports the temperatures and flows of the exhaust at the tested operating points of the engine.

In a first series of experiments, the NO_x conversions in the steady state were determined for the various operating points of the engine given in Table 9.1. These values were successively used to calculate the dosage of reducing agent required in unsteady state experiments. Two series of unsteady state experiments were carried out: cold start and warm start tests. In the warm start tests the temperatures of motor oil and cooling water were higher than 40°C at the start of the test. In the cold start tests motor oil and cooling water were at room temperature at the start of the test.

Table 9.1   Operating points and corresponding temperatures and exhaust flows.

Electrical power [kW]	Exhaust temperature after the engine [K]	Exhaust temperature before the SCR catalyst [K]	Exhaust temperature after the SCR catalyst [K]	Exhaust flow in dry conditions $[m^3_N/h]$	Exhaust flow in humid conditions $[m^3_N/h]$
100	500	470	460	424	457
75	440	415	406	354	378
50	365	338	335	303	320
40	335	308	306	290	304
30	285	265	264	283	295
20	245	230	229	273	283
10	200	187	187	265	274

9.2.3 Catalysts

The SCR catalysts used in the test stand experiments were prepared in house using the preparation procedure reported in chapter 3. A volume of about 10 liters was used and the active material was coated both on a cordierite (K69) and on a metal (M30) carrier. Table 9.2 reports the exact specifications and Figure 9.2 shows a photo of the cordierite catalyst K69.

The oxidation catalyst used in the investigations of the combined system of oxidation catalyst + SCR catalyst was obtained from Degussa. This is a Pt-based catalyst (90 g-Pt/ ft^3) coated on a metallic monolith with a volume of 1.9 liters and a cell density of 400 cpsi. The diameter and the length of the catalyst were 143 and 120 mm, respectively.
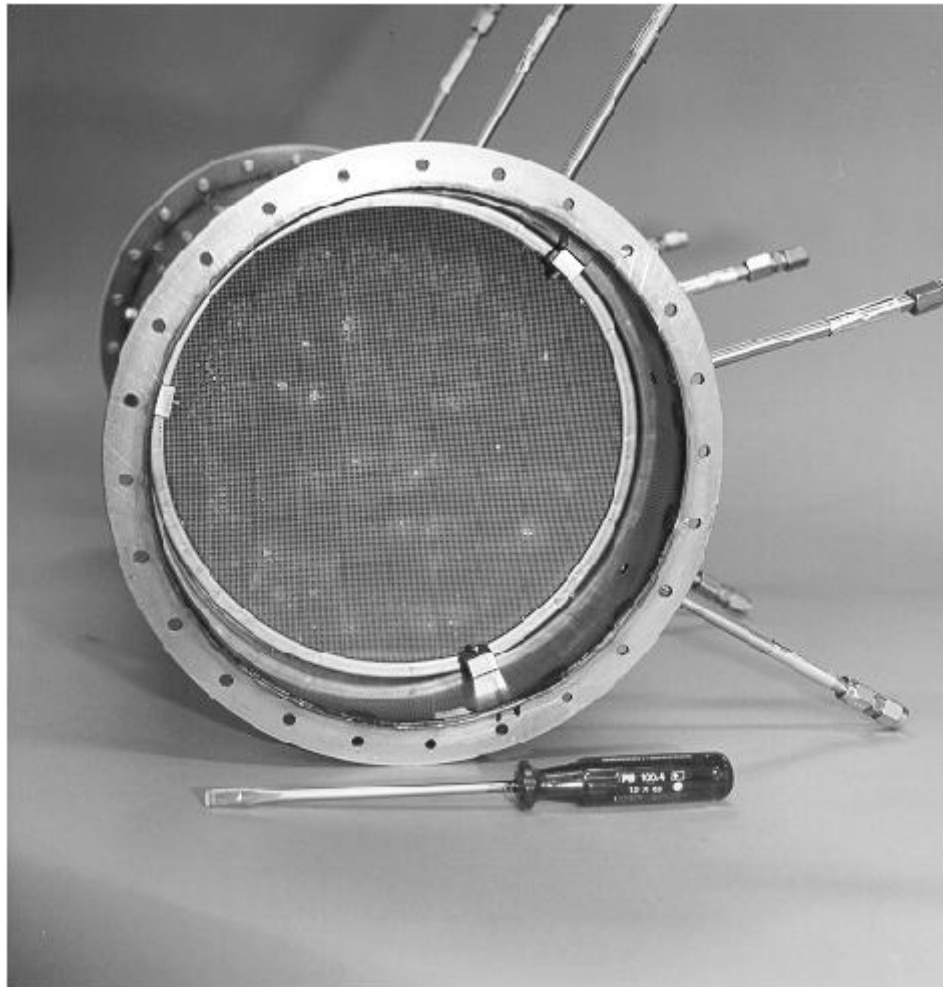

Figure 9.2   Catalyst K69.

Experiments on the diesel test stand

Table 9.2 Specifications of the SCR catalysts K69 and M30.

| Catalysts	K69	M30
support material	cordierite (2 MgO·2 Al_2O_3·5 SiO_2)	heat resistant steel
cell density	300 cpsi	400 cpsi
cell geometry	square	triangular
pitch* * without coating	1.3 mm	1.25 mm
wall thickness* * without coating	170 μm	50 μm
geometric surface* * without coating	23 m^2	29 m^2
catalyst geometry	cylinder	cylinder
catalyst length	151 + 75 mm	101 + 101 mm
catalyst volume	9.85 dm^3	9.18 dm^3
frontal dimensions	diameter = 241 mm	diameter = 240 mm
coating thickness	50 μm	50 μm
active mass (coated)	1900 g	2200 g

9.2.4 Measurement of the standard exhaust gas components

CO, CO_2 and N_2O were measured by means of a multi-component IR spectrometer (Perkin Elmer MCS 100). The NO feed concentration entering the SCR catalyst was determined by an electrochemical analyzer AEG 4000 S. NO_x downstream of the SCR

catalyst was measured by means of a chemiluminescence detector (Tecan CLD 502). Oxygen concentrations were measured using a paramagnetic oxygen analyzer (Helantec OX2). Unburned hydrocarbons were determined with a flame ionization detector FID (J.U.M. VE7).

9.2.5 Measurement of NH_3 and HNCO

The on-line measurement of NH_3 and HNCO was performed using an apparatus developed by our group [1]. A constant gas stream is extracted from the exhaust and its NH_3 and HNCO are continuously absorbed into a constant stream of absorbing solution. A partial stream of the solution ($\approx 40\%$) is alkalized by the addition of a constant stream of sodium hydroxide solution. Ammonia may then directly be measured by an ammonia-sensitive electrode. Another partial stream of $\approx 40\%$ is acidified by the addition of a constant stream of hydrochloric acid and is subsequently heated in a small flow-through heat exchanger to $\approx 60°C$. This causes the hydrolysis of isocyanic acid into ammonium ions and carbon dioxide:

$$HNCO + H^+ + H_2O \rightarrow [NH_4]^+ + CO_2$$
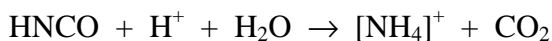
The solution stream is subsequently alkalized by the addition of a constant stream of sodium hydroxide solution thus yielding free ammonia. Therefore, ammonia measured in this stream corresponds to the sum NH_3 + HNCO. The concentration of HNCO is obtained by difference between the two measurements.

9.3   Results and Discussion

9.3.1   Catalyst K69 (cordierite support)

Figure 9.3 reports the curves of DeNOx vs. NH_3-slip for catalyst K69 using urea solution as reducing agent. At the lowest operating point (20 kW/225°C) only 32% DeNOx were obtained. However, NO_x conversions higher than 90% were observed at exhaust temperatures above 300°C. At the operating point 100 kW/465°C, the NO_x conversion again decreased to $\approx$ 70%.

Experiments on the diesel test stand

Catalyst K69 showed a high selectivity for SCR. The formation of N_2O was found to be very low. 10 ppm N_2O were detected at 100 kW/465°C; at lower temperatures N_2O was practically not detected. Moreover, an slight overconsumption of reducing agent was observed at 100 kW/465°C, meaning that some ammonia is oxidized to nitrogen

Figure 9.4 reports the curves of DeNOx vs. NH_3-slip for catalyst K69 using ammonia solution as the reducing agent. Other experiments have shown that the delayed thermo-hydrolysis of urea will lead to a lower SCR performance if urea is used instead of ammonia [2]. The different behavior of the curves in Figure 9.3 and 9.4 at the operating point 100 kW/465°C indicates that the thermohydrolysis of urea is rate limiting at these operating conditions. At lower temperatures no influence of the reducing agent on the SCR performance has been observed.
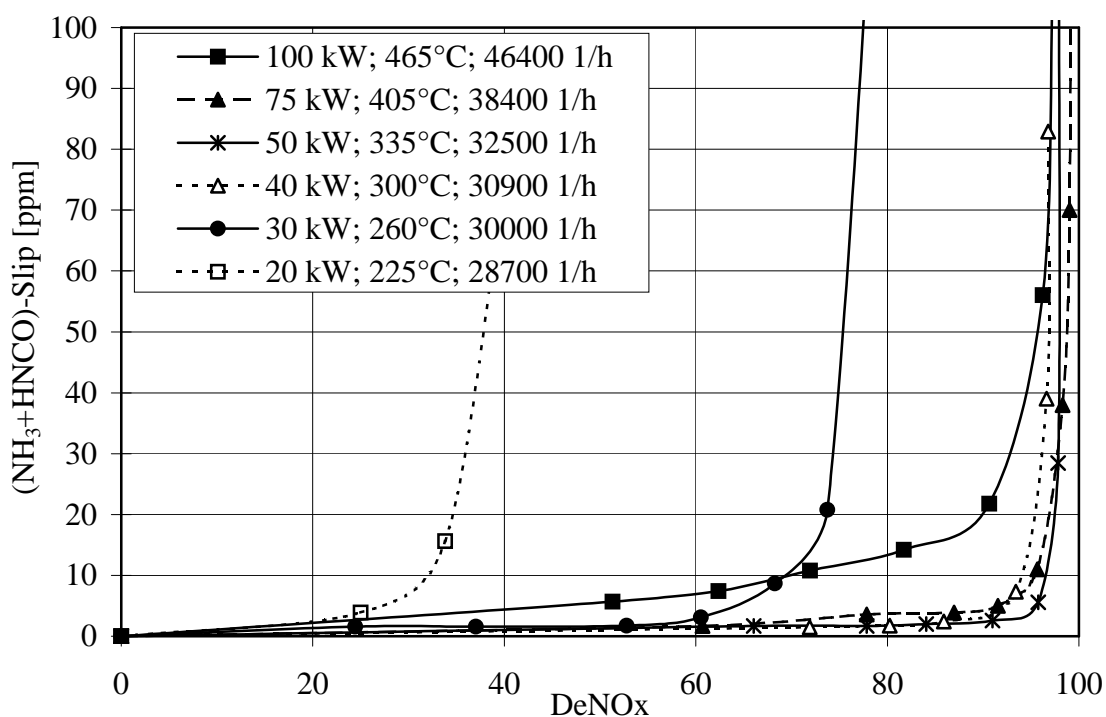

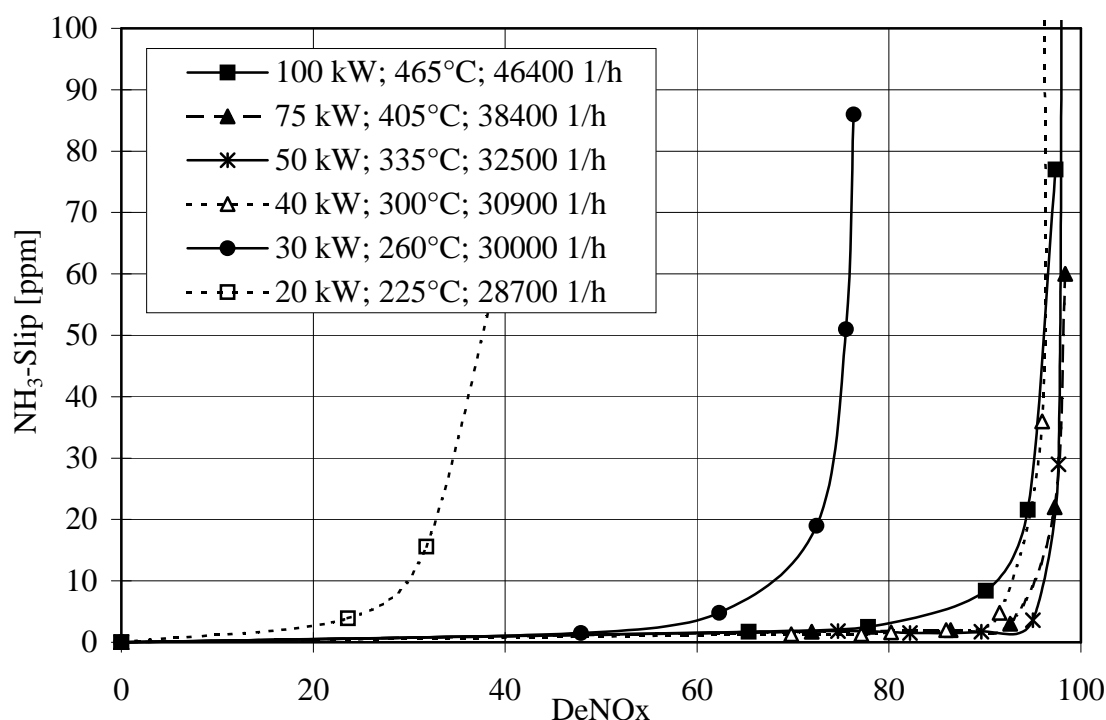**Figure 9.3**   Curves of DeNOx vs. NH_3-slip for catalyst K69. Reducing agent = urea solution. GHSV=28000 - 47000 h^{-1}.

Figure 9.4   Curves of DeNOx vs. NH_3-slip for catalyst K69. reducing agent = ammonia solution. GHSV=28000 - 47000 h^{-1}.

The test stand experiments were compared with laboratory experiments using a simulated test gas mixture of 1000 ppm NO, 5% H_2O, 10 % N_2, balance N_2 and variable amounts of NH_3. A catalyst sample K70 was used, which had been prepared according to the same procedure (chapter 3). K70 contained 1.4 grams of active mass and was supported on a monolithic cordierite carrier with a volume of 7.3 cm^3 and a cell density of 370 cpsi. In the laboratory tests, ammonia was used as reducing agent and the test gas mixture was free from CO_2 and hydrocarbons.

Figure 9.5 reports the results. Comparing Figure 9.4 with 9.5 shows that the NO_x conversion in real exhaust gas is definitely lower than in the simulated exhaust at temperatures below 300°C. This suggests that, at low temperatures, the SCR reaction is inhibited by hydrocarbons contained in real exhaust. On the other hand, at temperatures above 300°C, the SCR catalyst will oxidize most of the hydrocarbons, thus yielding practically equal values of DeNOx in both gas compositions.
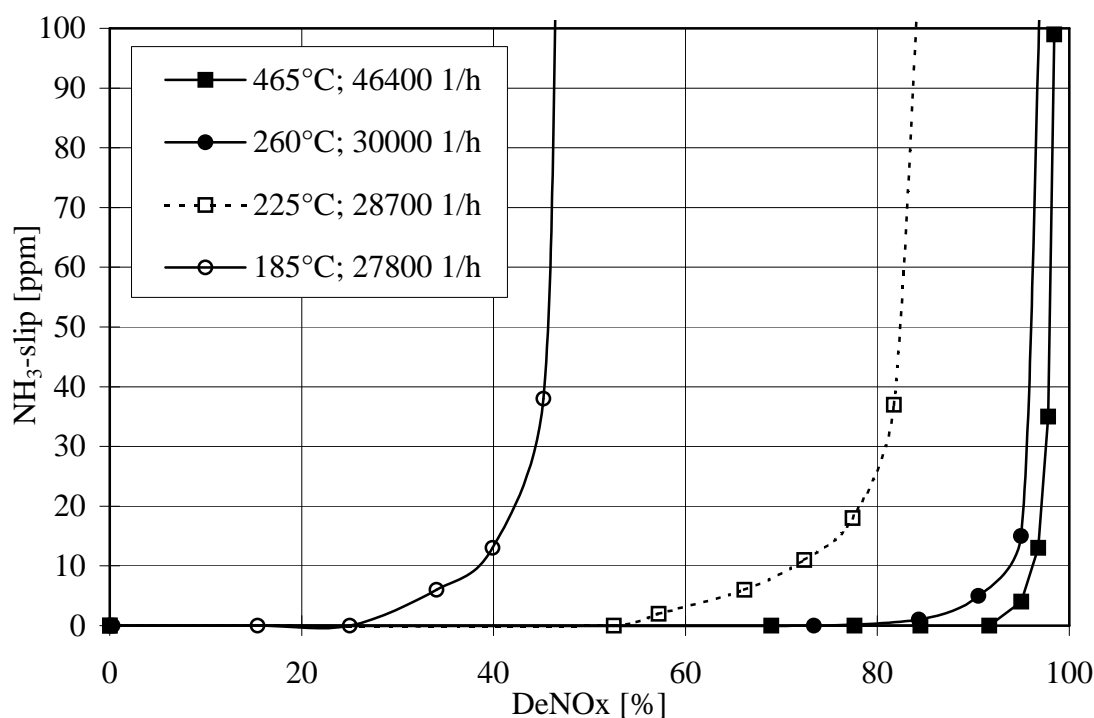
Experiments on the diesel test stand

Figure 9.5 Curves of DeNOx vs. NH_3-slip for K70. Lab tests with a synthetic gas mixture at the same values of temperature and GHSV as the test stand experiments. Reducing agent = gaseous ammonia. GHSV=28000 - 47000 h^{-1}.

9.3.2 Catalyst M30 (metal support)

Catalyst M30 had a higher amount of active mass than catalyst K69: the thinner walls of the metal monolith allow for a higher amount of active mass per volume of catalyst (see Table 9.2). Figure 9.6 reports the curves of DeNOx vs. NH_3-slip for this catalyst using urea solution as reducing agent. Although the amount of active mass is higher, catalyst M30 reaches lower DeNOx-values than catalyst K69 at low temperatures (compare Figure 9.3 with 9.6). Further laboratory investigations could not give an explanation for this effect. In our opinion, the impurities of the metallic carrier, mainly Zn, should be responsible for the lower SCR activity. It is a well known fact that basic compounds have a negative effect on the SCR performance [3] and Zn has basic properties.
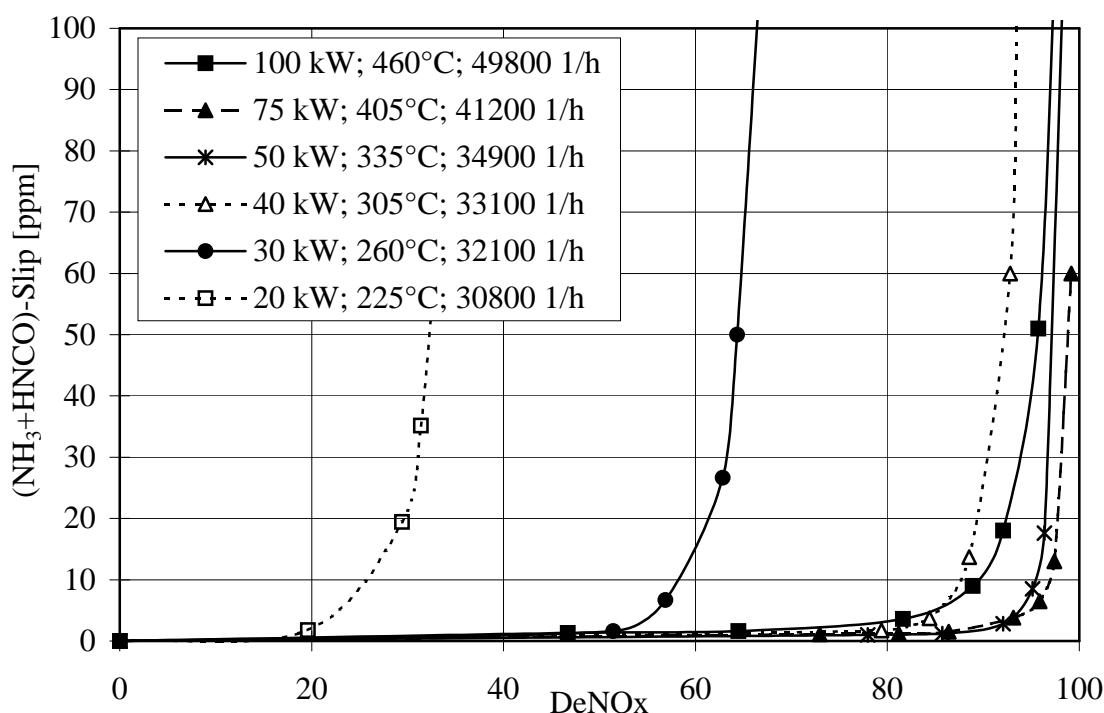
Figure 9.6   Curves of DeNOx vs. NH_3-slip for catalyst M30. Reducing agent = urea solution. GHSV=30000 - 50000 h^{-1}.

In spite of the lower intrinsic activity, catalyst M30 showed a higher NO_x conversion than catalyst K69 at the operating point 100 kW/465°C with urea (compare Figure 9.3 and 9.6). Moreover, catalyst M30 showed practically the same SCR performance with urea and ammonia. These observations suggest that the higher cell density of catalyst M30, enhancing the collisions of the urea drops to the catalyst surface, favored the thermohydrolysis of urea.

9.3.3   The combined system: oxidation catalyst + SCR catalyst

Additional experiments were made in order to investigate the effect of a pre-oxidation catalyst on the conversion of NO_x under real exhaust gas conditions. Figure 9.7 shows the curves of DeNOx vs. NH_3-slip for such a combined system. These curves were obtained using urea as the reducing agent. The comparison of Figure 9.3 (SCR catalyst

Experiments on the diesel test stand

alone) and 9.7 (combined system) shows that the addition of an oxidation catalyst enhances the NO_x conversion especially at low temperatures.
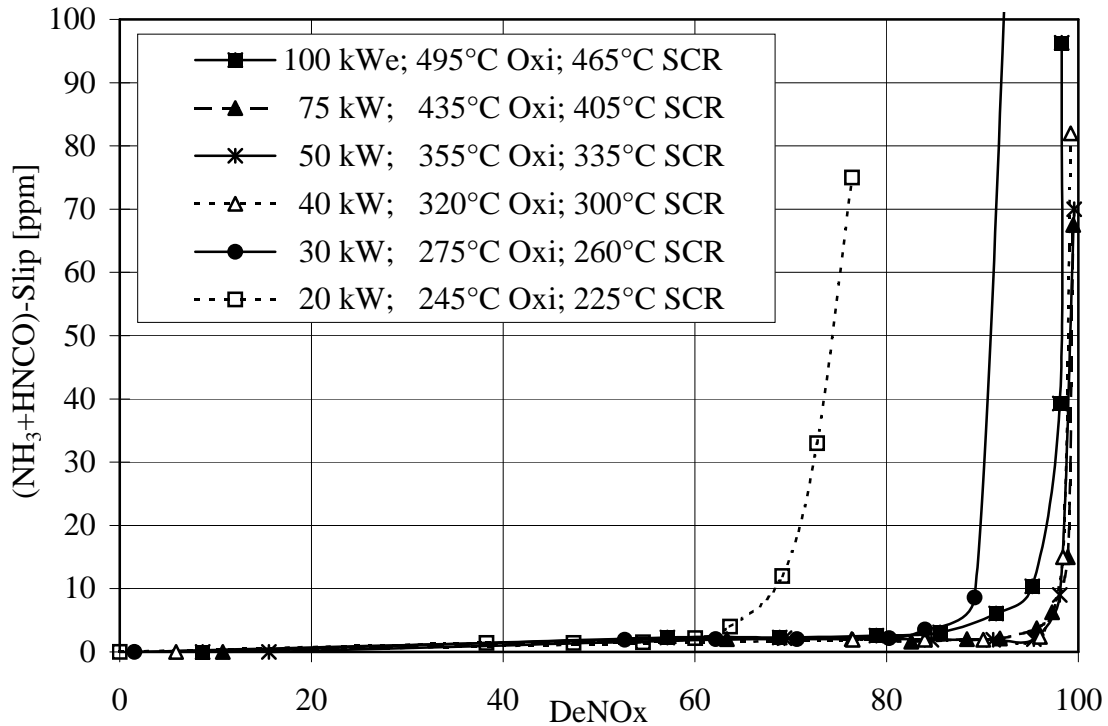

Figure 9.7   Curves of DeNOx vs. NH_3-slip for the combined system of oxidation catalyst + SCR   catalyst (K69). Reducing agent = urea solution. $GHSV_{SCR}$=28000-47000 h^{-1}.

Table 9.3 reports the conversion of NO to NO_2 on the oxidation catalyst in these experiments. At temperatures below 300°C the oxidation of NO to NO_2 was quite low, thus resulting in a negligible contribution of the fast SCR reaction to the NO_x conversion on the SCR catalyst. At the operating points 20kW/225°C and 30 kW/260°C, the SCR performances of the combined system were practically equal to the SCR performances evaluated in the laboratory tests (Figure 9.5). A synthetic gas mixture without hydrocarbons and with NO_x = pure NO was used in the laboratory tests. These

findings suggest that the beneficial effect of the oxidation catalyst on DeNOx were mainly due to the oxidation of hydrocarbons contained in real exhaust (see Table 9.4).

Table 9.3 Conversion of NO to NO_2 on the oxidation catalyst.

Electric Power [kW]	T Oxi-Cat [°C]	NO_2 in NO_x before OxiCat [%]	NO_2 in NO_x after OxiCat [%]
100	495	3	17
75	440	3	28
50	360	6	35
40	330	9	27
30	280	11	17
20	240	18	11
10	200	26	2

A major drawback of the additional oxidation catalyst is an increase of the exhaust back-pressure. An increased back-pressure has negative effects on the fuel economy and the maximum engine power. Therefore, it is highly undesirable. Table 9.5 reports the measured pressure drops of the piping alone and of the complete system. The values reported in Table 9.5 show that the pressure drops increase with increasing generator power. With increasing engine power the exhaust flow also increases. It is also evident that the oxidation catalyst contributes significantly to the total pressure drop, almost doubling the pressure drop of the complete system. The highest measured pressure drop was 115 mbar.

The addition of the oxidation catalyst brings about another problem by reducing the distance between the point of urea injection and the SCR catalyst. This distance should be as large as possible in order to allow complete mixing of the reducing agent with the exhaust gas. Figure 9.8 reports a typical radial concentration profile of ammonia

Experiments on the diesel test stand

measured for the case of a short distance ($\approx$ 50 cm) between the point of urea injection and the SCR catalyst.

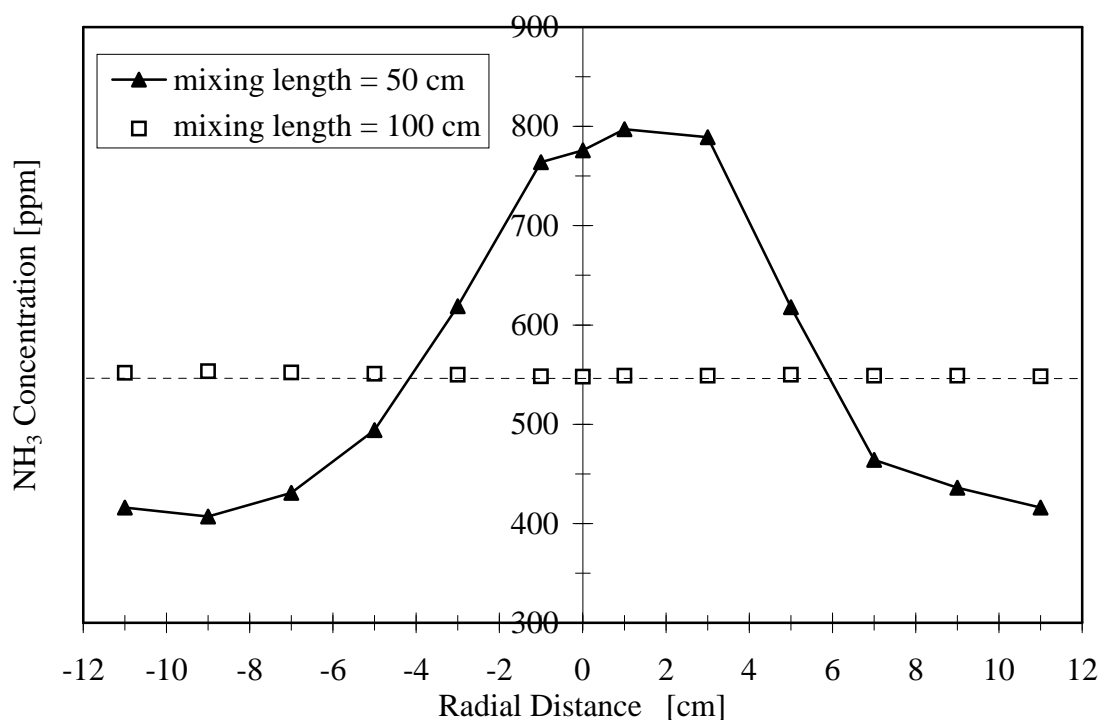**Table 9.4**   Oxidation of CO and unburned hydrocarbons on the oxidation catalyst.

Electric Power [kW]	T Oxi-Cat [°C]	CxHy before OxiCat [ppm C1]	CxHy after OxiCat [ppm C1]	CO before OxiCat [ppm C1]	CO after OxiCat [ppm C1]
100	495	87	21	88	8
75	440	92	18	74	4
50	360	105	21	83	3
40	330	115	23	94	3
30	280	125	26	145	3
20	240	127	31	194	5
10	200	162	82	250	48

Due to the separated flows in the individual channels of the monolithic catalyst, the radial concentration profile will extend into the catalyst itself. In the center channels the stoichiometric ratio α will be higher than at the circumference. When the catalyst is further operated at its kinetic limits (comparably high α), this will diminish the average NO_x conversion for a given ammonia slip.

Summarizing, bad mixing of reducing agent with the exhaust causes low NO_x conversions and high slips of ammonia, thus lowering significantly the SCR performance [4]. In the present experiments acceptable mixing of reducing agent and exhaust was obtained when the distance between the point of urea injection and the SCR catalyst amounted to about 1 meter (Figure 9.8).

Chapter 9

Table 9.5   Back-pressures measured at the test stand.

Electric Power [kW]	Δp (no catalyst) [mbar]	Δp (catalyst K69) [mbar]	Δp (OxiCat+K69) [mbar]	Δp (catalyst M30) [mbar]	Δp (OxiCat+M30) [mbar]
100	29	70	115	66	115
75	21	50	85	48	81
50	13	33	59	32	58
40	11	30	53	28	50
30	10	25	45	24	43
20	9	21	40	20	35
10	not meas.	18	34	16	29

Figure 9.8   Measured radial profile of NH_3 concentration detected on the cross area of the SCR catalyst. Nominal value of NH_3 concentration = 550 ppm.

9.3.4 Unsteady state investigations

The results of the steady state investigations were used to determine the dosage of the reducing agent (i.e. urea solution) in unsteady state experiments as they occur in the automotive application of the process. These investigations were carried out in the range 25 kW/245°C to 100 kW/465°C according to the test cycle reported in Figure 9.9. The duration of the test cycle was 40 minutes.
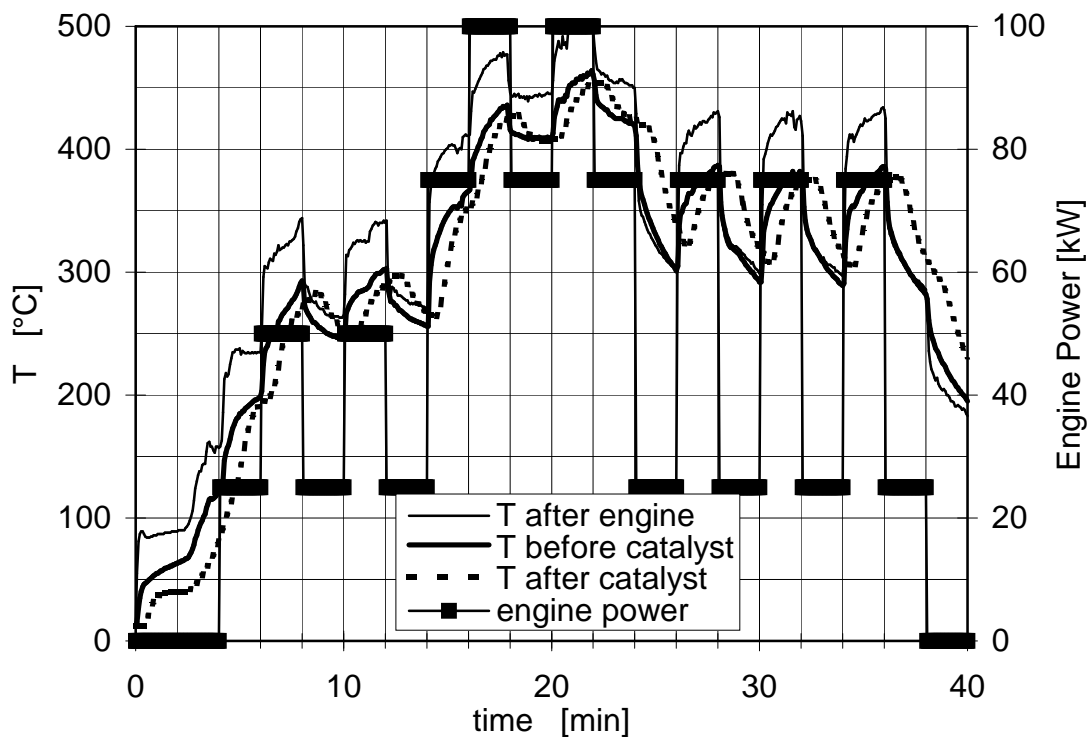

Figure 9.9 Engine powers and exhaust temperatures in the unsteady state experiments (cold start test).

The actual dosage of the reducing agent (urea solution) was calculated by a computer program. The actual engine power is used as a control signal for the NO_x concentration. The actual catalyst temperature is representative for the catalyst activity, as determined previously in the steady state investigations. The required amount of reducing agent is first calculated for a DeNOx of 100%, and subsequently the actual activity of the catalyst is used to calculate the effective dosage. In order to avoid solid deposits, the dosage of urea is only started when the exhaust temperature has reached 200°C.

Chapter 9

The unsteady state experiments were again carried out with the SCR catalyst alone and with the combined system including the oxidation catalyst. Table 9.6 reports the results of these investigations. It can be seen that the SCR catalyst alone can reduce the NO_x emissions clearly below the value of 3.5 g/kWh proposed in the forthcoming EURO IV legislation [5]. The combined system can reach an even higher NO_x removal.

Table 9.6   Overall DeNOx, NO_x and NH_3 emissions in the test cycle shown in Figure 9.9. (Reducing agent = urea solution)

	DeNOx [%]	NO_x IN [g/kWh]	NO_x OUT [g/kWh]	NH_3 OUT [g/kWh]
Cold Start				
K69	76	8.7	2.1	0.09
OxiCat + K69	81	8.1	1.5	0.06
M30	77	7.7	1.8	0.20
OxiCat + M30	79	7.2	1.5	0.18
Warm Start				
K69	80	8.7	1.7	0.04
OxiCat + K69	87	7.8	1.0	0.04
M30	85	7.5	1.1	0.10
OxiCat + M30	89	7.1	0.8	0.08

The emissions of HNCO were very low: traces of 1-2 ppm could only be observed at the highest operating point (100 kW/465°C). They are due to an incomplete thermohydrolysis of urea. Low emissions of ammonia were achieved using the dosage strategy described above. The slip of ammonia is mainly due to the release of ammonia adsorbed on the catalyst surface when a sudden increase of exhaust temperature occurs [6].

9.4   Conclusions

The test stand experiments have shown that an aftertreatment system based on the SCR process may reduce the NO_x emissions of automotive lean exhaust below the forthcoming EURO IV emission standards. NO_x conversions as high as $\approx$80% could be obtained using coated SCR catalysts with a volume of $\approx$10 liters.

The SCR catalysts coated on metal monoliths were found to be less active than the catalysts coated on cordierite monoliths. The metal impurities, mainly Zn, present in the metal foils of the carrier probably inhibit the SCR reaction. Conversely, the higher cell densities of metal carriers enhance the thermohydrolysis of urea, probably due to their better ability to trap the urea aerosol.

The experiments have also shown that the additional oxidation catalyst enhances the NO_x conversion at low temperatures. Laboratory tests suggested that the better NO_x conversion was mainly due to the combustion of hydrocarbons contained in the real exhaust. Due to the modest volume of the oxidation catalyst, the NO_2 concentration reaching the SCR catalyst was low, thus resulting in a negligible contribution of the fast SCR reaction to the removal of NO_x. A larger oxidation catalyst could increase the NO_x conversion at low temperatures considerably.

The disadvantages of the oxidation catalyst are an increased back-pressure and less favorable conditions for the mixing of the reducing agent with the exhaust. These aspects should be carefully assessed when designing an optimized system.

9.5   References

[1]   M. Koebel and M. Elsener, *Kontinuierlich arbeitender Analysator zur Ammoniak-bestimmung in Abgasen von SCR und SNCR-Anlagen*, TM-51-91-17, Paul Scherrer Institut (1991)

[2]   M. Koebel, M Elsener and G. Madia, *SAE Paper* N. 2001-01-3625

155

[3]   M. Kleemann, *Beschichtung von Cordierit-Wabenkörpern für die selektive kata-lytische Reduktion von Stickoxiden*, Thesis ETH Nr. 13401, Zurich (1999)

[4]   F. Bettoni, *Untersuchungen zum stationären und dynamischen Verhalteneines Entstickungssystems nach dem SCR-Prinzip mit realem Dieselabgas,* Thesis ETH Nr. 12443, Zurich (1997)

[5]   G. Emmerling and F.I. Zuther, *Motorische Verbrennung - aktuelle Probleme und moderne Lösungsansätze*, Berichte zur Energie- und Verfahrenstechnik, Schriftenreihe Heft 99.1, Erlangen (1999), 581

[6]   M.Koebel, M. Elsener and M. Kleemann, *Catal. Today* **59** (2000), 335

10

Thermal stability of TiO$_2$-WO$_3$-V$_2$O$_5$ catalysts

10.1 Introduction

A high thermal stability of vanadia-tungsta-titania catalysts is a prerequisite for the automotive application of urea-SCR. Many authors suggested that sintering of anatase and anatase-to-rutile phase transition are the major factors responsible for the deactivation of vanadia-titania catalysts at temperatures exceeding 500°C [1,2]. This effect has been partly attributed to the observed decrease of the catalyst surface area and to the intrinsically lower activity of the rutile-based catalysts [3]. Anatase sintering and anatase-to-rutile phase transition depend strongly on the thermal history and on the composition of the catalyst. Surface vanadium species speed up the growth of anatase and the anatase-to-rutile phase transition [1,4,5]. High surface area anatase sinters and undergoes phase transition at lower temperatures than samples with low surface area [6]. At temperatures approaching 690°C, melting of V$_2$O$_5$ should also contribute to the deactivation of the catalyst [6].

Went et al. [7] found that the surface structure of vanadyl species present in TiO$_2$-V$_2$O$_5$ catalysts has a pronounced effect on the activity and the selectivity for the reduction of NO$_x$ by ammonia. Raman analysis of TiO$_2$-V$_2$O$_5$ catalysts showed that at vanadia loadings below a monolayer the vanadia is present as monomeric vanadyl and polymeric vanadate species. As the vanadia loading is increased above the dispersive

capacity of the support, crystallites of V_2O_5 form at the expense of the polymeric species leading to a decrease of the SCR selectivity. On the other hand, increasing the loading of vanadia causes the formation of more polymeric vanadate species, which are estimated to be approximately 10 times more active than monomeric species. Therefore, an optimum SCR activity is attained at some intermediate vanadia loading.

The following experiments were made with catalyst samples having different vanadia contents (1, 2 and 3 wt-% V_2O_5). The effect of various ageing treatments on the physical properties of the catalyst and on the surface species was studied and correlated with the practically measured SCR activity and selectivity of the catalysts.

10.2   Experimental

10.2.1 Catalyst samples and reactor

The tested catalysts were prepared in house according to the method reported in chapter 3. The final treatment was a calcination step in air at 500°C for 4 hours ("new catalyst"). The anatase support contained ≈8 wt-% WO_3 and the vanadia content of the three samples amounted to 1.1, 2.26 and 3.0 wt-%. For simplicity, the samples will be further denoted as 1, 2 and 3 wt-% V_2O_5.

The activity tests were carried out using monolithic samples with a volume of 6.9 cm^3 and a total coating mass of 1.2 g in the test rig described in chapter 2. The monolithic carriers consisted of cordierite and had a cell density of 370 cpsi (cells per square inch). Powdered SCR catalysts (160 μm < d_P < 200μm) were used for the BET surface area determination, XRD, XPS and Raman measurements.

The different investigations were carried out with the new catalyst samples and after performing the following ageing procedures:

- ageing 1: the catalyst was aged for 100 hours at 550°C;

- ageing 2: the catalyst was aged for 100 hours at 550°C and for 30 hours at 600°C;

- ageing 3: the catalyst was aged for 100 hours at 550°C, for 30 hours at 600°C and for 15 hours at 650°C.

Ageing procedure 3 is extreme because the temperature approaches the melting point of V_2O_5 (690°C). However, in the practical application of urea-SCR, temperatures up to 650°C must be considered. Such temperatures may occur at extreme operating points of the diesel engine (low rpm and high load).

10.2.2 BET surface area determination

N_2 adsorption isotherms were measured at 77 K with a Micromeritics ASAP 2000 apparatus, after pre-treating the samples overnight under vacuum at 200°C. For calculating the BET specific surface area, relative pressures in the range 0.05 - 0.2 were used, assuming that each N_2 molecule occupies a surface of 0.162 nm^2.

10.2.3 X-ray diffraction (XRD) measurements

Diffraction patterns were recorded with a Philips X'Pert powder diffractometer with Fe Kα radiation. Measurements were carried out in the 2θ range extending from 10 to 90° using a step size of 0.05°.

10.2.4 X-ray photoelectron spectroscopy (XPS) measurements

XPS measurements were performed on an ESCALAB 220i XL instrument (VG Scientific) using Mg Kα radiation from a twin-anode assembly which was operated at a power of 300 W (15 kV, 20 mA). The vacuum in the analysis chamber was better than $5 \cdot 10^{-9}$ mbar. The instrument was operated in the constant analyzer energy mode at a pass energy of 20 eV, giving a FWHM (full width at half maximum) for the Ag $3d_{5/2}$

peak of clean metallic silver equal to 0.9 eV. Binding energy (BE) values were referenced to the Ti $2p_{3/2}$ signal (458.7 eV), giving charging always lower than 6 eV. The quantification of the XPS spectra was carried out using the cross-sections calculated by Scofield [8]. For quantification of vanadium, overlapping O 1s satellites were subtracted from the spectrum according to the intensities measured for a clean copper sample.

10.2.5 Raman spectroscopy measurements

Raman spectra were acquired with a confocal Raman microscope (Labram, DILOR) equipped with a 50x magnification objective (laser spot size ~ 5 µm) and a thermoelectrically cooled CCD detector. The Raman spectra were obtained in a backscattering geometry with the yellow line (λ = 568.2 nm) of a Kr-ion laser (Coherent Innova 302). The power at the sample was kept at 2.5±0.2 mW. No laser-induced damage was observed at this laser power, as shown by visual inspection of the sample and by the constancy of the Raman spectrum with acquisition time. Raman spectra were routinely acquired in the range from 300 to 1500 cm^{-1} using a 1800 grooves/mm grating. In order to avoid effects due to a changing degree of hydration, the Raman spectra were collected immediately after the ageing treatments.

10.3   Results

10.3.1 DeNO$_x$ activity measurements

Figure 10.1 reports the NO$_x$ conversion (DeNO$_x$) at 10 ppm of ammonia slip at 300°C for catalysts with 1, 2 and 3 wt-% V_2O_5 in new conditions and after the ageing procedures 1, 2 and 3.

In new conditions a high NO$_x$ conversion was obtained with catalysts containing 2 wt-% and 3 wt-% V_2O_5, whereas the catalyst with 1 wt-% V_2O_5 showed only low SCR activity. The catalyst with 3 wt-% V_2O_5 showed a decrease in the SCR activity upon

ageing, whereas the SCR performance of the catalysts with 1 and 2 wt-% V_2O_5 slightly improved after the ageing procedures 1 and 2. Ageing procedure 3 led to a drastic decrease of the SCR performance of the catalyst with 3 wt-% V_2O_5. The catalyst with 2 wt-% V_2O_5 showed only a slight reduction of SCR activity after the ageing procedure 3.
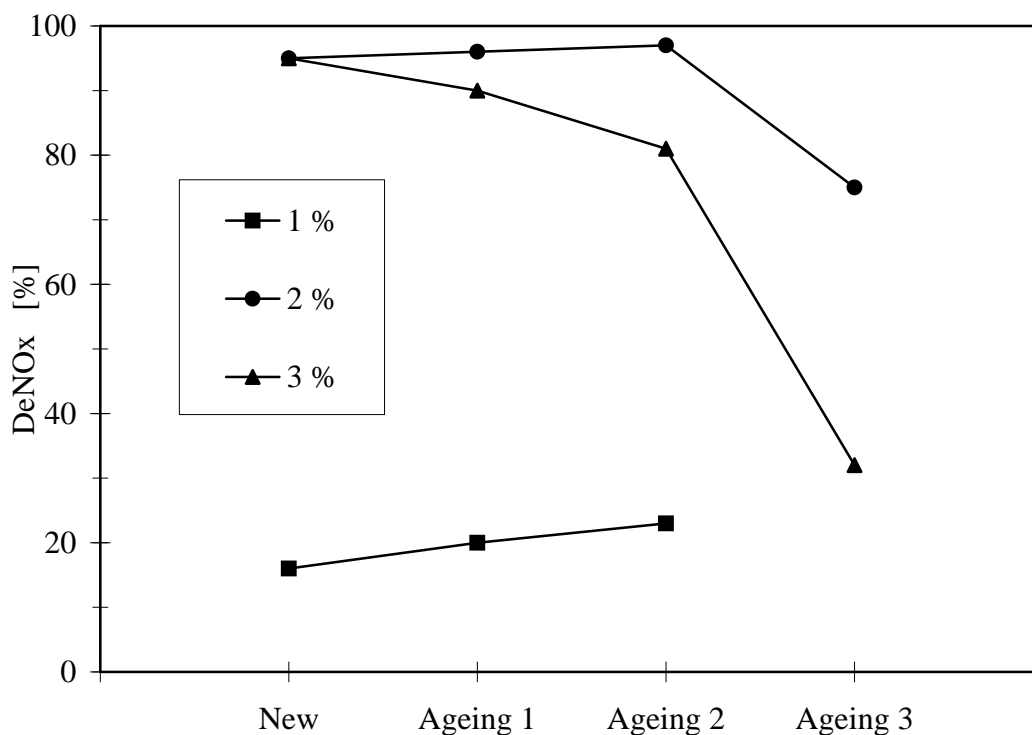

Figure 10.1 DeNO$_x$ at 10 ppm NH$_3$-slip in new conditions and after ageing procedures 1, 2 and 3 for SCR catalysts with 1, 2 and 3 wt-% V_2O_5. T=300°C. Feed: 1000 ppm NO, NH$_3$, 5% H_2O, 10% O_2, balance N_2. GHSV=52000 h^{-1}.

10.3.2 BET surface area determination

The change of the BET specific surface area as a function of the applied ageing conditions is illustrated in Figure 10.2 for various V-loadings. The specific surface area of all catalysts decreased with increasing harshness of the ageing treatment. The loss of sur-

face area was related to the V-content, with the V-richest sample undergoing the most significant loss. The specific surface area of the WO_3-TiO_2 support only decreased by 20 % upon the ageing procedure 3. This is in agreement with previous observations that vanadia promotes the loss of surface area in these materials [6].
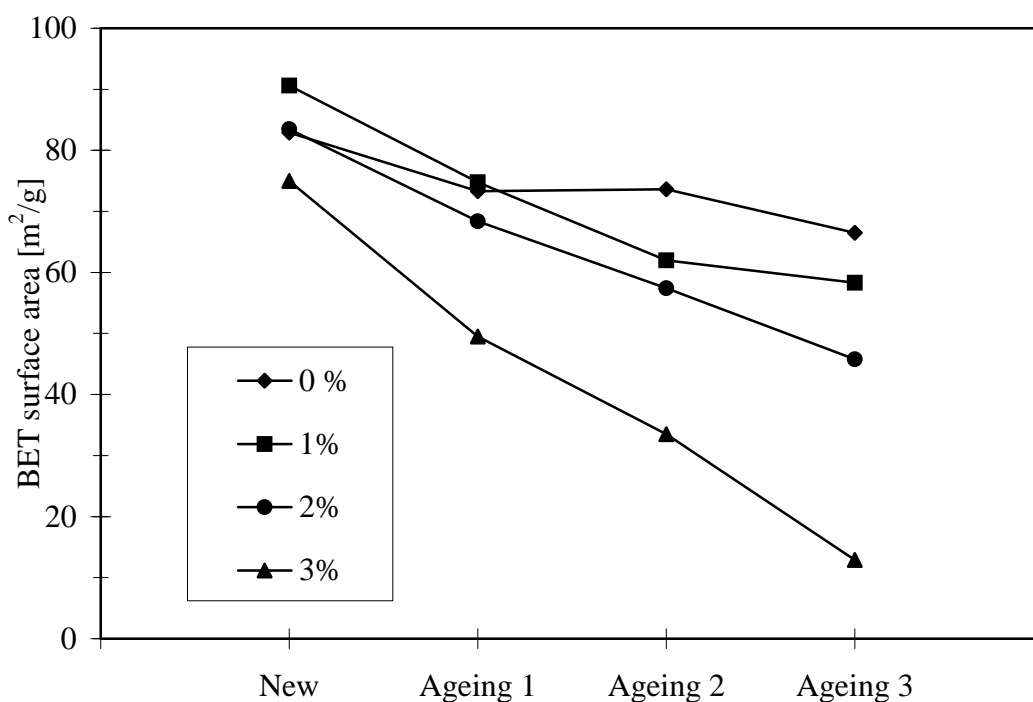

Figure 10.2   BET specific surface area vs. ageing procedure for various V_2O_5 contents

10.3.3 X-ray diffraction (XRD) measurements

Anatase (PDF 71-1167) was the only TiO_2 phase detected in all samples, indicating that significant rutilisation did not take place under all applied ageing conditions. From the FWHM (full width at half maximum) of the anatase (101) diffraction peak, the average dimension $d_{(101)}$ of the anatase particles perpendicularly to the (101) plane was calculated using the Scherrer equation:

$$d_{(101)} = \frac{K\lambda}{\sigma \cos \vartheta} \tag{10.1}$$

K is a constant that depends on the shape of the particles and is generally assumed to be 1, λ is the wavelength of the X-ray radiation, σ is the FWHM of the considered diffraction peak and ϑ its position [9]. The resulting average anatase particle size after the applied ageing procedures is shown in Figure 10.3.
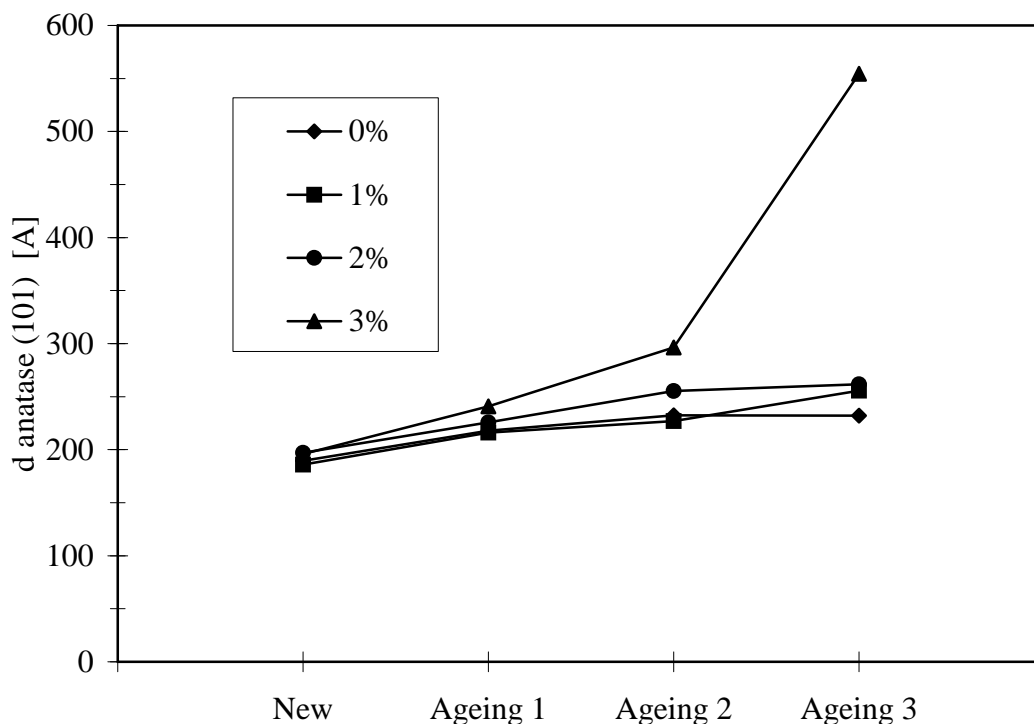

Figure 10.3   Average anatase particle dimension perpendicularly to the (101) plane vs ageing procedure for various V_2O_5 contents. The particle dimension was calculated by the Scherrer equation from the FWHM of the anatase (101) diffraction peak (see text).

The anatase particles grow larger with increasing ageing temperature for all studied V-loadings. This indicates that anatase sintering is involved in the observed loss of BET specific surface area. The fact that the catalyst with 3 wt-% V_2O_5 undergoes the largest change in particle size, above all after the most drastic treatment, suggests that growth of the anatase crystallites is favored by a higher V-content. Figure 10.4 shows the cor-

relation between the BET specific surface area and the anatase particle size calculated from the broadening of the (101) diffraction peak. The continuous line represents the calculated specific surface area of spherical anatase particles as a function of their diameter.
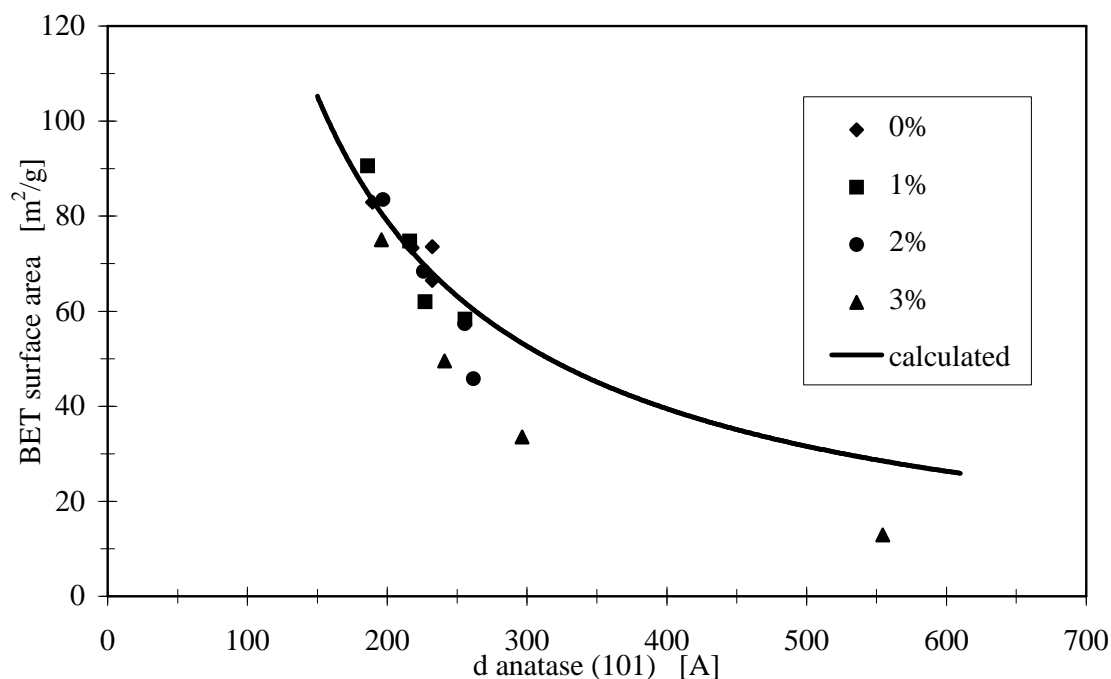

Figure 10.4 BET specific surface area vs. average anatase particle dimension perpendicularly to the (101) plane after various ageing procedures and for various V_2O_5 contents. The continuous line corresponds to the specific area of spherical anatase particles having a diameter equal to $d_{(101)}$ calculated as: $A_{BET} = (6/\rho_{anatase})/d_{(101)}$.

It can be seen that, for V_2O_5-contents equal to 0 and 1 wt-%, the measured BET surface area is in good agreement with the values calculated for spherical anatase particles, indicating that no significant pore clogging is occurring. For a 2 wt-% V_2O_5-content the agreement is still good after the ageing procedure 2, whereas a significant deviation is observed after the ageing procedure 3. After all the ageing procedures, the catalyst con-

Chapter 10

taining 3 wt-% V_2O_5 shows a BET specific surface area lower than the value calculated for spherical anatase particles, indicating that, at higher V-contents, pore clogging is involved in the loss of surface area together with the sintering of anatase. Formation of crystalline WO_3 (PDF 46-1096 and/or PDF 76-1734) was observed in all samples after the ageing procedure 2. After the ageing procedure 3, the intensity of the diffraction peaks corresponding to WO_3 increased more for the catalyst containing 3 wt-% V_2O_5 than for the samples containing smaller amounts of V_2O_5.

10.3.4 Characterization of the catalyst surface

The XPS investigations have shown that the V $2p_{3/2}$ BE generally increased with increasing V-loading and with increasing ageing temperature. The V $2p_{3/2}$ BE measured for all catalysts in new conditions and after the ageing procedures 1 and 2 was significantly lower than the value reported in the literature for bulk V(V)-containing phases (516.8-517.7 eV) [10], thus indicating the existence of very well dispersed vanadia on the TiO_2-WO_3 support [11]. Exposure of the catalysts containing 2 and 3 wt-% V_2O_5 to the ageing procedure 3 caused an increase of the V $2p_{3/2}$ BE to values typical of bulk V_2O_5, indicating a decrease of the vanadia dispersion at T=650°C, with the formation of multilayer regions.

The Raman investigations evidenced three surface vanadia species: monomeric tetrahedrally co-ordinated VOx units (feature at ~1200 cm^{-1}), polymeric metavanadate species (broad band extending from ~850 to ~960 cm^{-1}) and crystalline vanadia (peak at ~992 cm^{-1}). The V-loading and the ageing temperature influence the nature and distribution of the surface vanadia species (Figure 10.5 and 10.6).

In the case of the catalyst containing 2 wt-% V_2O_5, ageing treatments at increasingly high temperatures led to higher intensity between ~910 and ~970 cm^{-1}, thus indicating the growth of metavanadate and/or metatungstate chains by polymerisation of monomeric VO_x and WO_x units.

The change of the Raman features of the catalyst containing 3 wt-% V_2O_5 with increasing temperature is quite different. The intensity of the polyvanadate species reaches a maximum after the ageing procedure 1 and then starts decreasing. After the ageing procedure 3, a peak at 992 cm^{-1}, attributed to crystalline vanadia, appears [12]. The corresponding XRD measurements did not show any diffraction peaks corresponding to crystalline vanadia, probably, because the vanadia crystallites were too small for producing a well-defined XRD pattern.

The band around 800 cm^{-1} consists of the overlapping contribution of a second-order anatase feature and of the W-O-W stretching of octahedrally co-ordinated W units [13,14]. In the case of the catalyst containing 3 wt-% V_2O_5, the intensity of this band strongly increased with increasing ageing temperature, whereas it remained constant for the catalyst containing 2 wt-% V_2O_5. This difference in the Raman spectra corresponds to the different evolution of the XRD patterns after ageing at increasing temperature.

A more detailed description of the surface characterization of the catalyst has been reported in a recent paper [15].
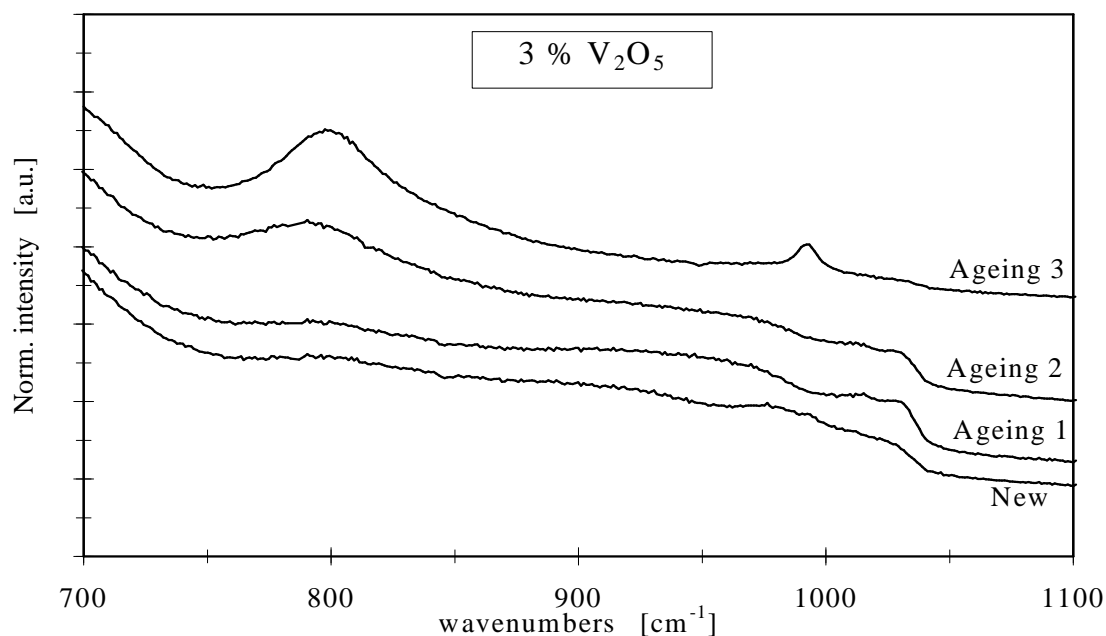
Figure 10.5   Raman spectra obtained after exposure of an SCR catalyst with 3 wt-% V_2O_5 to various ageing procedures. The spectra were normalized using the anatase peak at 637 cm^{-1}. (carried out by F. Raimondi)
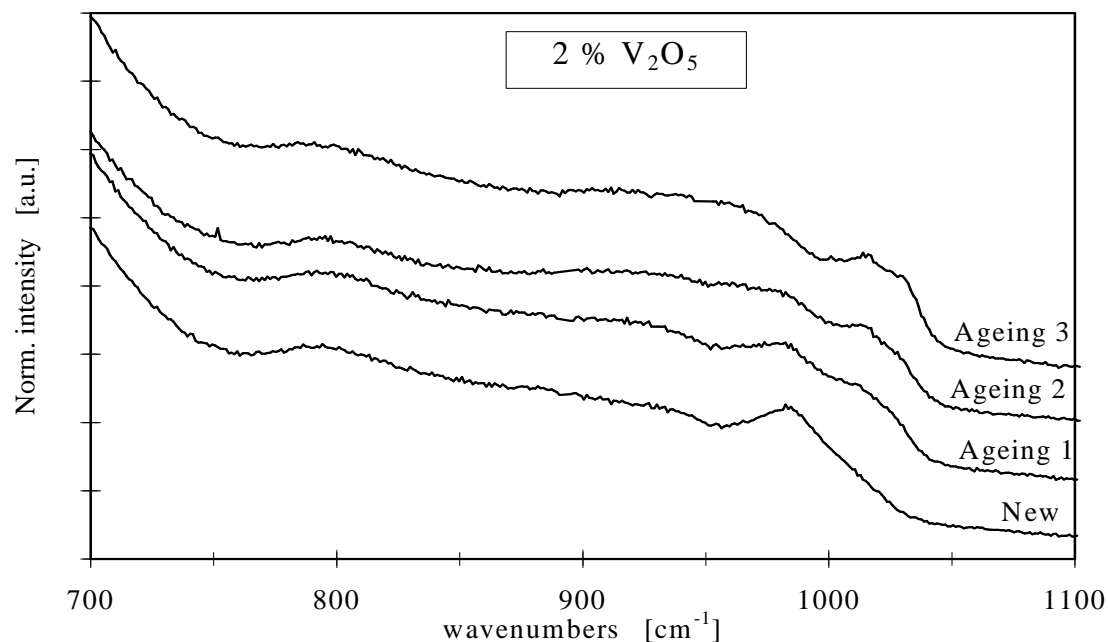

Figure 10.6   Raman spectra obtained after exposure of an SCR catalyst with 2 wt-% V_2O_5 to various ageing procedures. The spectra were normalized using the anatase peak at 637 cm^{-1}. (carried out by F. Raimondi)

Thermal stability of TiO$_2$-WO$_3$-V$_2$O$_5$ catalysts

10.4 Discussion

The results reported above indicate that the vanadium content strongly influences the thermal stability of SCR catalysts. The ageing treatments modify the surface vanadia species and the morphology of the anatase support influencing both the activity and the selectivity for the reduction of NO_x by ammonia. Characterization by BET surface area determination, XRD, XPS and Raman spectroscopy allowed to correlate the different structural modifications observed upon ageing for catalysts with various vanadium contents with the different changes of their SCR activity.

The SCR performance of the catalysts containing 2 and 3 wt-% V_2O_5 showed a very different response to the ageing procedure 1. The SCR activity of the catalyst containing 3 wt-% V_2O_5 decreased monotonously with increasing harshness of ageing so that the NO_x conversion after ageing procedure 3 was reduced to about 30% of its original value. On the other hand, the catalyst containing 2 wt-% V_2O_5 showed an increase of SCR activity after ageing procedures 1 and 2, and only a small loss of activity after ageing procedure 3.

XPS and Raman spectroscopy indicated that in all the catalysts investigated, after calcination at 500°C, vanadium was present in the form of supported monomeric vanadyl groups and metavanadate chains at sub-monolayer coverage. XRD experiments showed that sintering of the anatase particles was the main cause of the loss of catalyst surface area observed upon ageing. The lower anatase surface available to disperse the supported vanadia after the ageing treatment forced the supported monomeric vanadyl groups to polymerize as indicated by the increase of the Raman intensity at 960 cm^{-1} observed after ageing procedure 1 for both catalysts with 1 and 2 wt-% V_2O_5. The decrease of the fraction of anatase surface non-covered by vanadia upon ageing is confirmed by the increase of the V/Ti XPS ratio. After ageing procedure 1, the XPS V2p$_{3/2}$ BE was unchanged for the catalyst with 2 wt-% V_2O_5, whereas it increased significantly in the case of the catalyst containing 3 wt-% V_2O_5. This indicates that the vanadia did not form multilayer structures in the catalyst containing 2 wt-% V_2O_5, whereas significant three-dimensional growth occurred in the catalyst with 3 wt-% V_2O_5. The consequent loss of exposed V-sites explains the decrease in the SCR activity of the catalyst

with 3 wt-% V_2O_5 observed after ageing procedure 1. Moreover, the comparison of the BET specific surface area with the average anatase particle size given by XRD indicates that significant pore clogging occurred in the catalyst with 3 wt-% V_2O_5, causing the loss of accessible active sites. The formation of additional metavanadate chains without loss of vanadia surface area and without significant pore clogging explains the higher activity observed for the catalyst containing 2 wt-% V_2O_5 after ageing procedure 1.

The situation after ageing procedure 2 was quite similar to the one described above. In the case of the catalyst containing 2 wt-% V_2O_5, the fraction of vanadium in metavanadate chains increased, leading to a further increase of the SCR activity. On the other hand, the number of accessible active sites in the catalyst containing 3 wt-% V_2O_5 was reduced by additional pore clogging and a further decrease of the SCR activity was observed.

Ageing procedure 3 affected negatively the catalytic activity of all studied catalysts. For both the catalysts with 2 and 3 wt-% V_2O_5, the XPS V2p$_{3/2}$ BE reached values typical of bulk substances containing V(V) species, indicating extensive three-dimensional growth of the supported vanadia. However, Raman spectroscopy showed that the degree of multilayer formation was not the same for the two catalysts: the catalyst with 3 wt-% V_2O_5 showed the typical fingerprint of crystalline vanadia, whereas this signal was absent in the case of the catalyst containing 2 wt-% V_2O_5. The formation of crystalline vanadia and severe pore clogging were responsible for the low SCR activity of the catalyst with 3 wt-% V_2O_5 after the ageing procedure 3. On the other hand, the less extensive pore clogging and the lower loss of active V-sites due to multilayer formation caused only a modest reduction of the SCR activity of the catalyst containing 2 wt-% V_2O_5.

Summarizing, there exists an optimum vanadium content resulting in high SCR activity and good thermal stability. Quite obviously, the SCR activity increases with the amount of accessible V-sites. This explains the low activity of the catalyst with 1 wt-% V_2O_5 in comparison to the catalysts with 2 and 3 wt-% V_2O_5. As shown in Figures 10.2 and 10.4, a higher V-content is associated with a larger decrease of the anatase surface and

with a more extensive pore clogging upon ageing. Moreover, the anatase surface required to disperse the supported vanadia increases with higher V-loading.

The comparison has shown that the catalyst containing 2 wt-% V_2O_5 represents an optimal compromise. Its amount of V-active sites is high enough for a high SCR activity, but low enough to prevent severe sintering of the anatase upon ageing. As a result, the vanadia surface species remain well-dispersed, a large amount of catalytically active metavanadate chains is formed and multilayer formation occurs only after exposure to drastic ageing conditions. A higher V-content causes a drastic decrease of anatase surface area upon ageing. Since the amount of supported vanadia present exceeds the dispersion capability of the support, extensive multilayer growth occurs and eventually crystalline vanadia is formed. Therefore, the thermal stability of catalysts containing amounts of V_2O_5 higher than 2 wt-% is significantly lower.

10.5 Conclusions

The vanadium content was found to have a major influence on both the SCR activity and the thermal stability of TiO_2-WO_3-V_2O_5 catalysts. The catalyst containing 2 wt-% V_2O_5 represents an optimal compromise between high SCR activity and good thermal stability over a wide range of ageing treatments. At lower vanadium contents, the small amount of active vanadium sites results in low SCR activity. Catalysts containing a higher vanadium content show a significantly lower thermal stability, due to vanadium-induced loss of anatase surface area upon ageing. This results in the formation of less active vanadia multilayer species and severe pore clogging.

10.6 References

[1]   R.Y. Saleh, I.E. Wachs, S.S. Chan and C.C. Chersic, *J. Catal.* **98** (1986), 102

[2]   V.A. Nikolov and A.I. Anastasov, *Ind. Chem. Eng. Res.* **31** (1992), 80

[3]   I.M. Pearson, H. Ryu, W.C. Wong and K. Nobe, *Ind Chem. Eng. Prod. Res. Dev.* **22** (1983), 381

[4]   D.J. Cole, C.F. Cullis and D.J. Hucknall, *J. Chem. Soc.*, *Faraday Trans. 1* **72** (1976), 2185

[5]   P. Forzatti, E. Tronconi, G. Busca and P. Tittarelli, *Catal. Today* **1** (1987), 209

[6]   G. Oliveri, G. Ramis, G. Busca and V.S. Escribano, *J. Mater. Chem.* **3** (1993) 12, 1239

[7]   G.T. Went, L.J. Leu, R.R. Rosin and A.T. Bell, *J. Catal.* **134** (1992), 492

[8]   J.H. Scofield, *J. Electron Spectrosc. Relat. Phenom.* **8** (1976), 129

[9]   H.P. Klug and L.E. Alexander, *X-ray Diffraction Procedures*, Wiley-Interscience (1974)

[10] J. Nickl, Ch. Schild, A. Baiker, M. Hund and A. Wokaun, *Fresenius J. Anal. Chem.* **346** (1993), 79

[11] M.A. Reiche, T. Bürgi, A. Baiker, A. Scholz, B. Schnyder and A. Wokaun, *Appl. Catal. A* **198** (2000), 155

[12] I.E. Wachs, *Catal. Today* **27** (1997), 437

[13] S.S. Chan, I.E. Wachs, L.L. Murrel, L. Wang and W. Keith Hall, *J. Phys. Chem.* **88** (1984), 5831.

[14] L.J. Alemany, L. Lietti, N. Ferlazzo, G. Busca, E. Giamello and F. Bregani, *J. Catal.* **155** (1995), 117

[15] G. Madia, M. Elsener, M. Koebel, F. Raimondi and A. Wokaun, submitted to *Appl. Catal. B*

Outlook

It has been shown that the temperature window of the SCR process may be widened by increasing the volumetric activity of the catalyst and by utilizing the accelerating effect of NO_2, i.e. the fast SCR reaction.

Increasing the vanadium content and the cell density are both effective in increasing the volumetric activity of the catalyst. However, an excessive vanadium content should be avoided due to detrimental effects on the thermal stability. A catalyst with 2 wt-% V_2O_5 was found to be an acceptable compromise between a high activity and a good thermal stability for temperatures up to ≈650°C. Its amount of V-active sites is sufficient to yield a high SCR activity, but low enough to prevent severe sintering of the support upon thermal ageing. As a result, the vanadia surface species remain well dispersed, a large amount of active metavanadate chains are formed and multilayer formation occurs only during drastic ageing treatments.

NO_2 was found to be very effective in enhancing the NO_x conversion at temperatures below 300°C. The NO_x conversion increases with NO_2 contents up to 50% of total NO_x, because an increasing amount of NO_x can react in the fast SCR reaction. Conversely, if $NO_{2,IN}/NO_{x,IN} > 50\%$, the slow kinetics of the SCR reaction involving NO_2 lower the conversion of NO_x. Furthermore, at temperatures below 200°C, the reaction between NH_3 and NO_2 may form ammonium nitrate, which may deposit in solid or liquid form in the catalyst pores leading to temporary deactivation. Therefore, a lower boundary for the operating temperature exists also in the case of the fast SCR reaction. This temperature is around 180°C for continuous operation.

Due to the high oxidizing power of NO_2 a continuous oxidation of soot at low temperatures may also be envisaged. Therefore, future work should focus on developing an integrated DeNOx-DeSoot system which takes advantage of NO_2 for both the SCR

reaction and the oxidation of soot. Such a combination may be a valid technical solution for reaching the forthcoming emission standards of both NO_x and soot.

Several engineering aspects must still be developed in order to turn the SCR process into a practical aftertreatment technology for automotive applications. One important issue is the improvement of the dosing strategy for the reducing agent with the goal of minimizing the ammonia slip during load changes. The availability of cheap and fast sensors for NO_x or NH_3 would be highly welcome as they allow for a more effective closed loop control of the process than the present open loop control. Furthermore, a dosing system for solid urea would have distinctive advantages over the use of urea solution. The main advantages are a much simpler infrastructure for distributing solid urea and the absence of the freezing problem related to urea solution ($\approx$ -11°C for the solution with 32.5 wt-% of urea).

The introduction of a hydrolyzing catalyst upstream of the SCR catalyst can lower the undesirable slip of isocyanic acid observed under certain operating conditions, e.g. high engine load. The benefit of an additional "guard catalyst" to minimize ammonia slip by its selective oxidation to nitrogen is still a subject of controversial discussion. These additional catalysts increase the size of the system and render it more complex, and also increase its costs.

Outlook

List of Publications

The following list summarizes the papers which resulted from this study.

"Reaction pathways in the selective catalytic reduction process with NO and NO_2 at low temperatures", M. Koebel, M. Elsener and G. Madia, *Ind. Chem. Eng. Res*. **40** (2001), 52.

"NO_x-Verminderung in Dieselabgasen mit Harnstoff-SCR bei tiefen Temperaturen", M. Koebel, M. Elsener and G. Madia, *MTZ Motortechnische Zeitschrift* **62** (2001) 2, 166.

"Selective catalytic reduction of NO and NO_2 at low temperatures", M. Koebel, G. Madia and M. Elsener, submitted to *Catal. Today*.

"Enhanced reoxidation of vanadia by NO_2 in the fast SCR reaction", M. Koebel, G. Madia, F. Raimondi and A. Wokaun, submitted to *J. Catal*.

"Side reactions in the selective catalytic reduction of NO_x with various NO_2 fractions", G. Madia, M. Koebel, M. Elsener and A. Wokaun, submitted to *Ind. Eng. Chem. Res.*

"Thermal stability of vanadia-tungsta-titania catalysts in the SCR process", G. Madia, M. Elsener, M. Koebel, F. Raimondi and A. Wokaun, submitted to *Appl. Catal. B*.

"The effect of an oxidation pre-catalyst on the NO_x reduction by ammonia SCR", G. Madia, M. Koebel, M. Elsener and A. Wokaun, submitted to *Ind. Eng. Chem. Res.*.

Curriculum Vitae

Name :   Madia, Giuseppe Salvatore

Date of birth :   December 1, 1973

Place of birth : Aarau (Switzerland)

Nationality :   Italian, from San Giovanni in Fiore (CS)

Education :

1979-1984   Primary School *Dante Alighieri*, San Giovanni in Fiore (CS), Italy

1984-1987   Secondary School *Gioacchino da Fiore*, San Giovanni in Fiore (CS),
                Italy

1987-1992   High School *Liceo Scientifico Statale,* San Giovanni in Fiore (CS),
                Italy

1992-1997   Chemical Engineering studies at the University of Calabria, Arcava-
                cata di Rende (CS), Italy

1999-2002   Ph.D. Thesis under the supervision of Prof. Dr. A. Wokaun (ETH Zu-
                rich) at the Paul Scherrer Institute in Villigen (AG)